Merging Neutron Stars

Matthias Hanauske

and Luciano Rezzolla

Institute for Theoretical Physics, Frankfurt

Frankfurt Institute of advanced Studies (FIAS), Frankfurt

WE-Heraeus summer school on “Nuclear Physics in Astrophysics”
Max Planck Institute for Nuclear Physics (MPIK), Heidelberg , 10-14.09.19

GOETHE UNIVERSITÄT FRANKFURT AM MAIN

erc

MAX-PLANCK-INSTITUT FÜR KERNPHYSIK HEIDELBERG

WILHELM UND ELSE HERAEUS-STIFTUNG

Plan of the lectures

- Lecture I: the **math** of neutron-star mergers

- Lecture II: the **physics/astrophysics** of neutron-star mergers

- Alcubierre, ***"Introduction to 3+1 Numerical Relativity"***, Oxford University Press, 2008
- Baumgarte and Shapiro, ***"Numerical Relativity: Solving Einstein's Equations on the Computer"***, Cambridge University Press, 2010
- Gourgoulhon, ***"3+1 Formalism in General Relativity"***, Lecture Notes in Physics, Springer 2012
- Rezzolla and Zanotti, "Relativistic Hydrodynamics", Oxford University Press, 2013

Merging Neutron Stars

- Lecture I: The math of neutron-star mergers
  - Introduction
  - A brief review of General Relativity
  - Numerical relativity of neutron-star mergers
    - The 3+1 decomposition of spacetime
    - ADM equations
    - BSSNOK/ccZ4 formulation
    - Initial data, gauge conditions, excising parts of spacetime and gravitational wave extraction
- Lecture II: The physics/astrophysics of neutron-star mergers
  - Introduction
  - GW170817 - the long-awaited event
  - Determining neutron-star properties and the equation of state using gravitational wave data
  - Hypermassive neutron stars and the post-merger gravitational wave emission
  - Detecting the hadron-quark phase transition with gravitational waves

The two-body problem in GR

- For BHs we know what to **expect**:

BH + BH ⟶ BH + GWs

- For NSs the question is more **subtle:**

hyper-massive neutron star (HMNS), ie

NS + NS ⟶ HMNS+**... ?** ⟶ BH+to

- **HMNS** phase can provide clear information on **EOS**

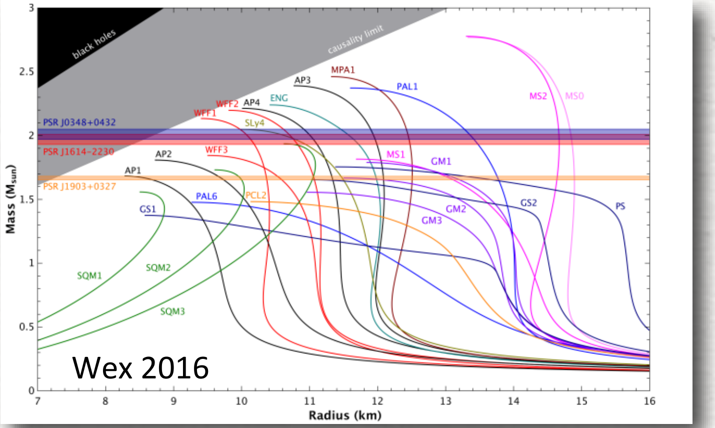

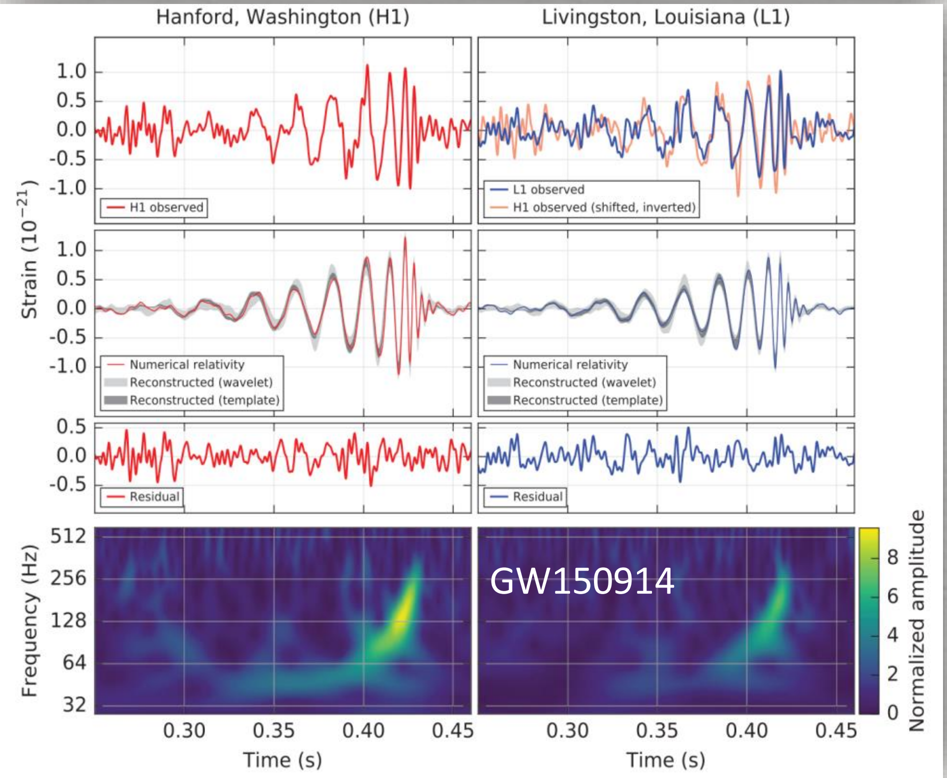

Abbott+ 2016

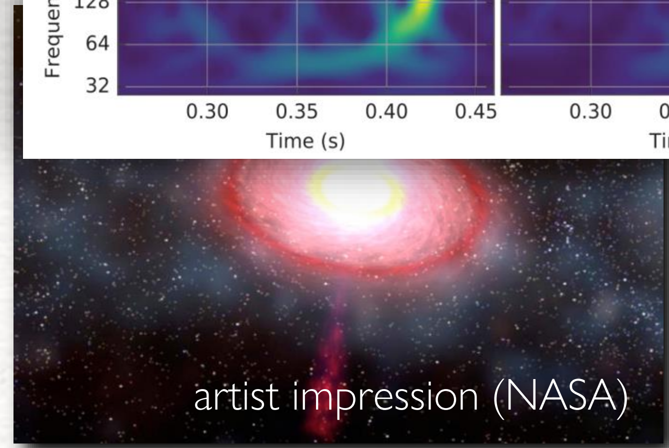

- **BH+torus** system may tell us on the central engine of **GRBs**

The two-body problem in GR

- For BHs we know what to **expect**:

BH + BH ⟶ BH + GWs

- For NSs the question is more **subtle:** the merger leads to an hyper-massive neutron star (HMNS), ie a metastable equilibrium:

NS + NS ⟶ HMNS+**... ?** ⟶ BH+torus+**... ?** ⟶ BH + GWs

- **ejected matter** undergoes nucleosynthesis of heavy elements

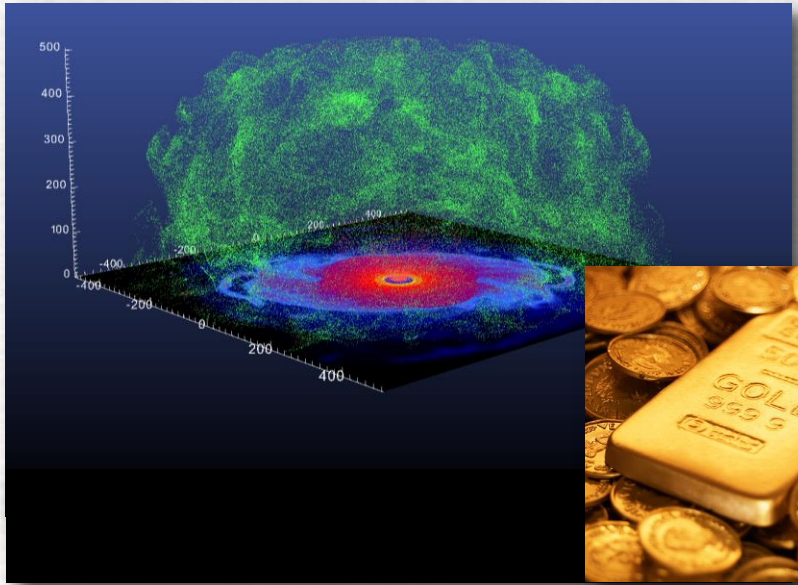

Broadbrush picture

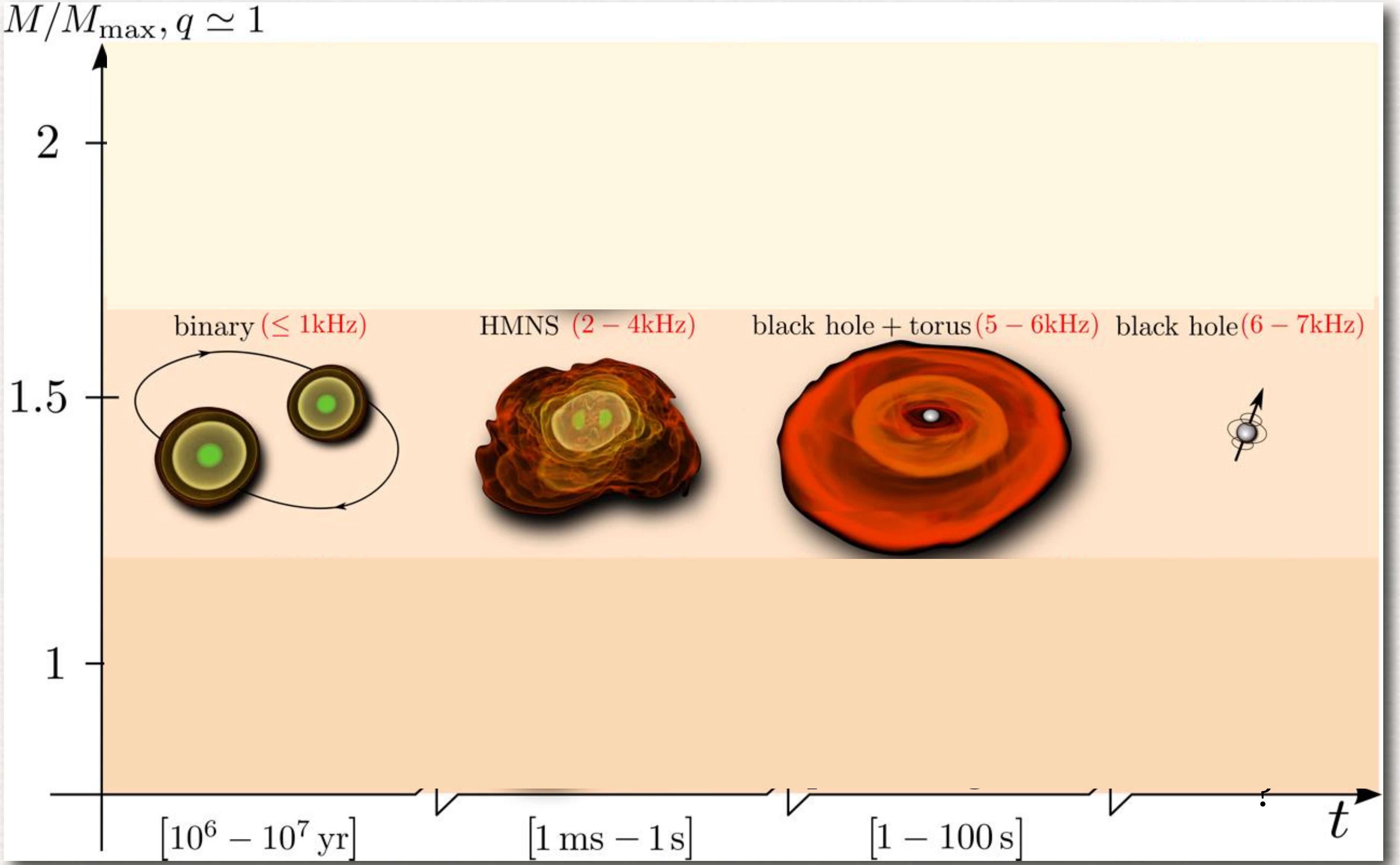

Computersimulation of a Neutron Star Merger in full General Relativity

Credits: Cosima Breu, David Radice and Luciano Rezzolla

Density

8.5 — 14

lg(rho) [g/cm^3]

Temperature

0 — 50

T [MeV]

merger → HMNS → BH + torus

Quantitative differences are produced by:

- total mass (prompt vs delayed collapse)
- mass asymmetries (HMNS and torus)
- soft/stiff EOS (inspiral and post-merger)
- magnetic fields (equil. and EM emission)
- radiative losses (equil. and nucleosynthesis)

Merging Neutron Stars

- Lecture I: The math of neutron-star mergers
  - Introduction
  - A brief review of General Relativity
  - Numerical relativity of neutron-star mergers
    - The 3+1 decomposition of spacetime
    - ADM equations
    - BSSNOK/ccZ4 formulation
    - Initial data, gauge conditions, excising parts of spacetime and gravitational wave extraction
- Lecture II: The physics/astrophysics of neutron-star mergers
  - Introduction
  - GW170817 - the long-awaited event
  - Determining neutron-star properties and the equation of state using gravitational wave data
  - Hypermassive neutron stars and the post-merger gravitational wave emission
  - Detecting the hadron-quark phase transition with gravitational waves

The long-awaited event GW170817

	Low-spin priors ($\|\chi\| \leq 0.05$)	High-spin priors ($\|\chi\| \leq 0.89$)
Primary mass m_1	1.36–$1.60\ M_\odot$	1.36–$2.26\ M_\odot$
Secondary mass m_2	1.17–$1.36\ M_\odot$	0.86–$1.36\ M_\odot$
Chirp mass $\mathcal{M}$	$1.188^{+0.004}_{-0.002} M_\odot$	$1.188^{+0.004}_{-0.002} M_\odot$
Mass ratio m_2/m_1	0.7–1.0	0.4–1.0
Total mass $m_{\rm tot}$	$2.74^{+0.04}_{-0.01} M_\odot$	$2.82^{+0.47}_{-0.09} M_\odot$
Radiated energy $E_{\rm rad}$	$> 0.025 M_\odot c^2$	$> 0.025 M_\odot c^2$
Luminosity distance $D_{\rm L}$	40^{+8}_{-14} Mpc	40^{+8}_{-14} Mpc
Viewing angle Θ	$\leq 55°$	$\leq 56°$
Using NGC 4993 location	$\leq 28°$	$\leq 28°$
Combined dimensionless tidal deformability $\tilde{\Lambda}$	≤ 800	≤ 700
Dimensionless tidal deformability $\Lambda(1.4 M_\odot)$	≤ 800	≤ 1400

Gravitational Wave GW170817 and Gamma-Ray Emission GRB170817A

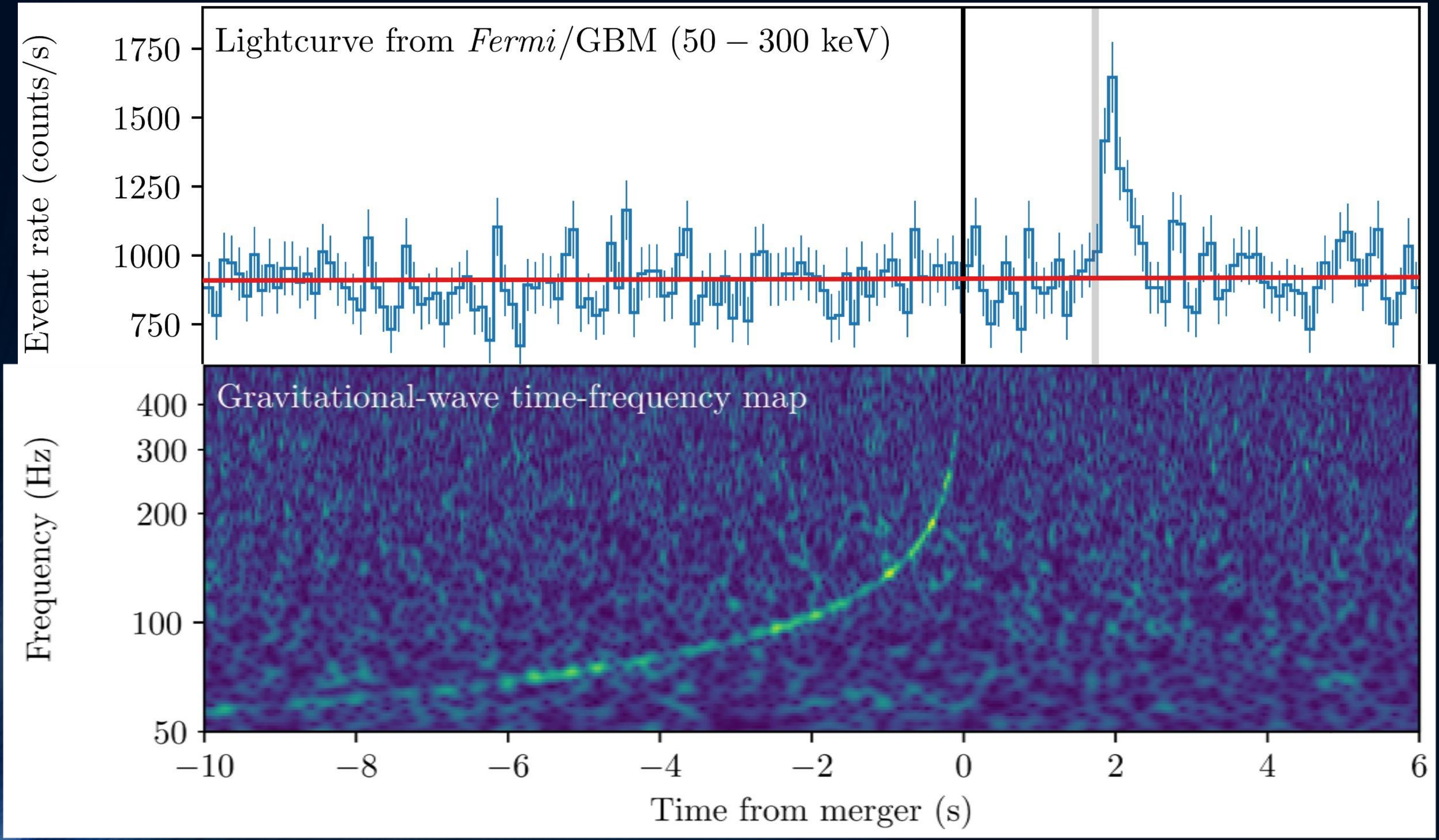

Measured Mass Ratio of GW170817 (for high and low spin assumption)

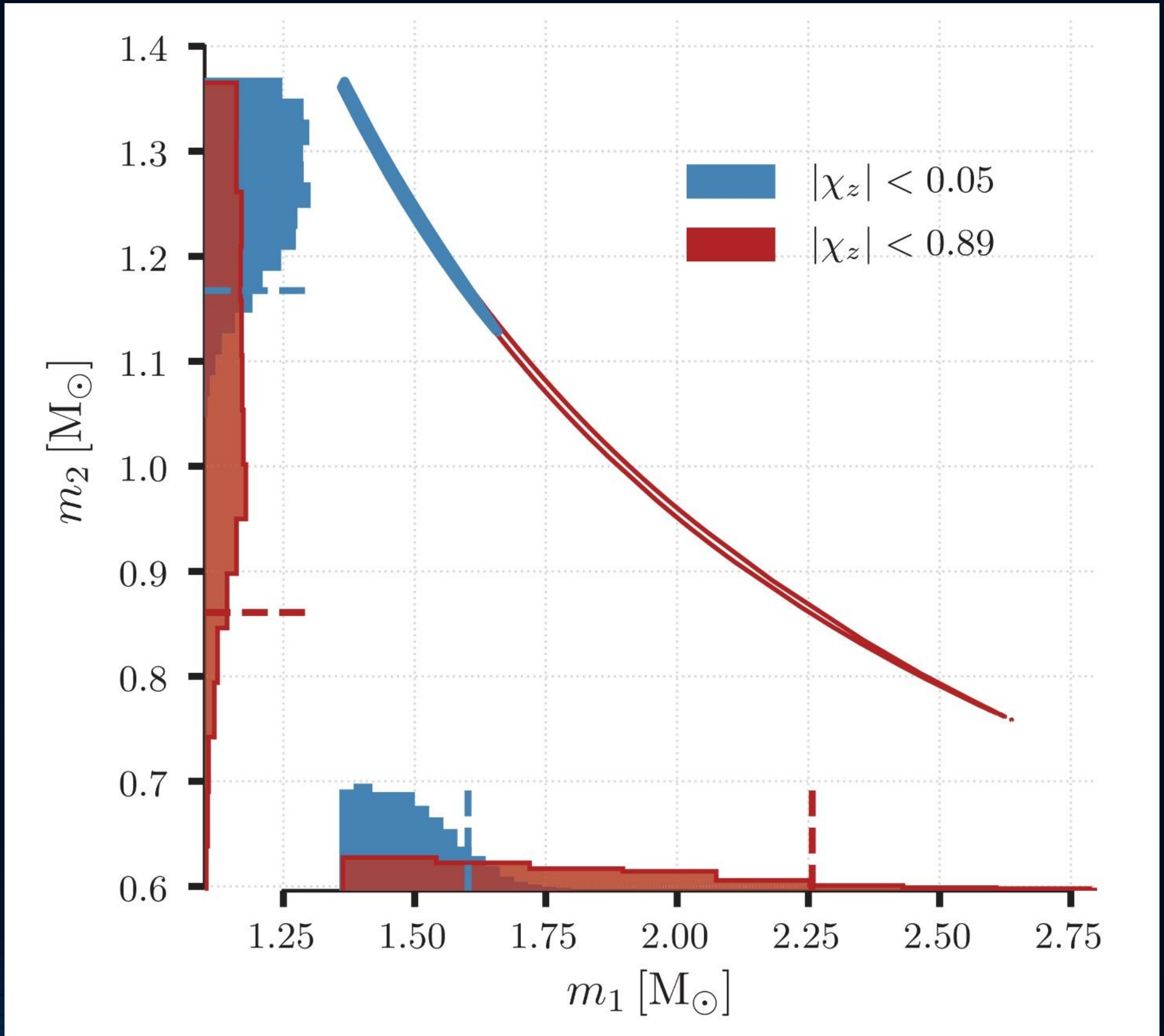

GW170817

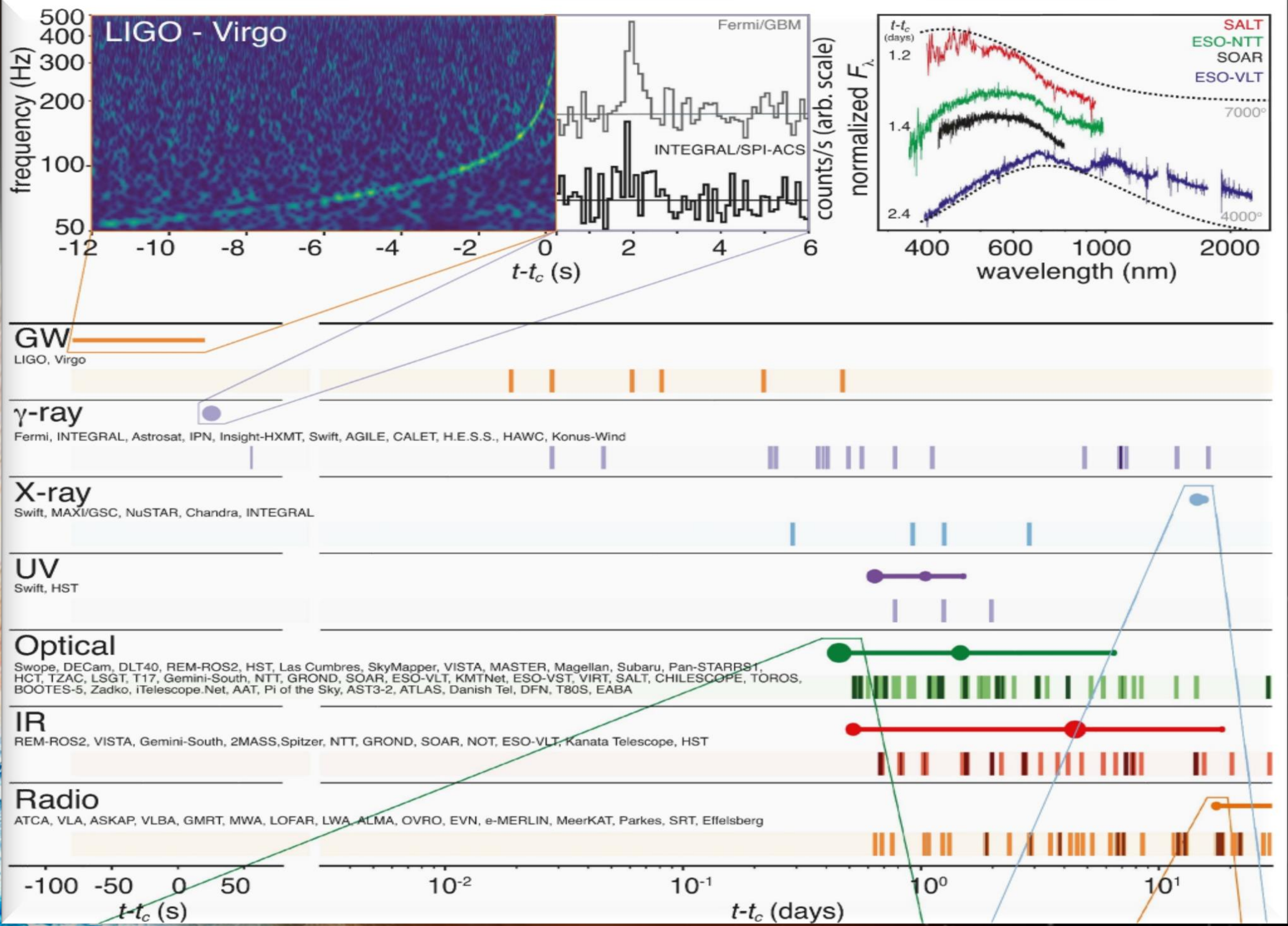
LIGO - Virgo
frequency (Hz)
500
400
300
200
100
50
-12
-10
-8
-6
-4
-2
0
2
4
6
t-t_c (s)
Fermi/GBM
INTEGRAL/SPI-ACS
counts/s (arb. scale)
normalized F_λ
t-t_c (days)
1.2
1.4
2.4
SALT
ESO-NTT
SOAR
ESO-VLT
7000°
4000°
400
600
1000
2000
wavelength (nm)
GW
LIGO, Virgo
γ-ray
Fermi, INTEGRAL, Astrosat, IPN, Insight-HXMT, Swift, AGILE, CALET, H.E.S.S., HAWC, Konus-Wind
X-ray
Swift, MAXI/GSC, NuSTAR, Chandra, INTEGRAL
UV
Swift, HST
Optical
Swope, DECam, DLT40, REM-ROS2, HST, Las Cumbres, SkyMapper, VISTA, MASTER, Magellan, Subaru, Pan-STARRS1, HCT, TZAC, LSGT, T17, Gemini-South, NTT, GROND, SOAR, ESO-VLT, KMTNet, ESO-VST, VIRT, SALT, CHILESCOPE, TOROS, BOOTES-5, Zadko, iTelescope.Net, AAT, Pi of the Sky, AST3-2, ATLAS, Danish Tel, DFN, T80S, EABA
IR
REM-ROS2, VISTA, Gemini-South, 2MASS, Spitzer, NTT, GROND, SOAR, NOT, ESO-VLT, Kanata Telescope, HST
Radio
ATCA, VLA, ASKAP, VLBA, GMRT, MWA, LOFAR, LWA, ALMA, OVRO, EVN, e-MERLIN, MeerKAT, Parkes, SRT, Effelsberg
-100
-50
0
50
t-t_c (s)
10^-2
10^-1
10^0
10^1
t-t_c (days)

GW170817, GRB170817A Localisation and unusual dimness of GRB

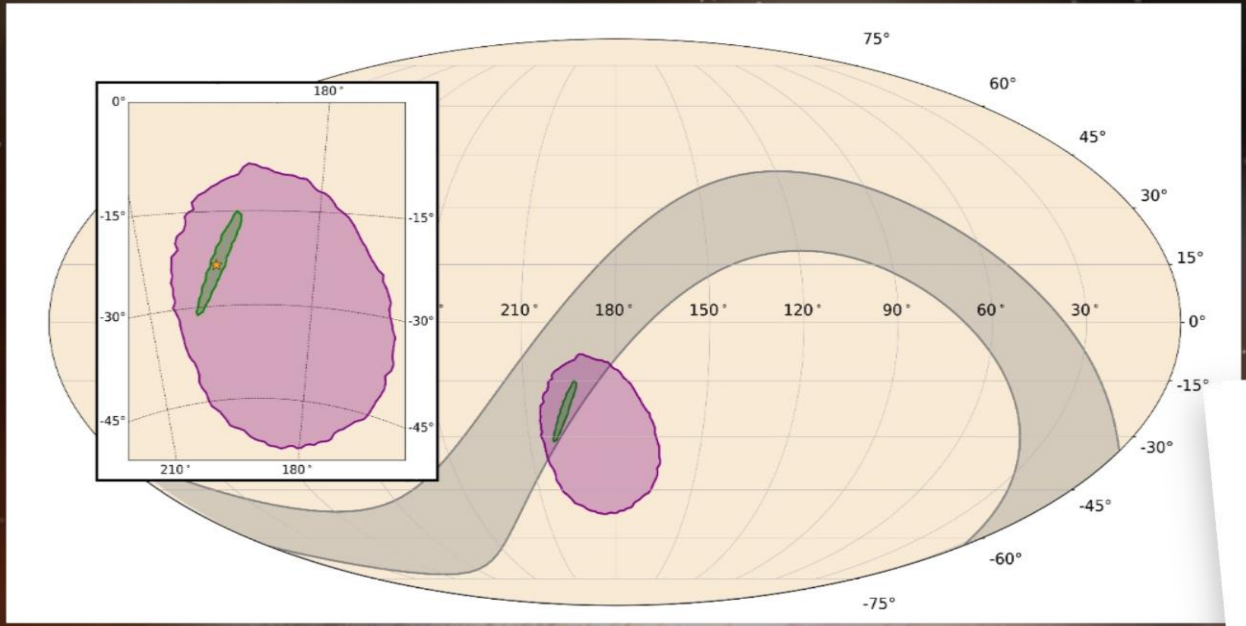

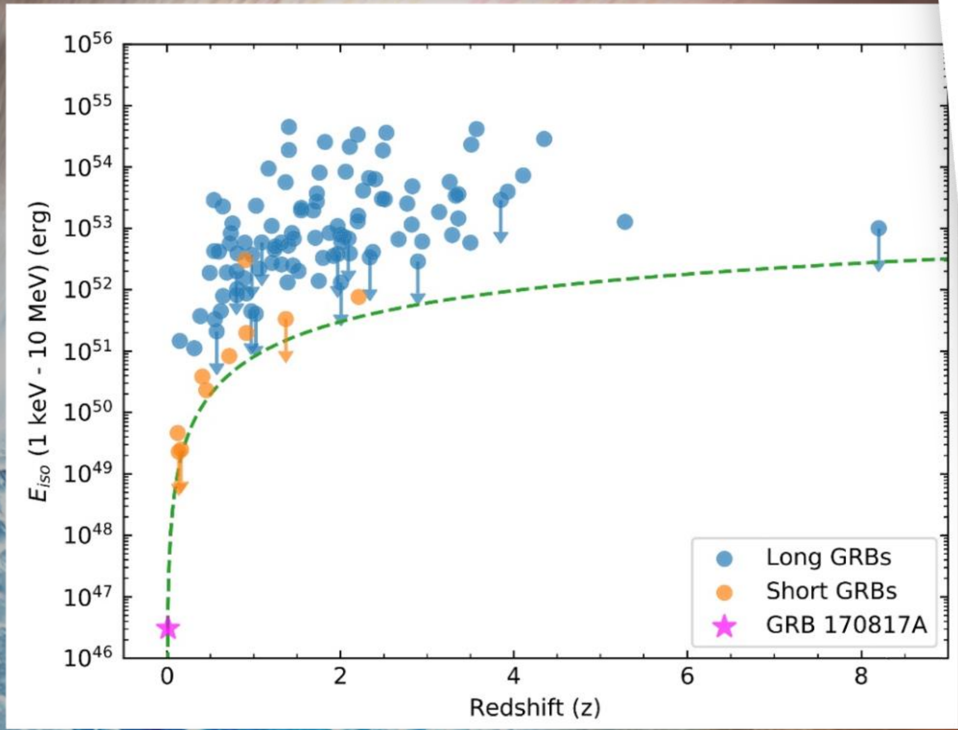

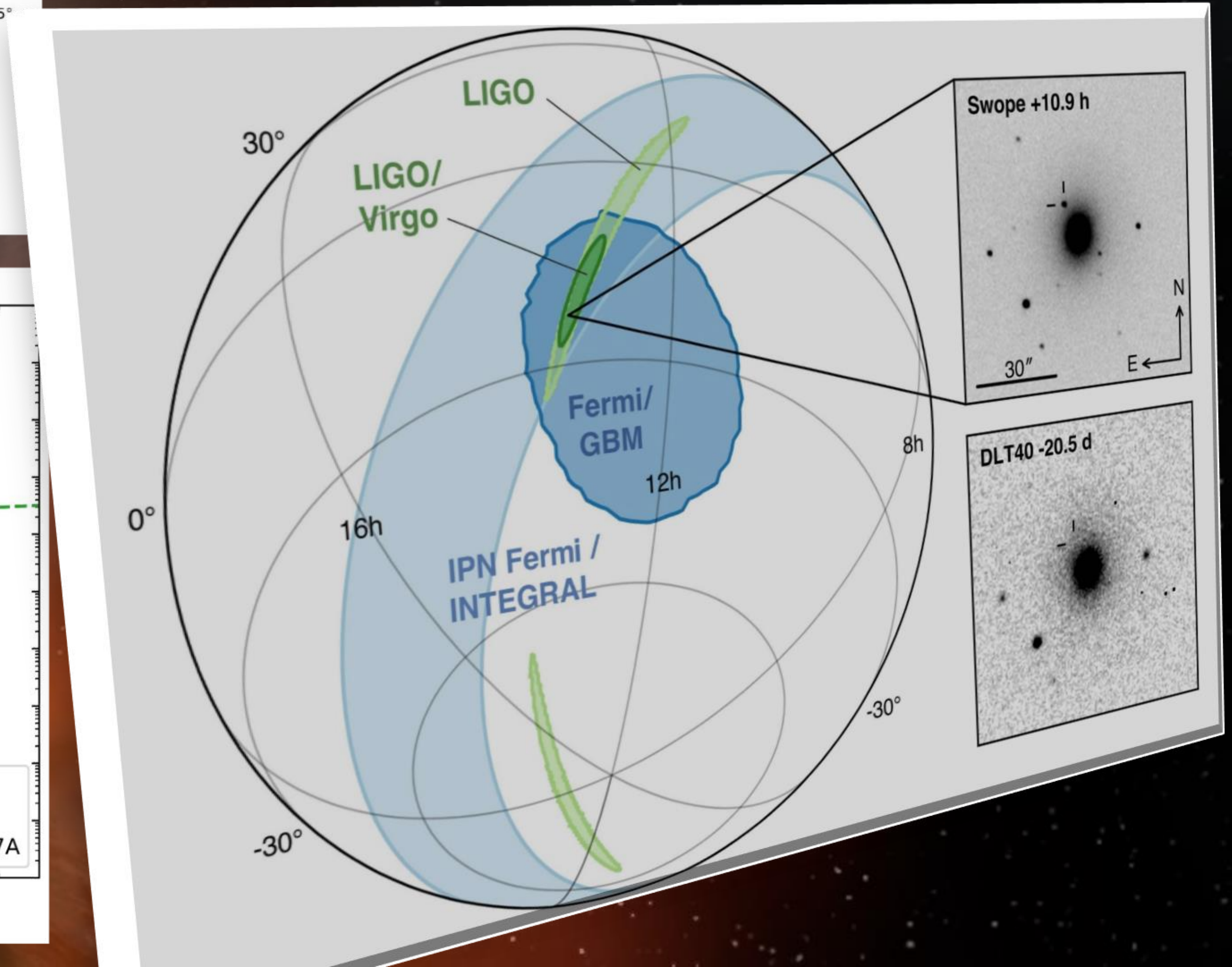

GW170817: Tidal Deformability Restrictions on the Equation of State (EOS) (for high and low spin assumption)

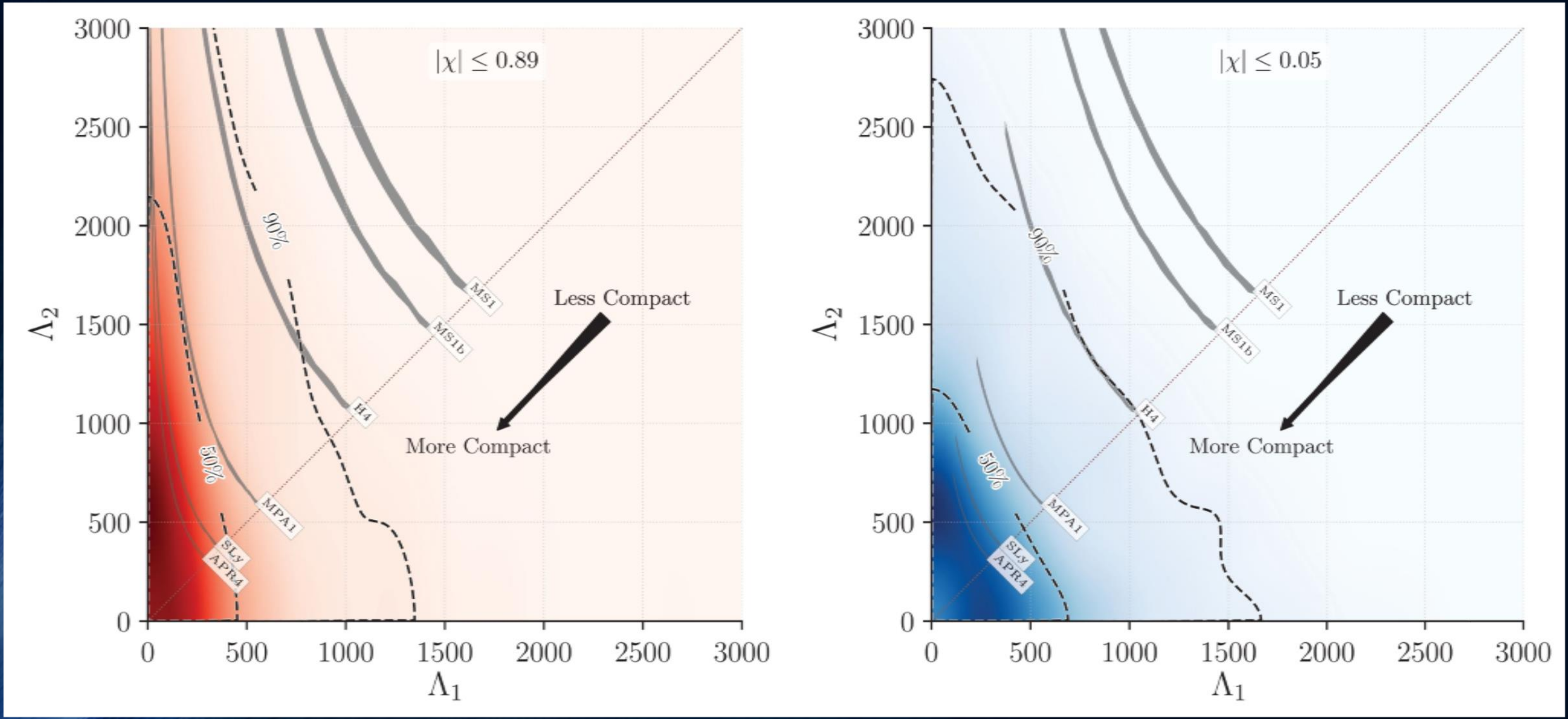

Merging Neutron Stars

- Lecture I: The math of neutron-star mergers
  - Introduction
  - A brief review of General Relativity
  - Numerical relativity of neutron-star mergers
    - The 3+1 decomposition of spacetime
    - ADM equations
    - BSSNOK/ccZ4 formulation
    - Initial data, gauge conditions, excising parts of spacetime and gravitational wave extraction
- Lecture II: The physics/astrophysics of neutron-star mergers
  - Introduction
  - GW170817 - the long-awaited event
  - **Determining neutron-star properties and the equation of state using gravitational wave data**
  - Hypermassive neutron stars and the post-merger gravitational wave emission
  - Detecting the hadron-quark phase transition with gravitational waves

GW170817: Constraining the Neutron Star Radius and EOS

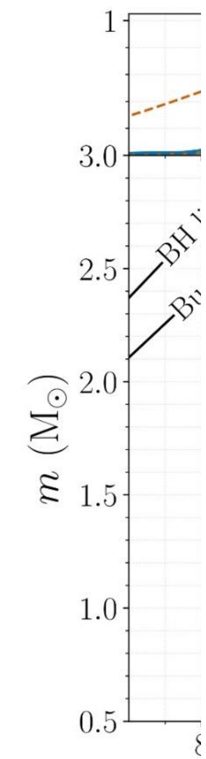

FIG. 3. Margin
and a parametr
posterior corre
the top left der
used for the po
of the 90% cre

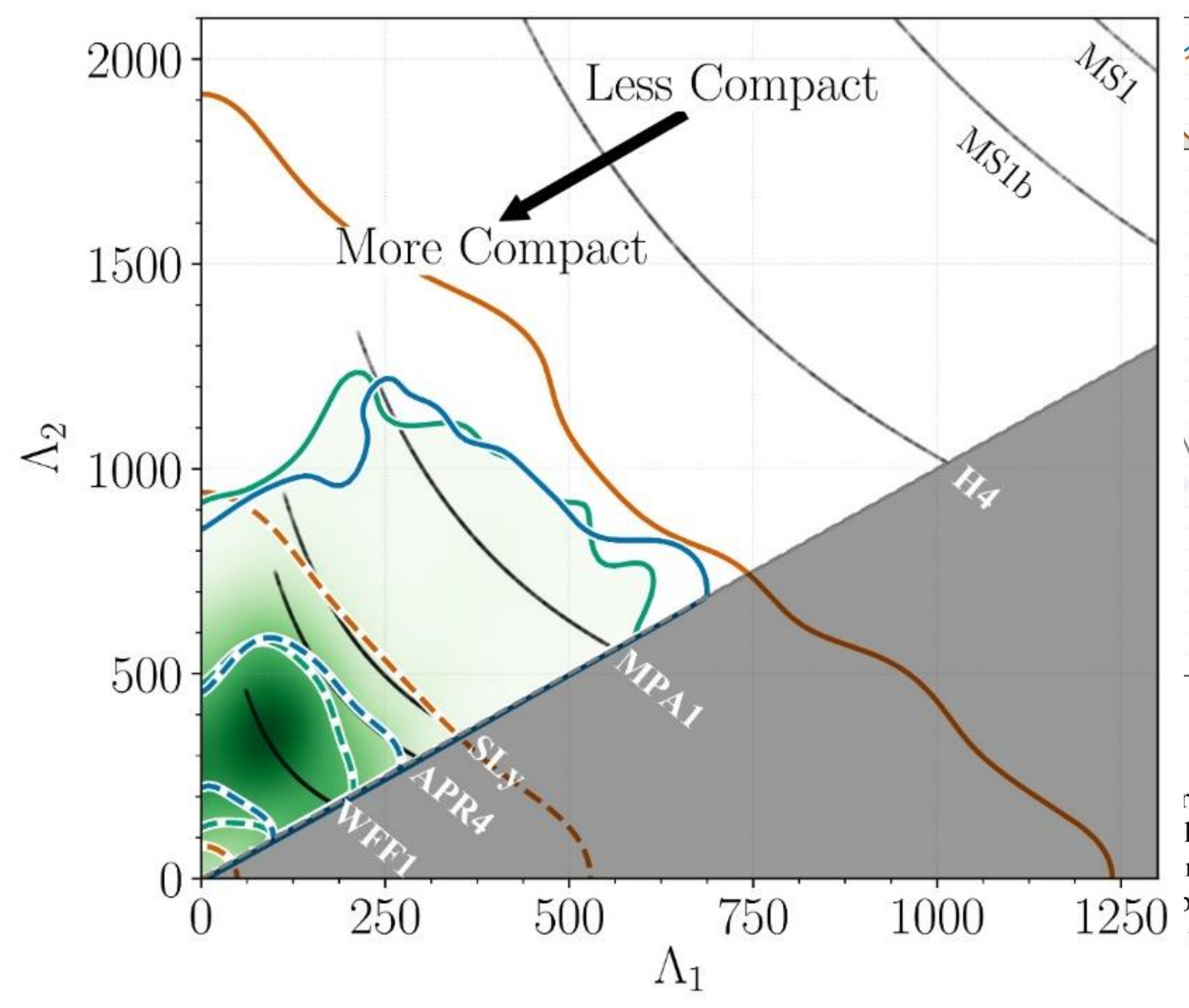

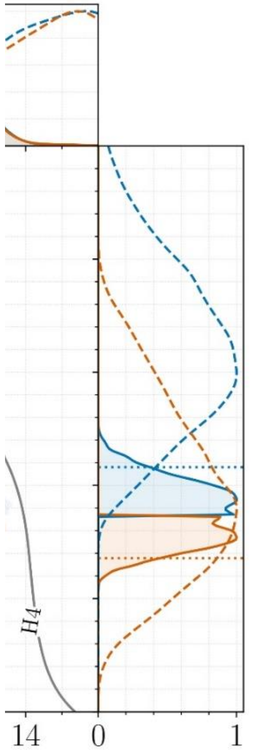

relations (left panel)
lue (bottom orange)
n grey. The lines in
plots, solid lines are
used for the bounds

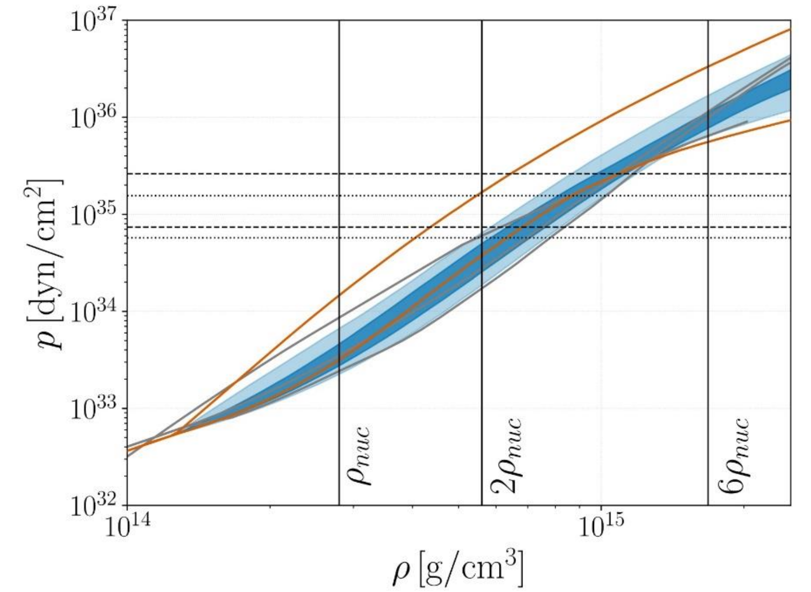

FIG. 2. Marginalized posterior (blue) and prior (orange) for the pressure p as a function of the rest-mass density ρ of the NS interior using the spectral EOS parametrization and imposing a lower limit on the maximum NS mass supported by the EOS of 1.97 $M_\odot$. The dark (light) blue shaded region corresponds to the 50% (90%) posterior credible level and the orange lines show the 90% prior credible interval. Horizontal lines denote the 90% credible interval for the central pressure of the heavier (dashed) and the lighter (dotted) binary components. Vertical lines correspond to once, twice, and six times the nuclear saturation density. Overplotted in grey are representative EOS models [121, 122, 124], using data taken from [19]; from top to bottom at $2\rho_{\rm nuc}$ we show H4, APR4, and WFF1.

GW170817: Measurements of neutron star radii and equation of state, *The LIGO /Virgo Collaboration*, arXiv:1805.11581v1

GW170817: ... us

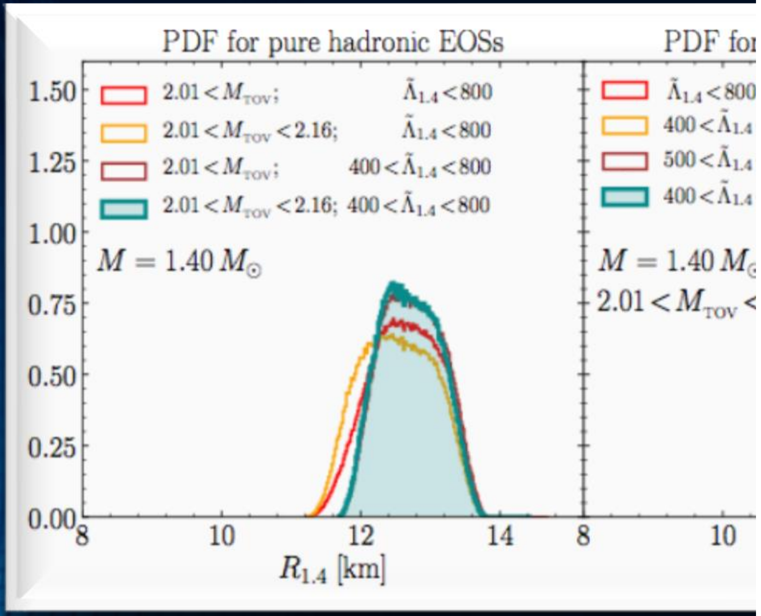

Reference	R_i [km]
Without a phase transition	
Bauswein et al. [42]	$10.68^{+0.15}_{-0.03} \leq R_{1.6}$
Most et al. [51]	$12.00 \leq R_{1.4} \leq 13.45$
Burgio et al. [54]	$11.8 \leq R_{1.5} \leq 13.1$
Tews et al. [55]	$11.3 \leq R_{1.4} \leq 13.6$
De et al. [56]	$8.9 \leq R_{1.4} \leq 13.2$
LIGO/Virgo [57]	$10.5 \leq R_{1.4} \leq 13.3$
With a phase transition	
Annala et al. [46]	$R_{1.4} \leq 13.6$
Most et al. [51]	$8.53 \leq R_{1.4} \leq 13.74$
Burgio et al. [54]	$R_{1.5} = 10.7$
Tews et al. [55]	$9.0 \leq R_{1.4} \leq 13.6$
This work	
NS	$R_{1.4} = 13.11$
HS Model-2	$12.9 \leq R_{1.4} \leq 13.11$
HS_T Model-1	$10.1 \leq R_{1.4} \leq 12.9$
HS_T Model-2	$10.4 \leq R_{1.4} \leq 11.9$

TABLE II. Constraints on the radius of neutron stars from GW170817 for models without a phase transition (top), works considering the possibility of a transition to quark matter (middle) and for EOSs of *Category III* in the present work (bottom).

$$12.00 < R_{1.4}/\mathrm{km} < 13.45$$

$$8.53 < R_{1.4}/\mathrm{km} < 13.74 \quad \bar{R}$$

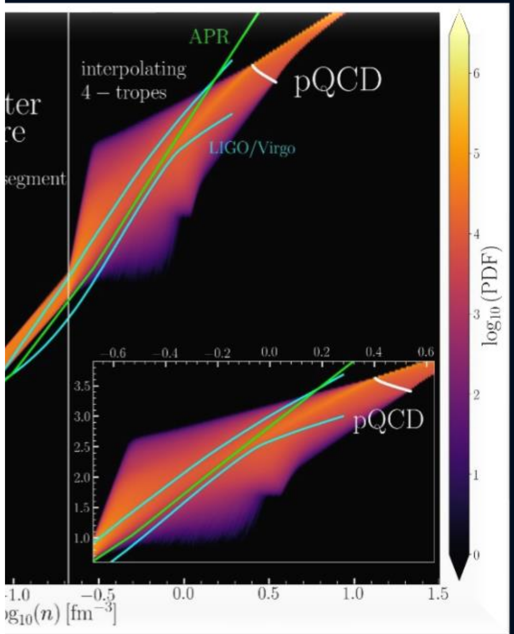

t, L.Weih, L.Rezzolla, J. fner-Bielich "New aints on radii and tidal mabilities of neutron rom GW170817", 1803.00549, pted in PRL)

See also: De, Finstad, Lattimer, Brown, Berger, Biwe... 172702 (2018) ; Nandi & Char, Astrophys. J. 857, 12 (201... Annala, Gorda, Kurkela, Vuorinen, PRL 120, 172703 (201... v, Piekarewicz, Horowitz, PRL 120, ... ros, PRD 97, 021501 (2018) ;

The Hadron-Quark Phase Transition and the Third Family of Compact Stars (Twin Stars)

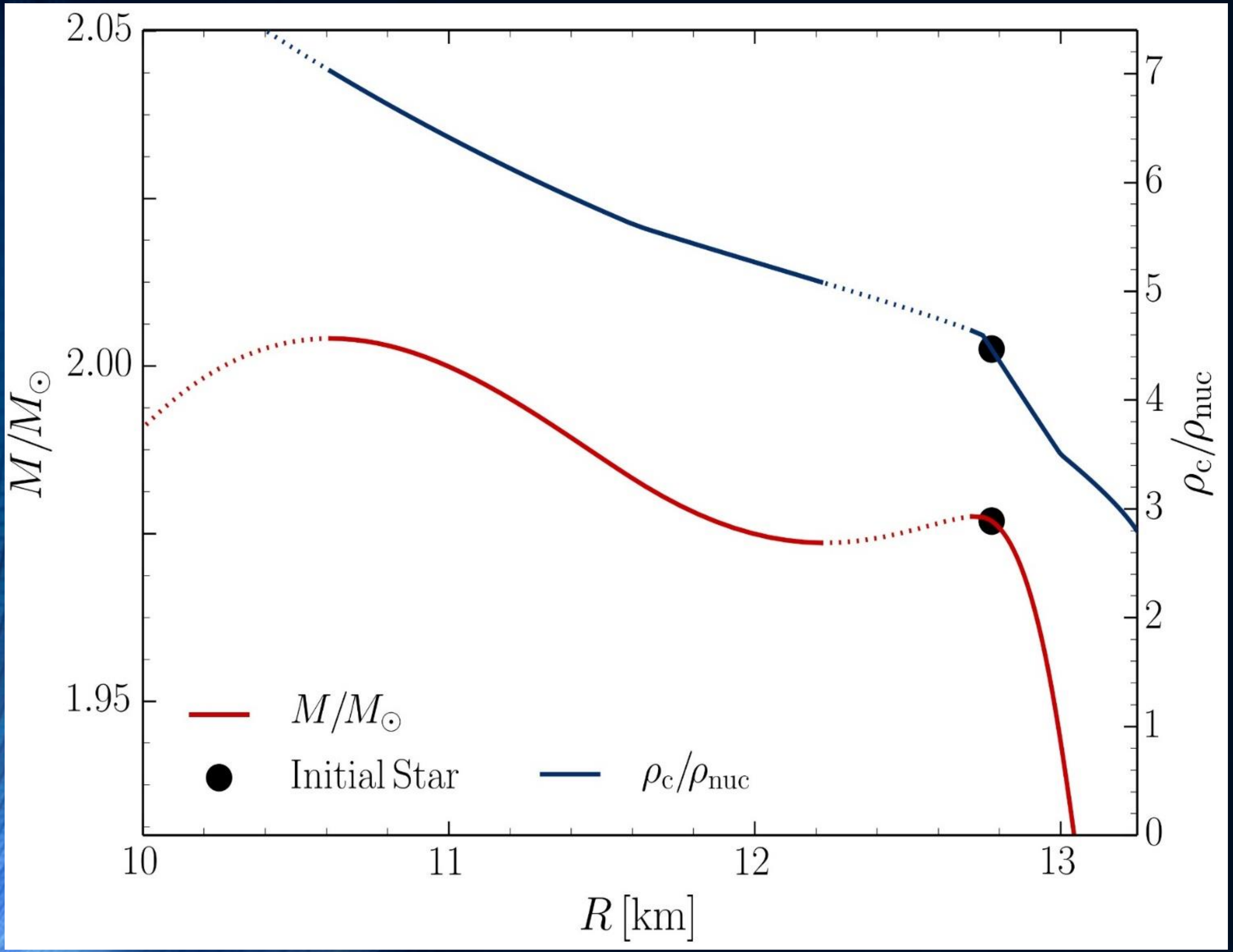

Glendenning, N. K., & Kettner, C. (1998). Nonidentical neutron star twins. Astron. Astrophys., 353(LBL-42080), L9.

Sarmistha Banik, Matthias Hanauske, Debades Bandyopadhyay and Walter Greiner, Rotating compact stars with exotic matter, Phys.Rev.D 70 (2004) p.12304

I.N. Mishustin, M. Hanauske, A. Bhattacharyya, L.M. Satarov, H. Stöcker, and W. Greiner, Catastrophic rearrangement of a compact star due to quark core formation, Physics Letters B 552 (2003) p.1-8

M.Alford and A. Sedrakian, Compact stars with sequential QCD phase transitions. Physical review letters, 119(16), 161104 (2017)..

D.Alvarez-Castillo and D.Blaschke, High-mass twin stars with a multipolytrope equation of state. Physical Review C, 96(4), 045809 (2017) .

A. Ayriyan, N.-U. Bastian, D. Blaschke, H. Grigorian, K. Maslov, D. N. Voskresensky, How robust is a third family of compact stars against pasta phase effects?, arXiv:1711.03926 [nucl-th]

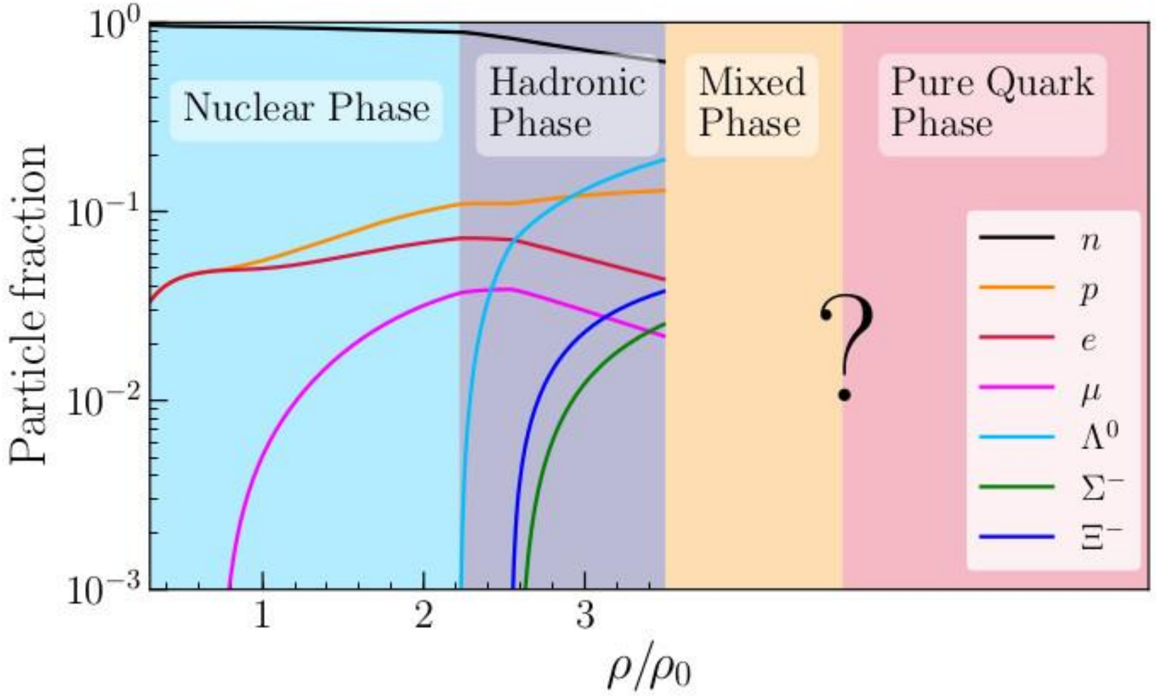

FIG. 1. Particle fractions as functions of the baryonic density for the FSU2H model [69, 70] up to the point where the HQPT is implemented, giving rise to a phase of deconfined quark matter which can be separated from the nuclear (or hadronic) phase by a mixed phase of hadrons and quarks. We note that the actual fractions of nucleons/hyperons and quarks u, d, s in the mixed and quark phases cannot be determined with the parametrizations used in this work.

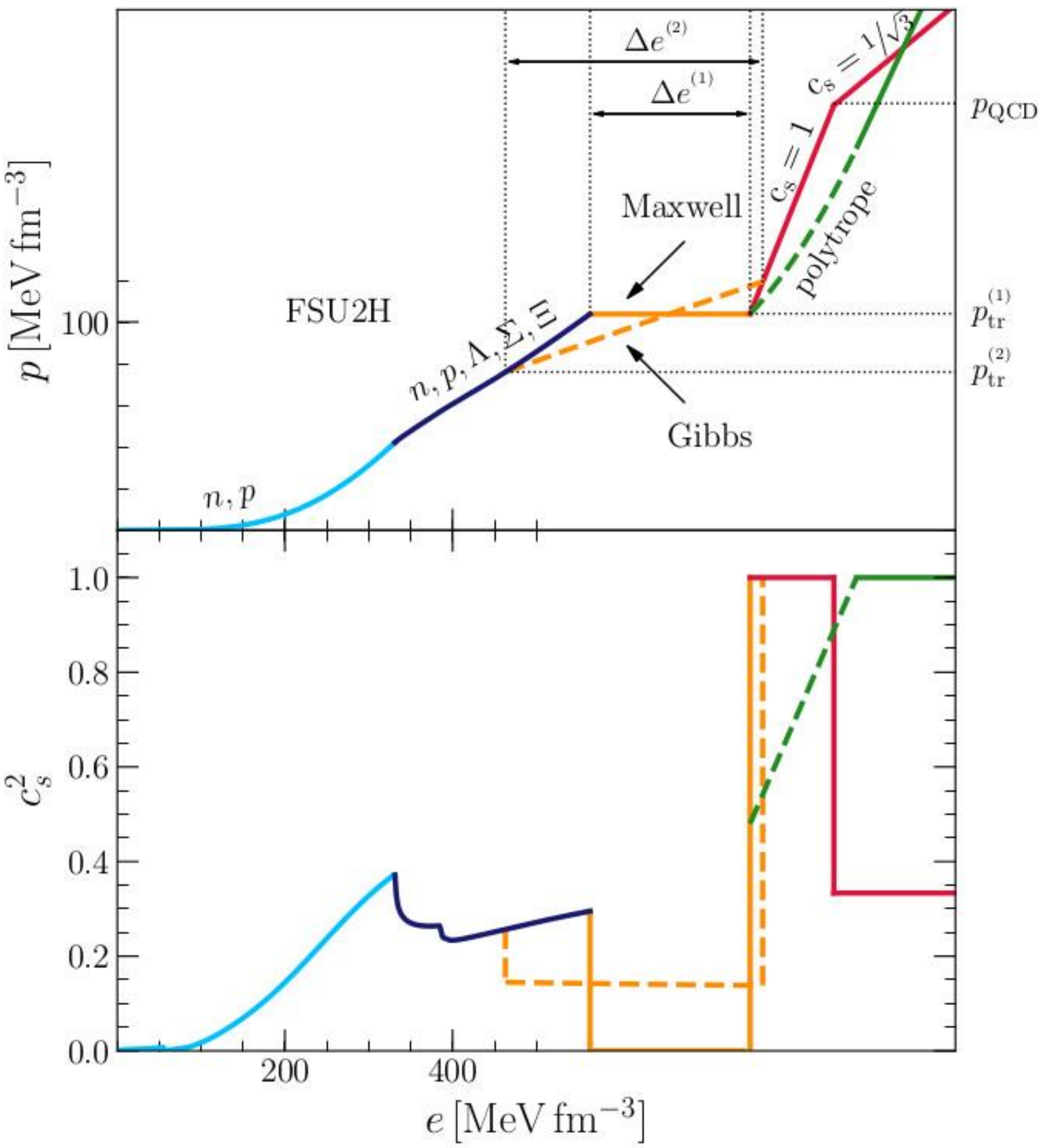

Mass-Radius Relations for Twin-Star EOSs

The mass and radius of a single, non-rotating and spherically symmetric neutron star can be easily calculated by solving the static TOV equation numerically for a given EOS.

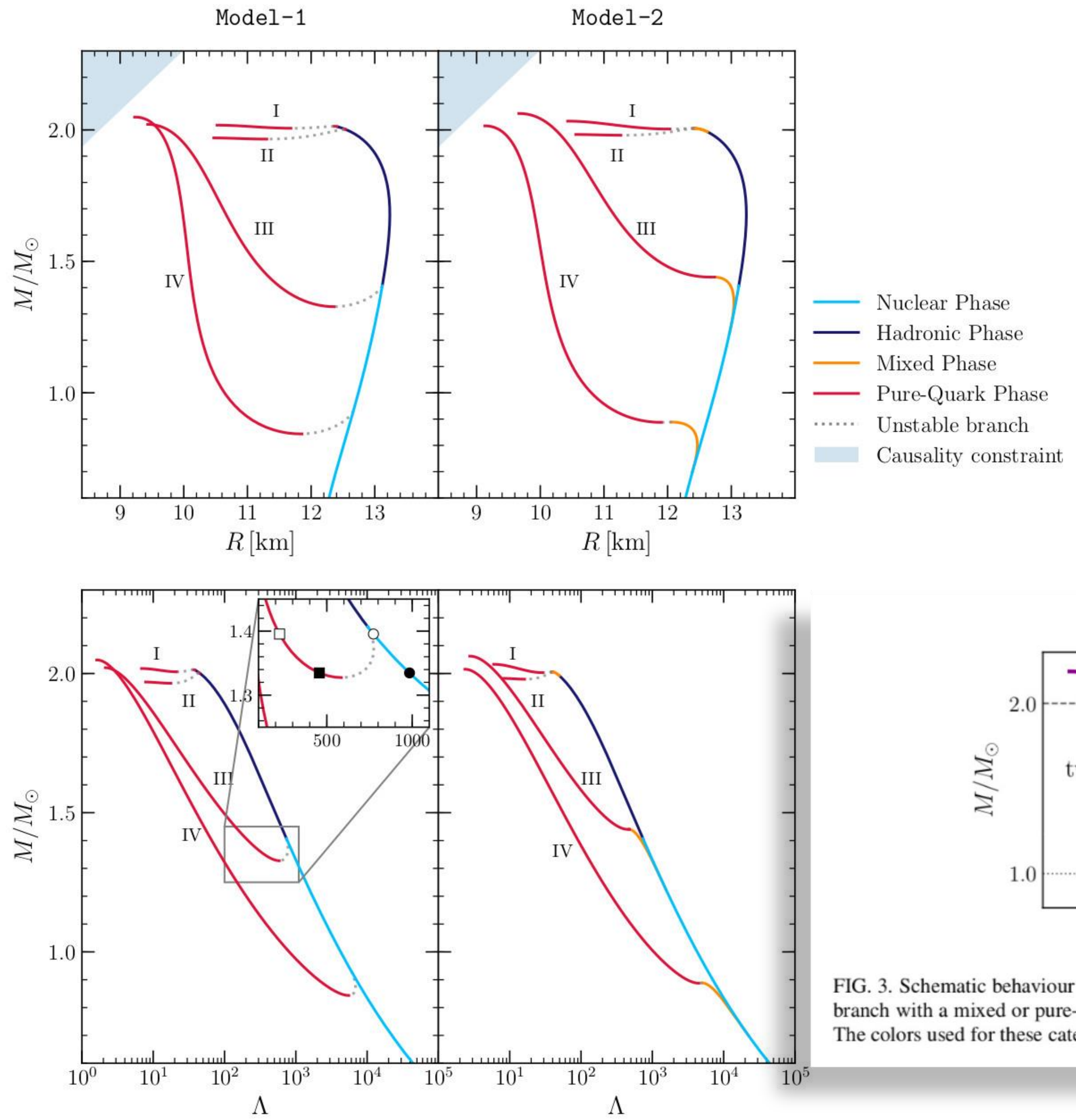

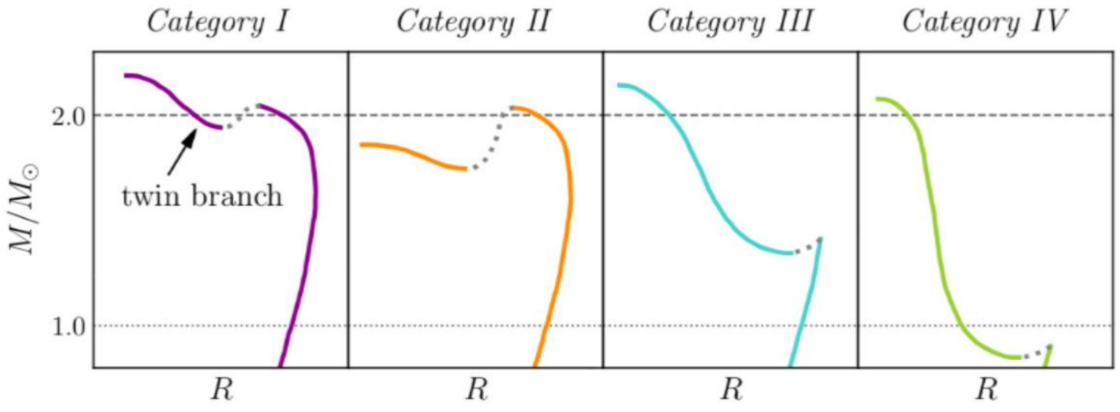

FIG. 3. Schematic behaviour of the mass–radius relation for the twin-star categories *I–IV* defined in the text. Note the appearance of a "twin" branch with a mixed or pure-quark phase; the twin branch has systematically smaller radii than the branch with a nuclear or hadronic phase. The colors used for these categories will be employed also in the subsequent figures.

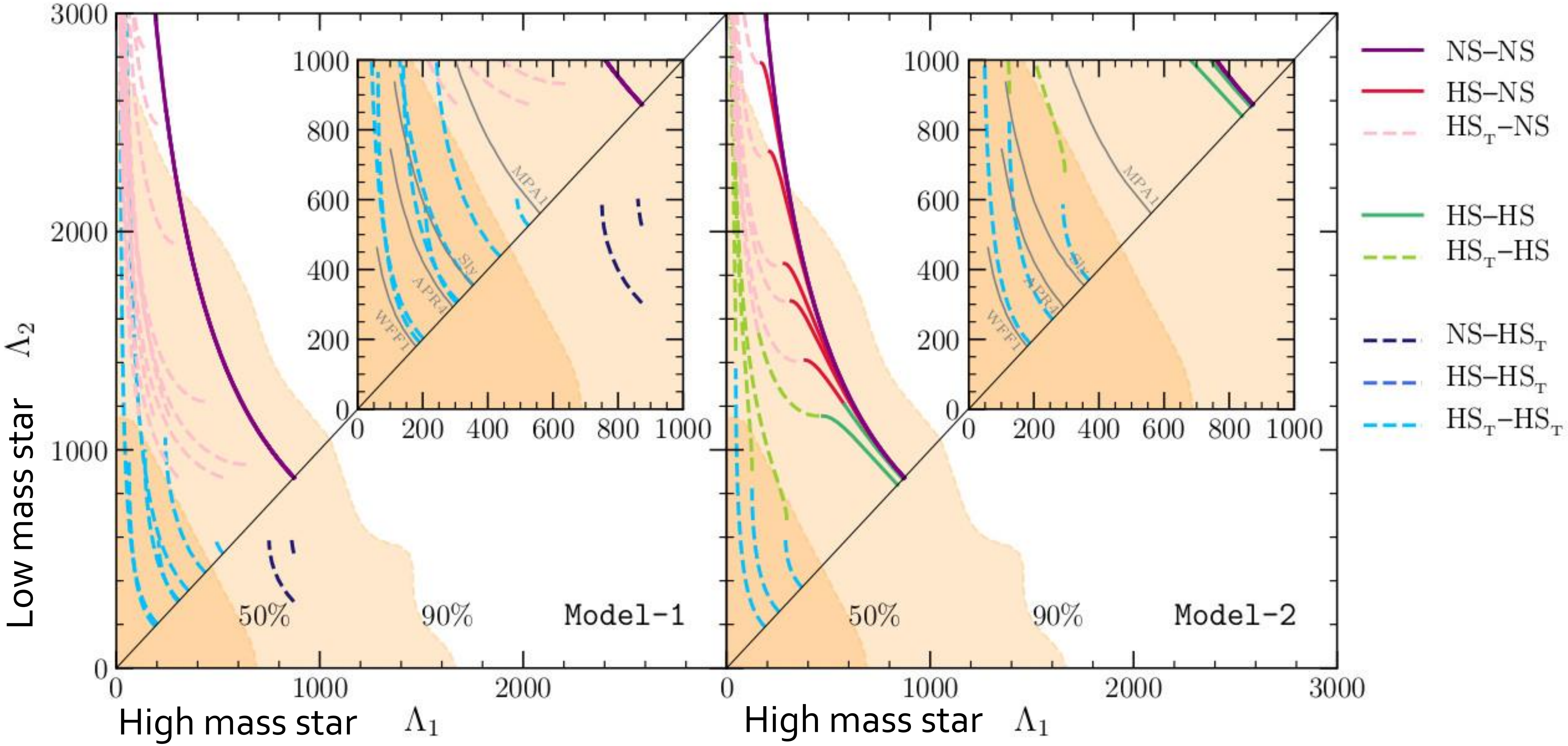

In a binary hybrid star merger the two masses of the individual stars can be different (q<1). As a result, the tidal deformability and the stars composition can be different. In this plot the total mass of the binary system has been fixed to the measured chirp mass of GW170817 (M=1.188 M_{solar}) and the different curve show results for EOSs of Category III.

Constraining the global parameters of the phase transition with GW170817

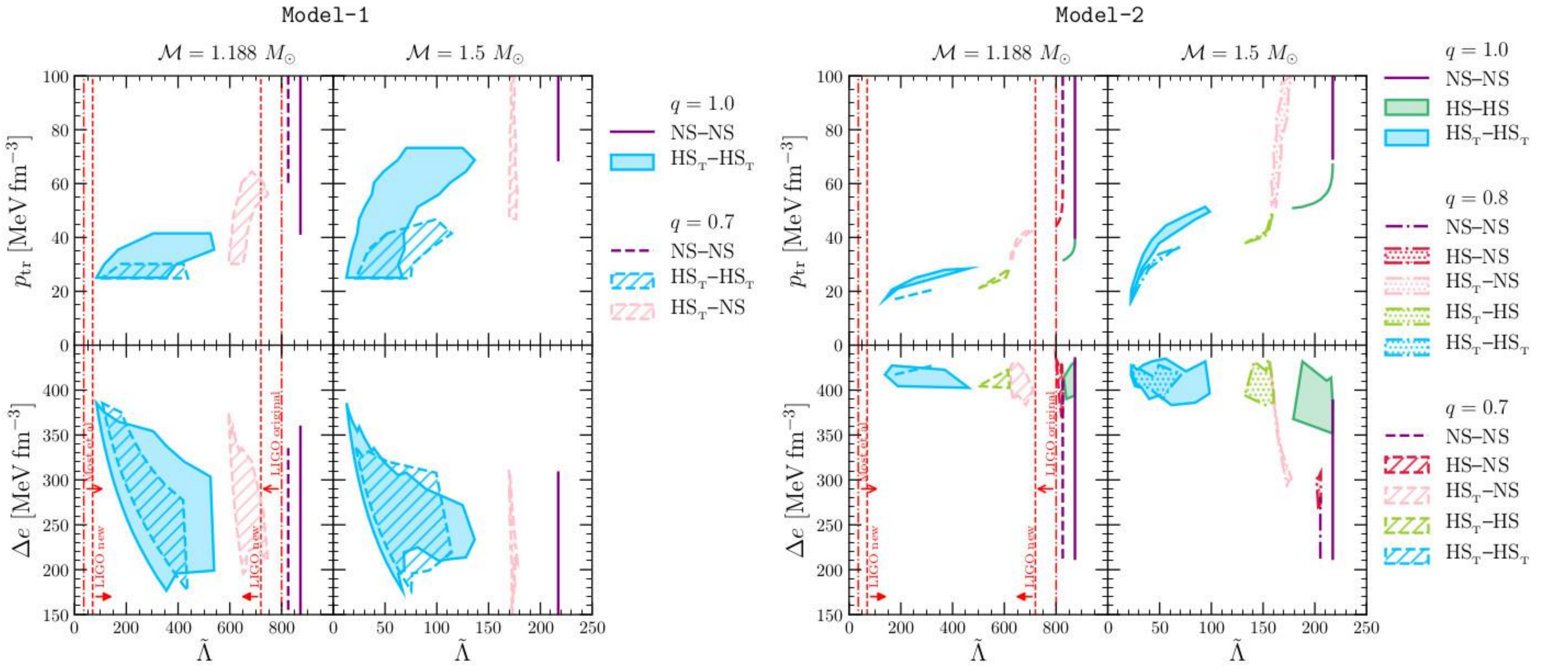

Gravitational Waves from Neutron Star Mergers

Neutron Star Collision (Simulation)

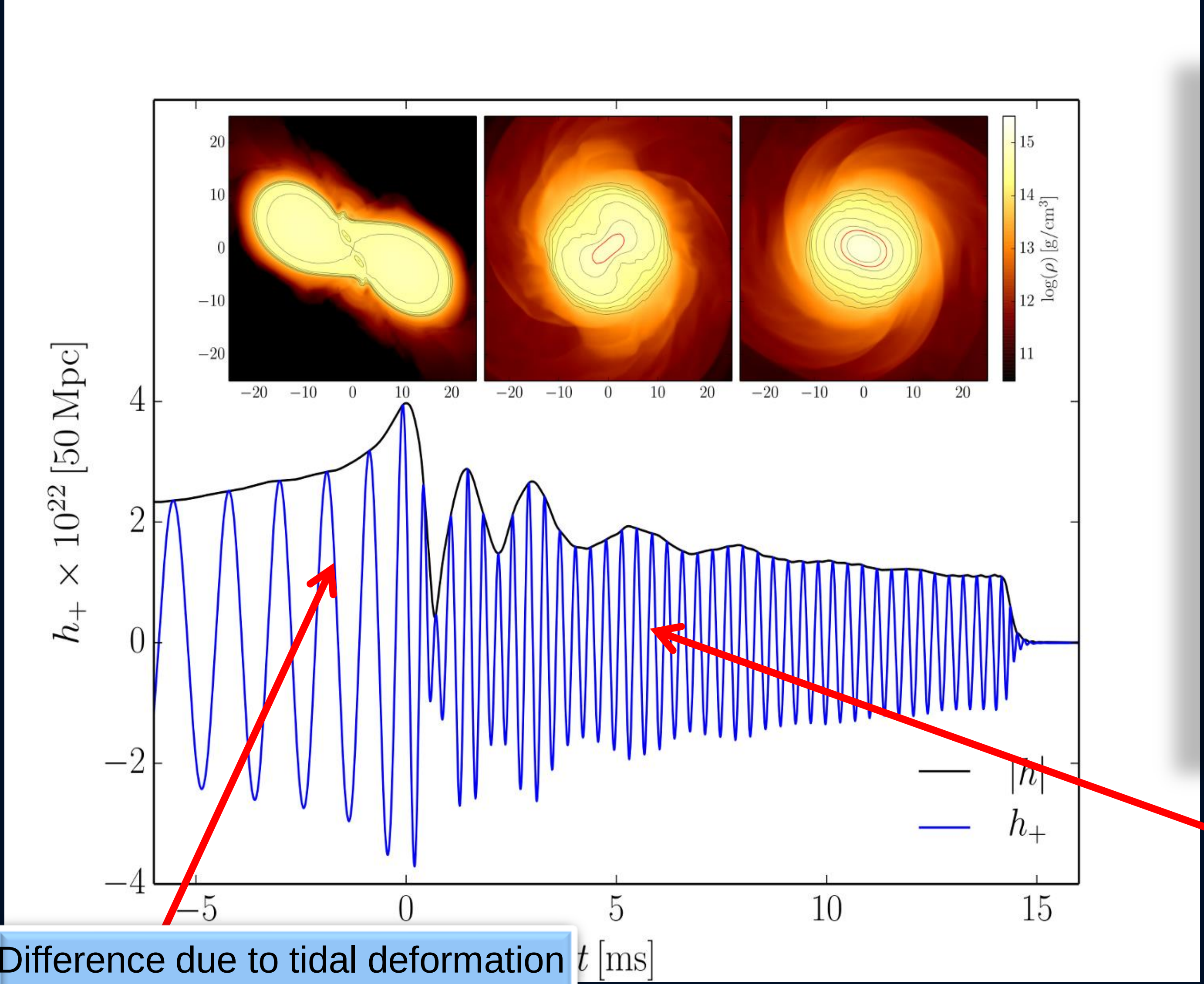

Difference due to tidal deformation in the late inspiral phase

Collision of two Black Holes
GW150914

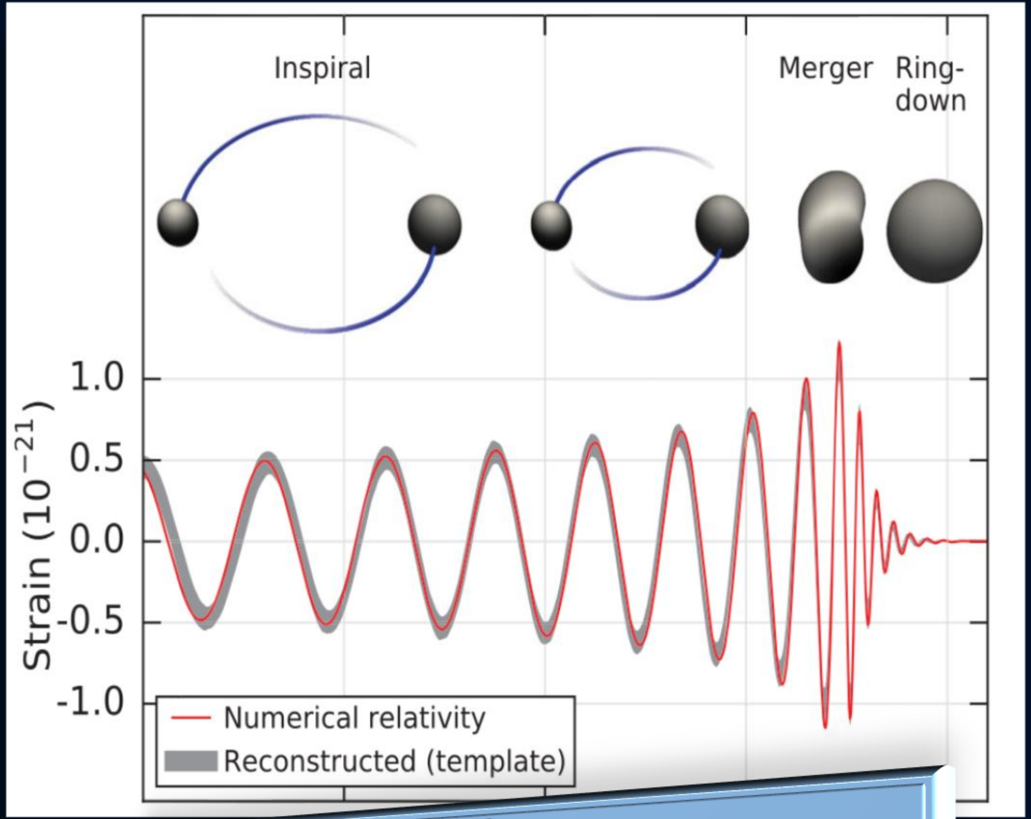

Main difference:

In binary neutron star mergers a **Post-Merger Phase** often exists

Binary Merger of two Neutron Stars for different EoSs

High mass simulations (M=1.35 Msolar)

Central value of the lapse function α_c (upper panel) and maximum of the rest mass density ρ_{max} in units of ρ_0 (lower panel) versus time for the high mass simulations.

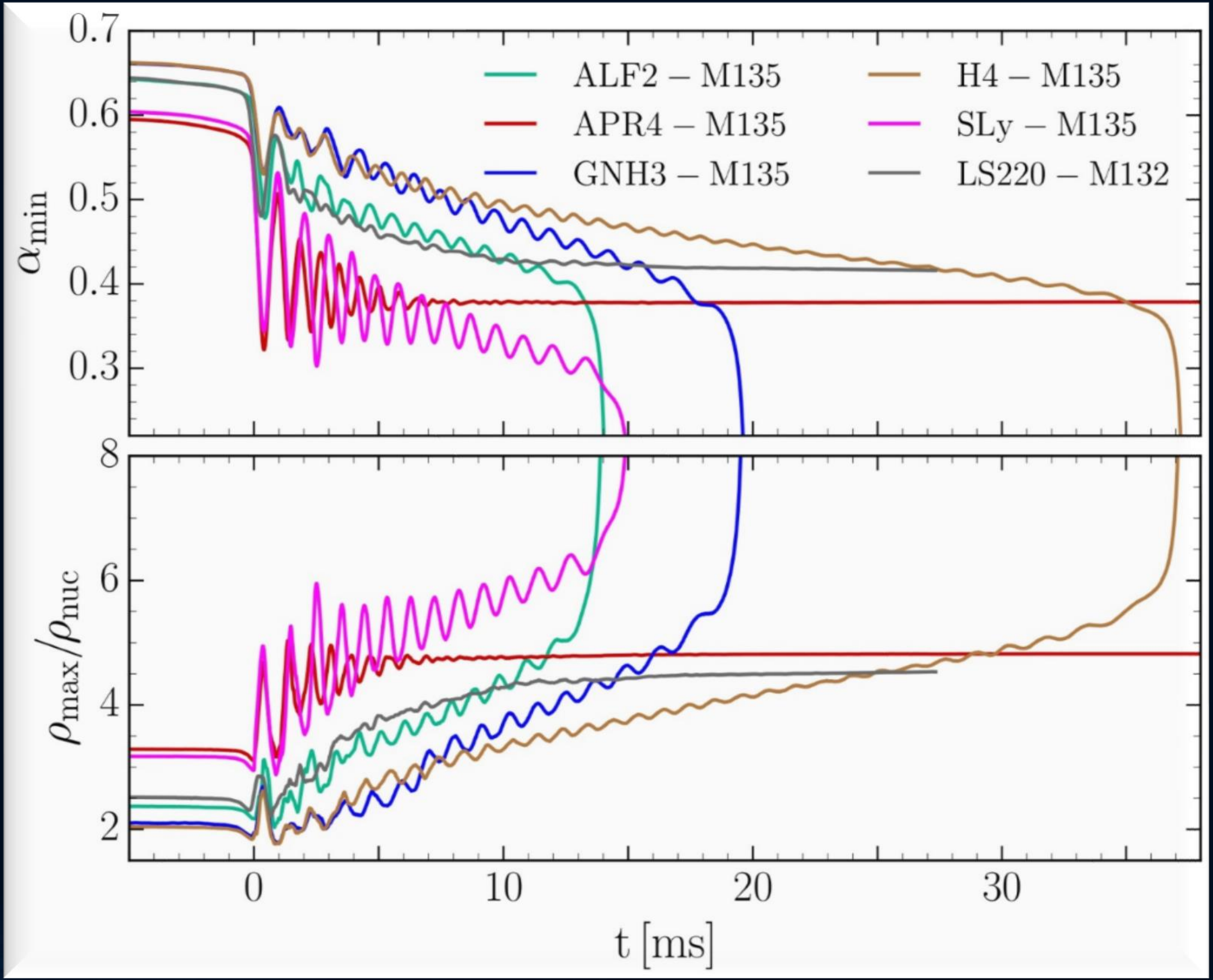

Hanauske, et.al. PRD, 96(4), 043004 (2017)

Evolution of the density in the post merger phase

ALF2-EOS: Mixed phase region starts at $3\rho_0$ (see red curve), initial NS mass: 1.35 M_{solar}

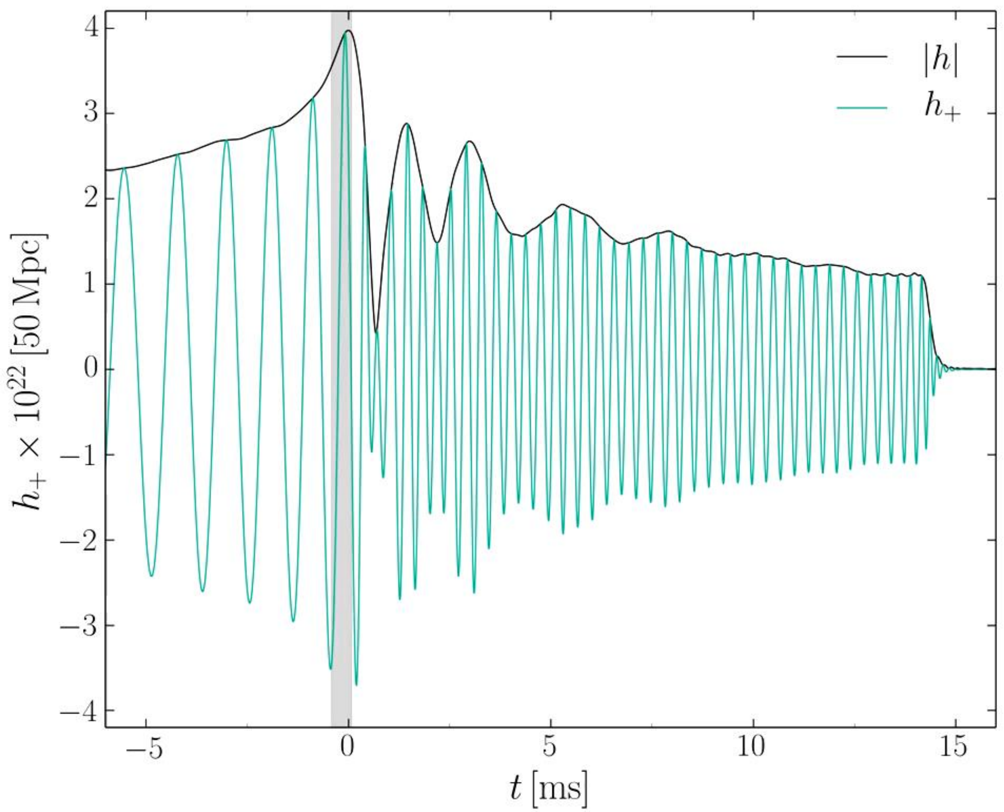

Gravitational wave amplitude
at a distance of 50 Mpc

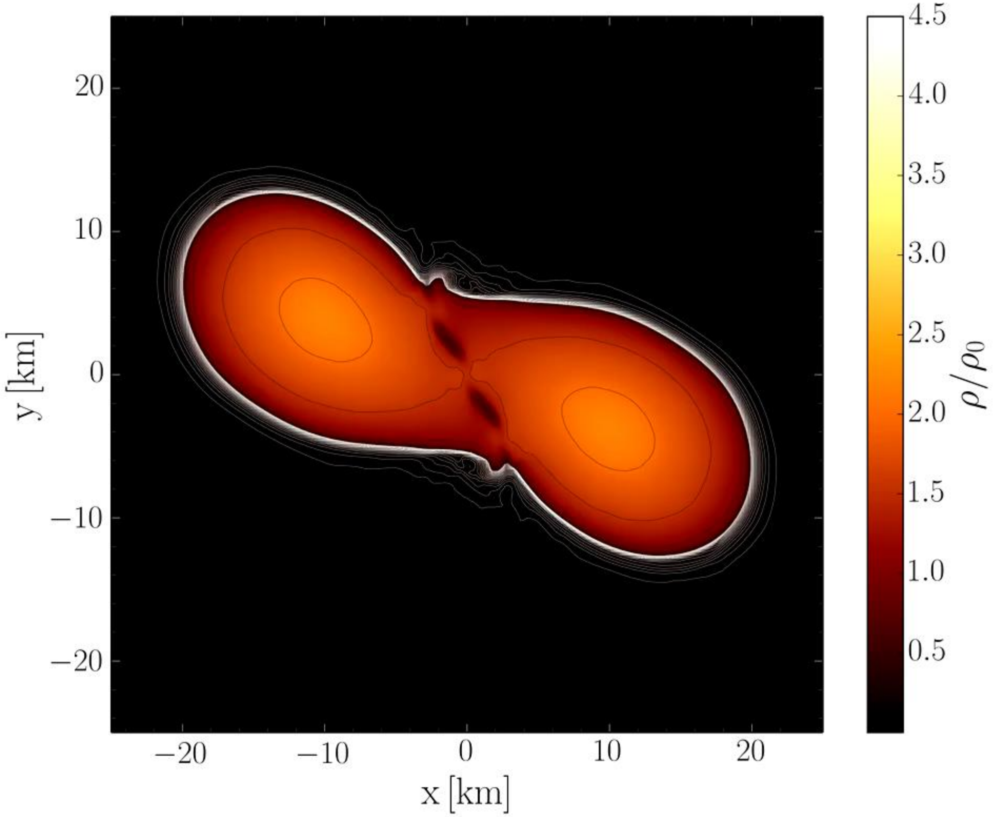

Rest mass density distribution ρ(x,y)
in the equatorial plane
in units of the nuclear matter density ρ_0

Anatomy of the GW signal

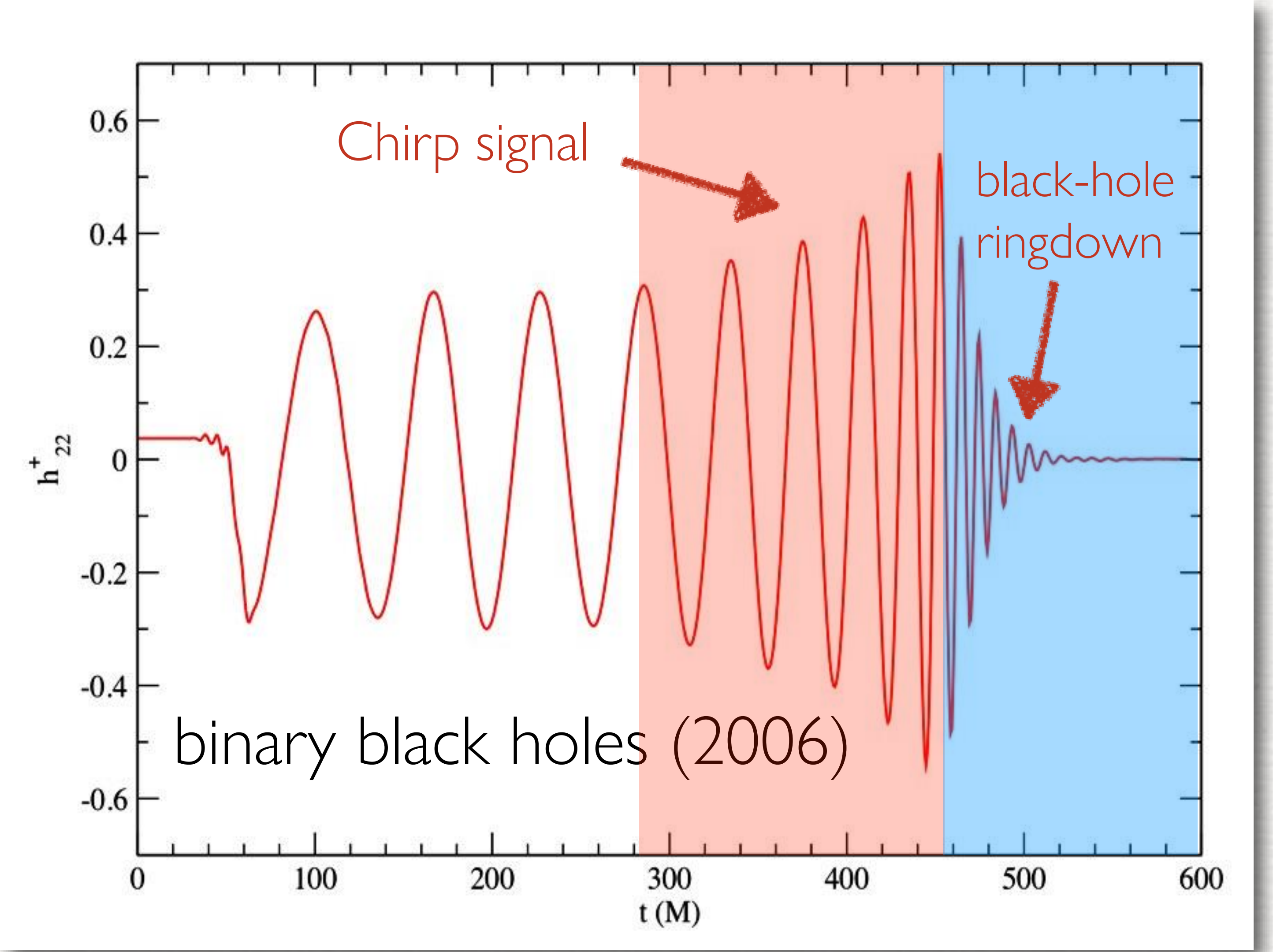

Anatomy of the GW signal

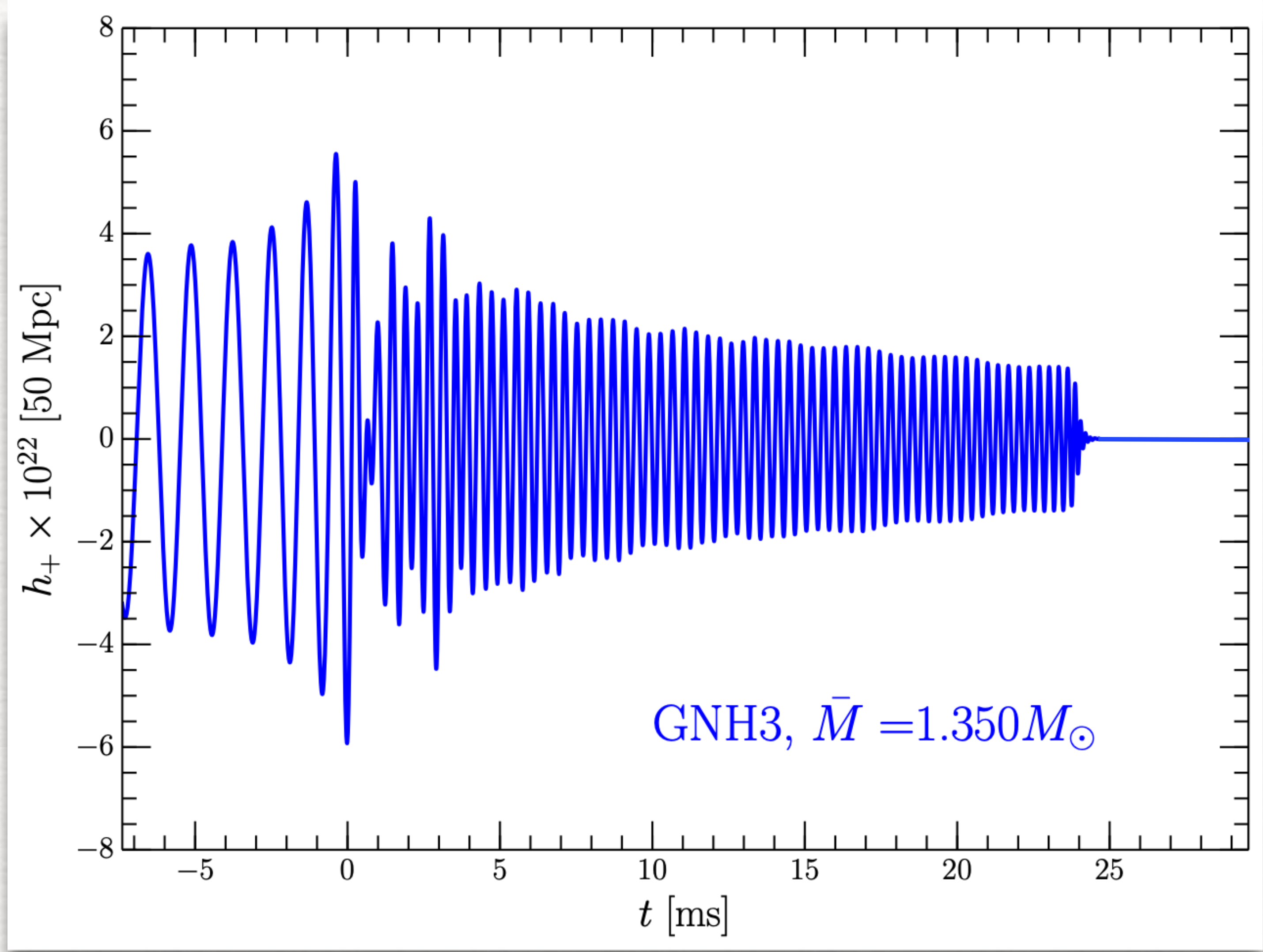

Anatomy of the GW signal

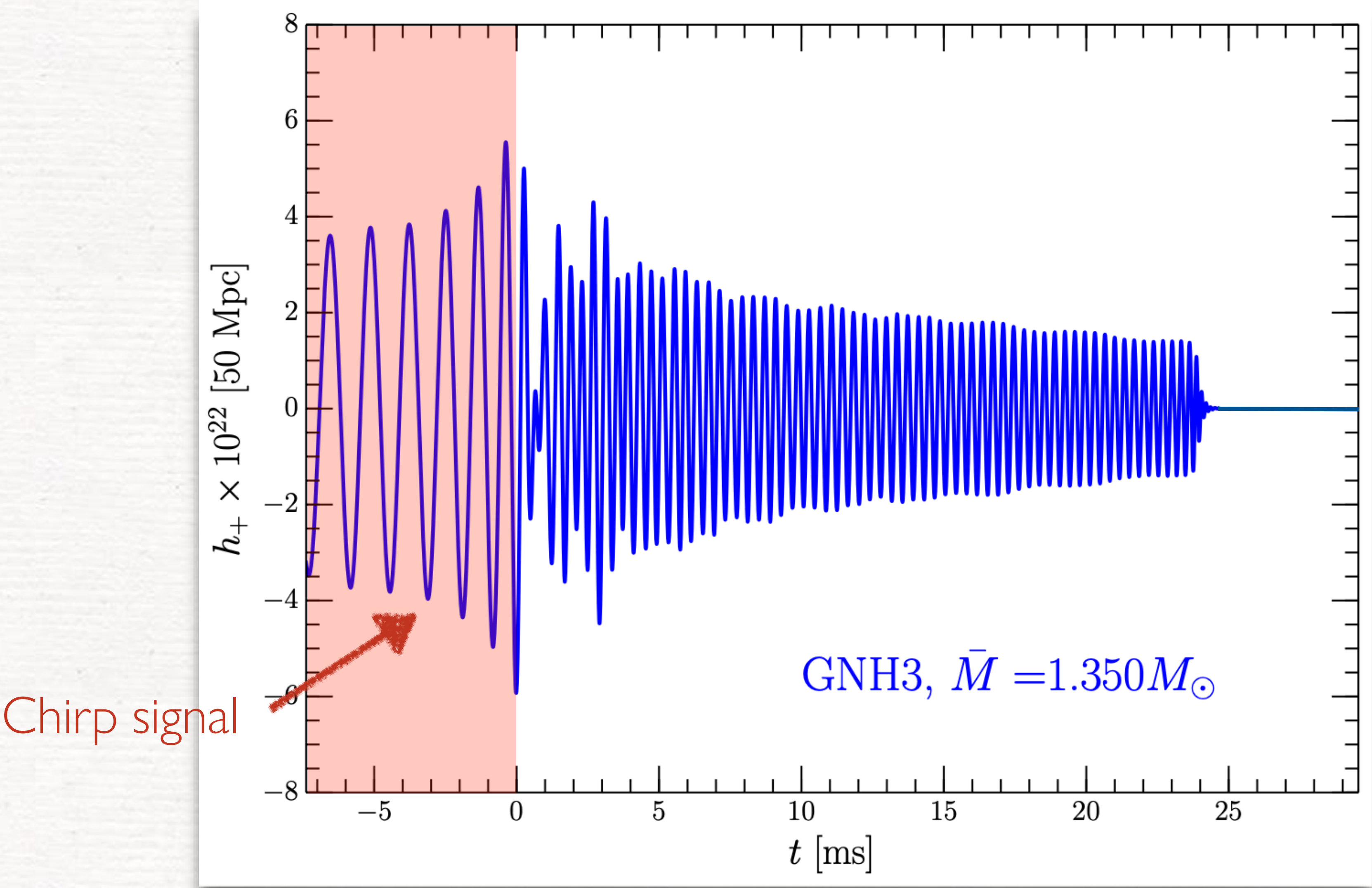

Inspiral: well approximated by PN/EOB; tidal effects important

Anatomy of the GW signal

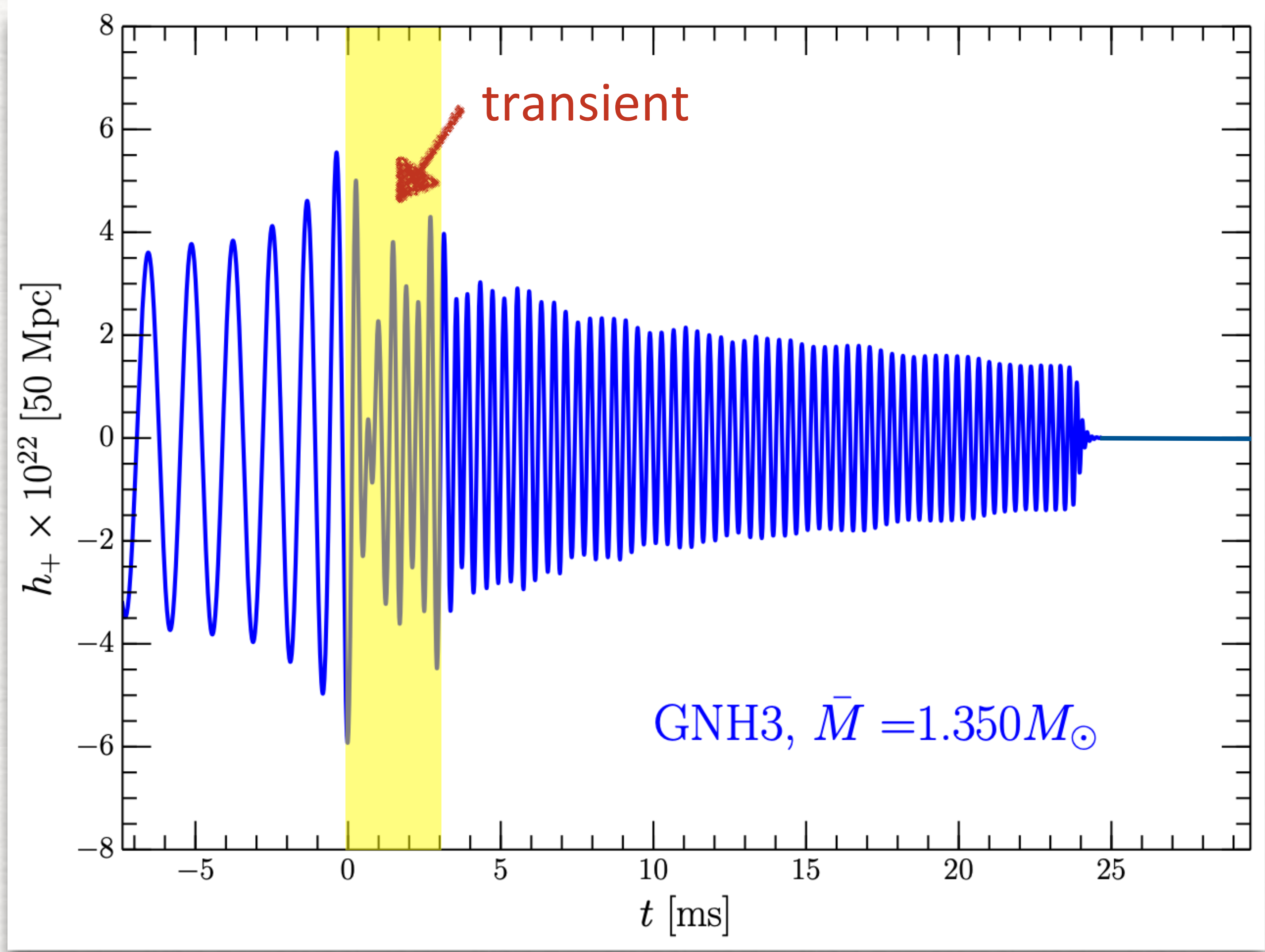

Merger: highly nonlinear but analytic description possible

Anatomy of the GW signal

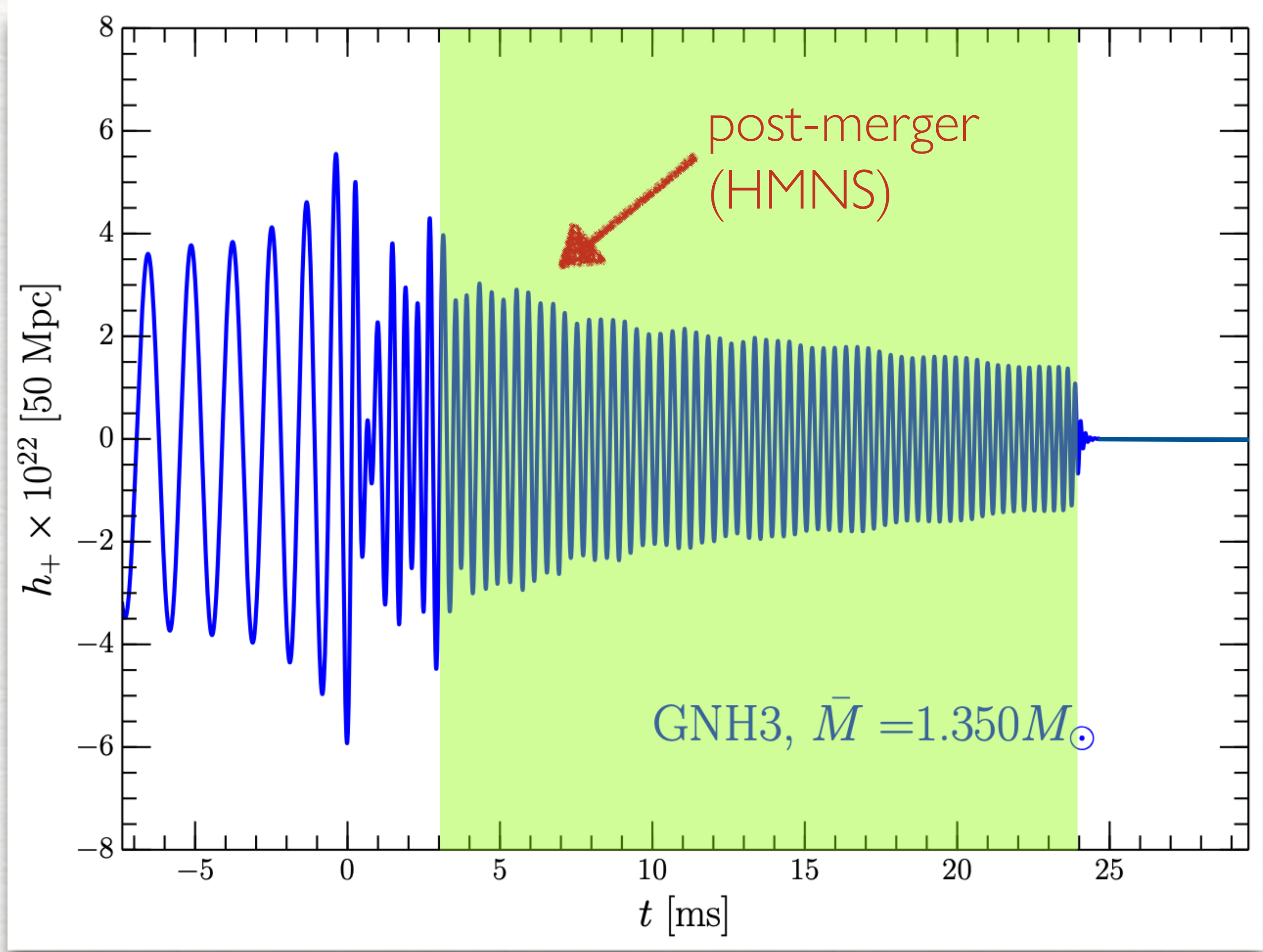

post-merger: quasi-periodic emission of bar-deformed HMNS

Anatomy of the GW signal

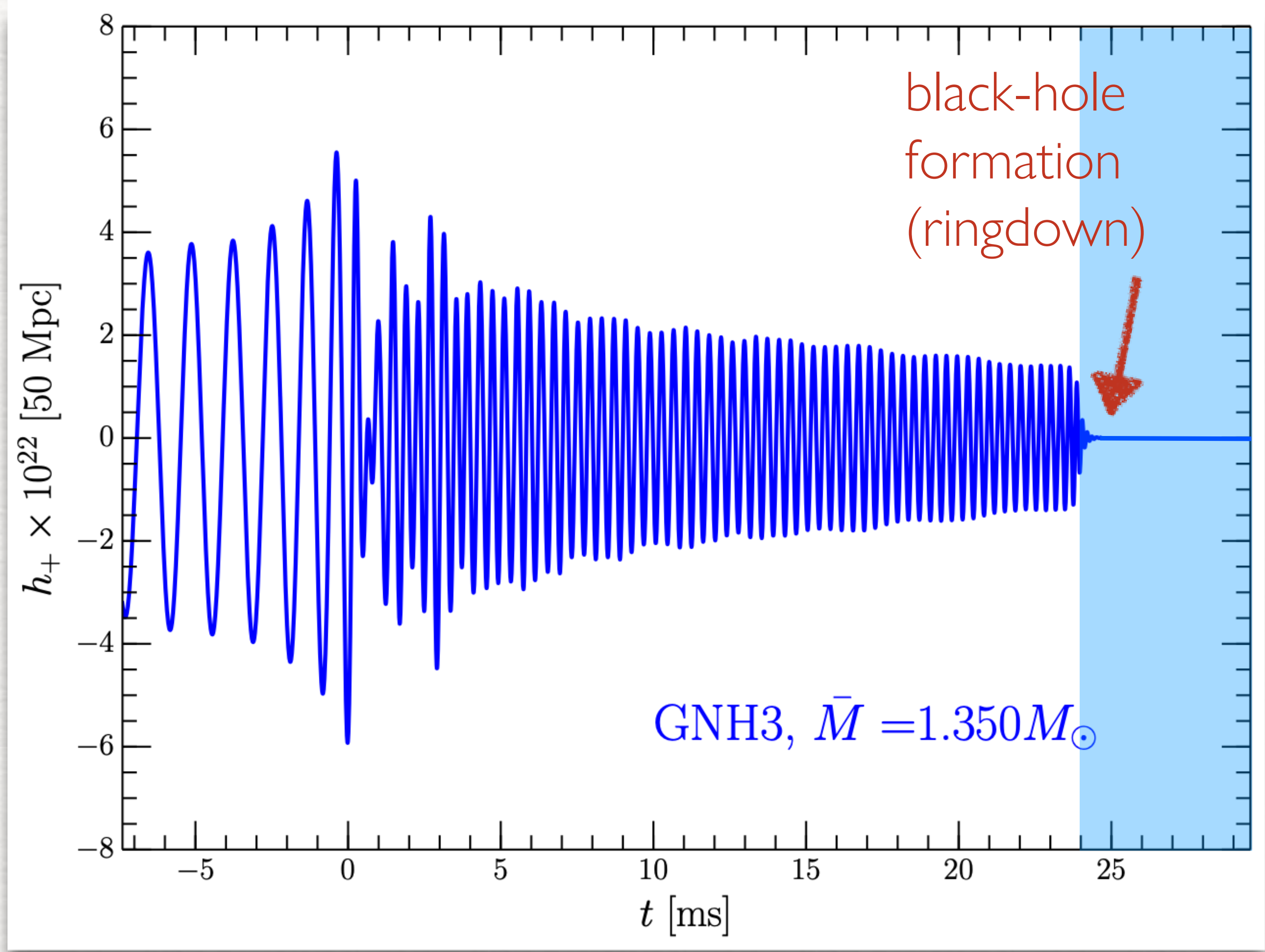

Collapse-ringdown: signal essentially shuts off.

In frequency space

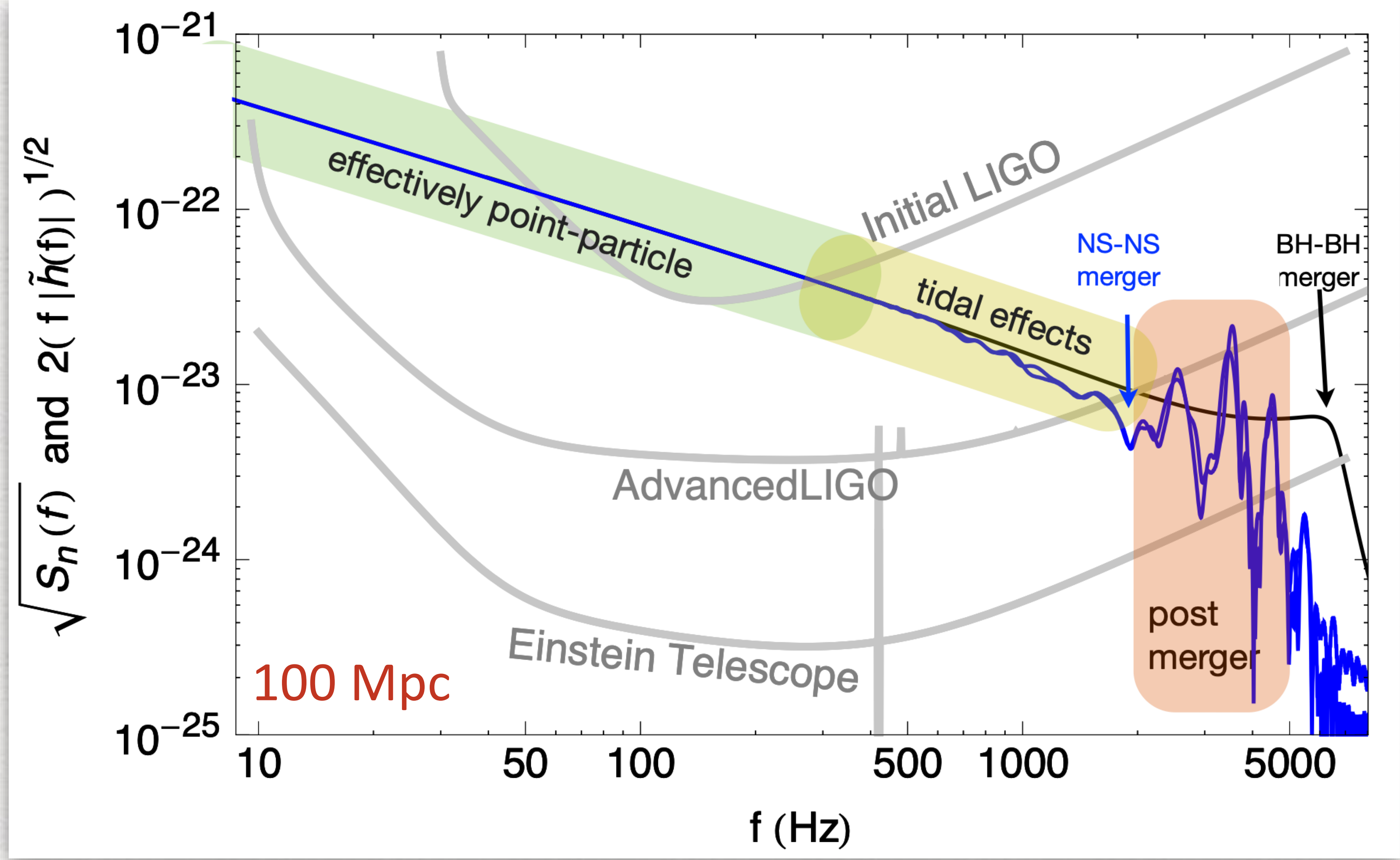

Read et al. (2013)

What we can do nowadays

Takami, LR, Baiotti (2014, 2015), LR+ (2016)

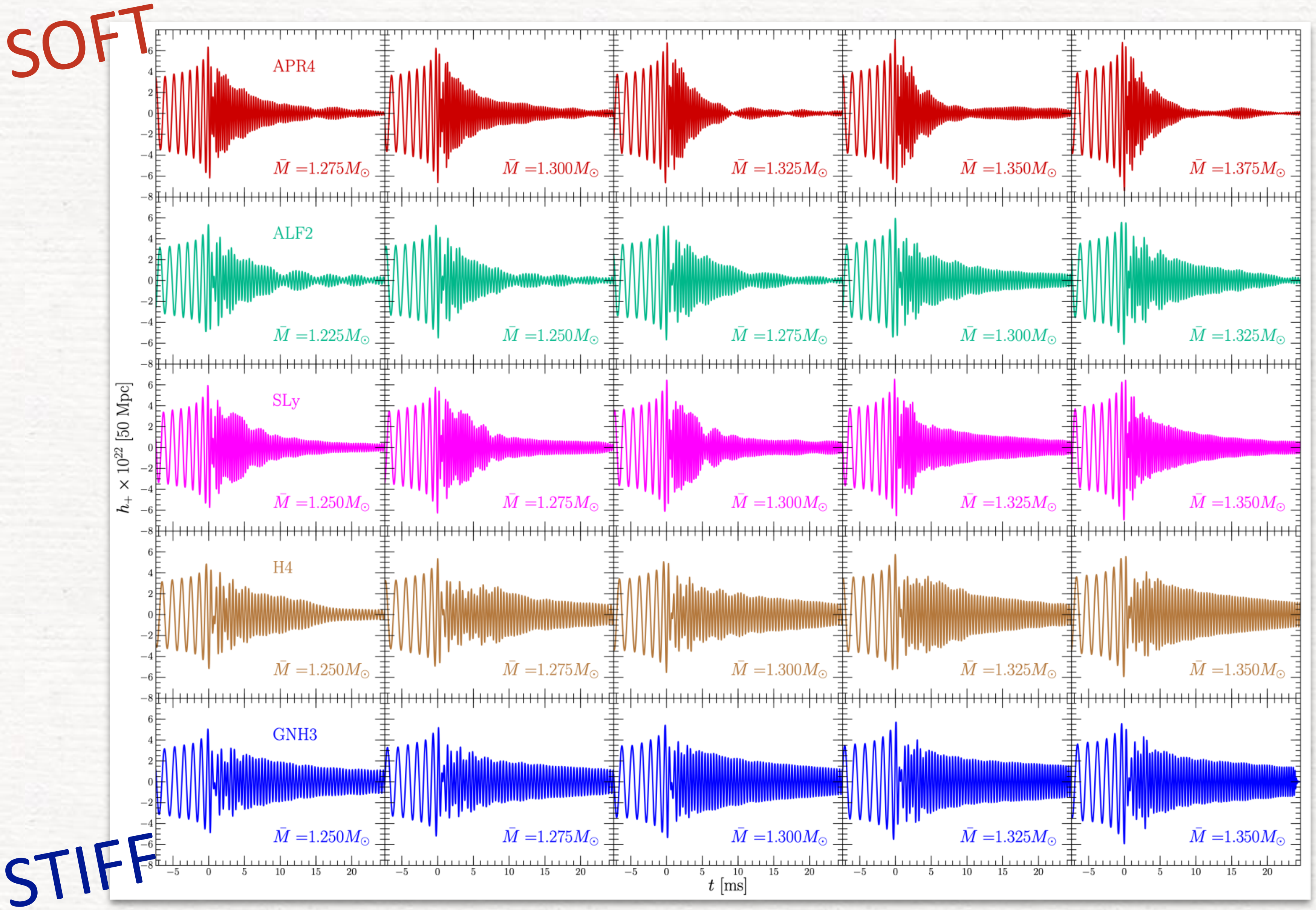

Time Evolution of the GW-Spectrum

The power spectral density profile of the post-merger emission is characterized by several distinct frequencies. After approximately 5 ms after merger, the only remaining dominant frequency is the f_2-frequency (See e.g. L.Rezzolla and K.Takami, PRD, 93(12), 124051 (2016))

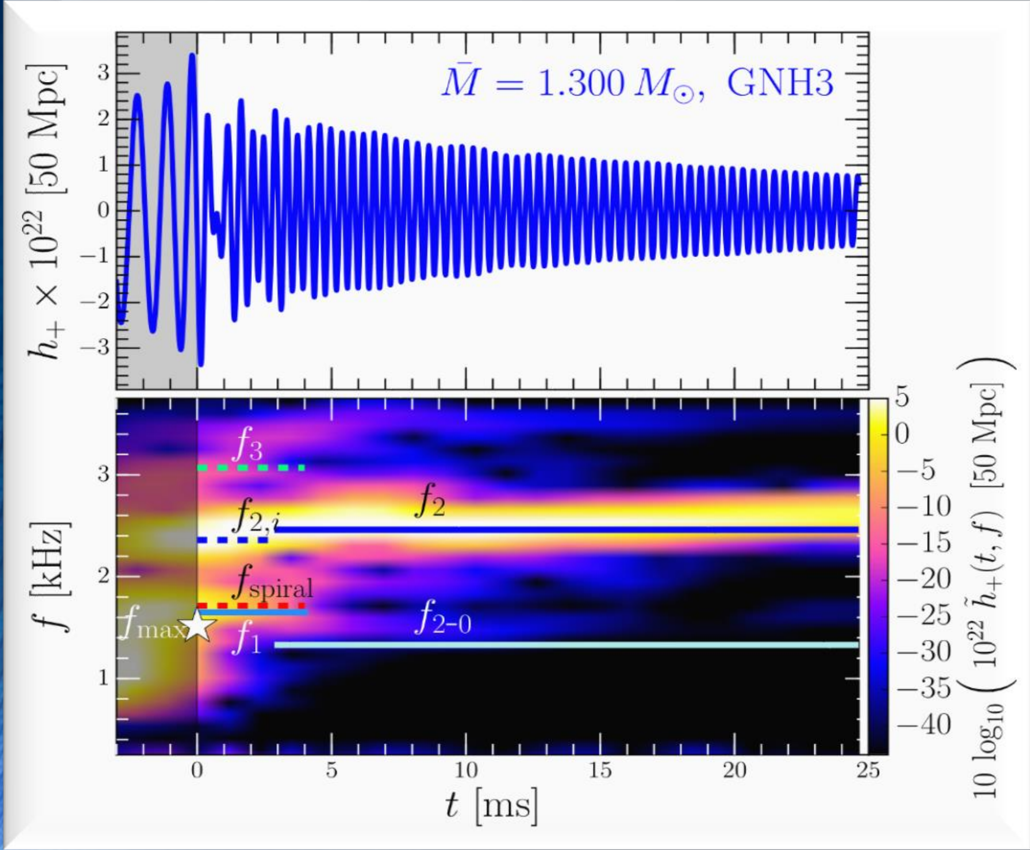

Stiff EOS

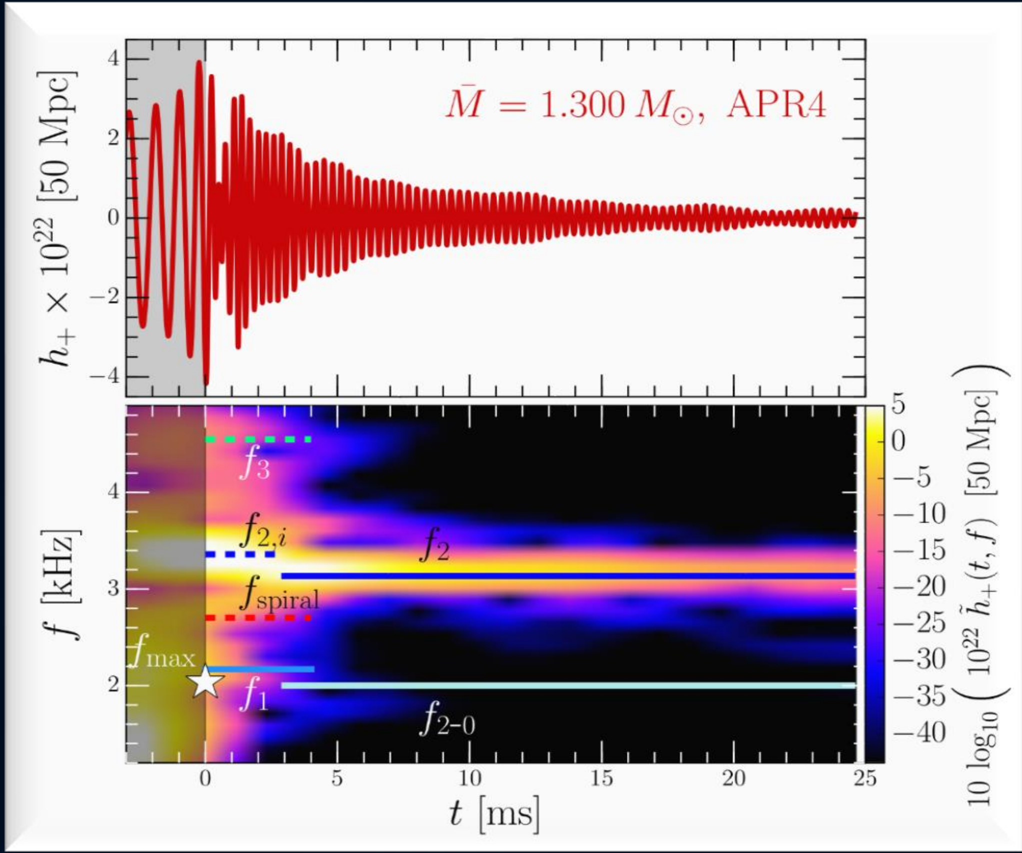

Soft EOS

Unfortunately, due to the low sensitivity at high gravitational wave frequencies, no post-merger signal has been found in GW170817.

But advanced detectors / next-generation detectors might be able to detect!!?

Evolution of the frequency spectrum of the emitted gravitational waves for the stiff GNH3 (left) and soft APR4 (right) EOS.

Extracting information from the EOS

Takami, LR, Baiotti (2014, 2015), LR+ (2016)

SOFT

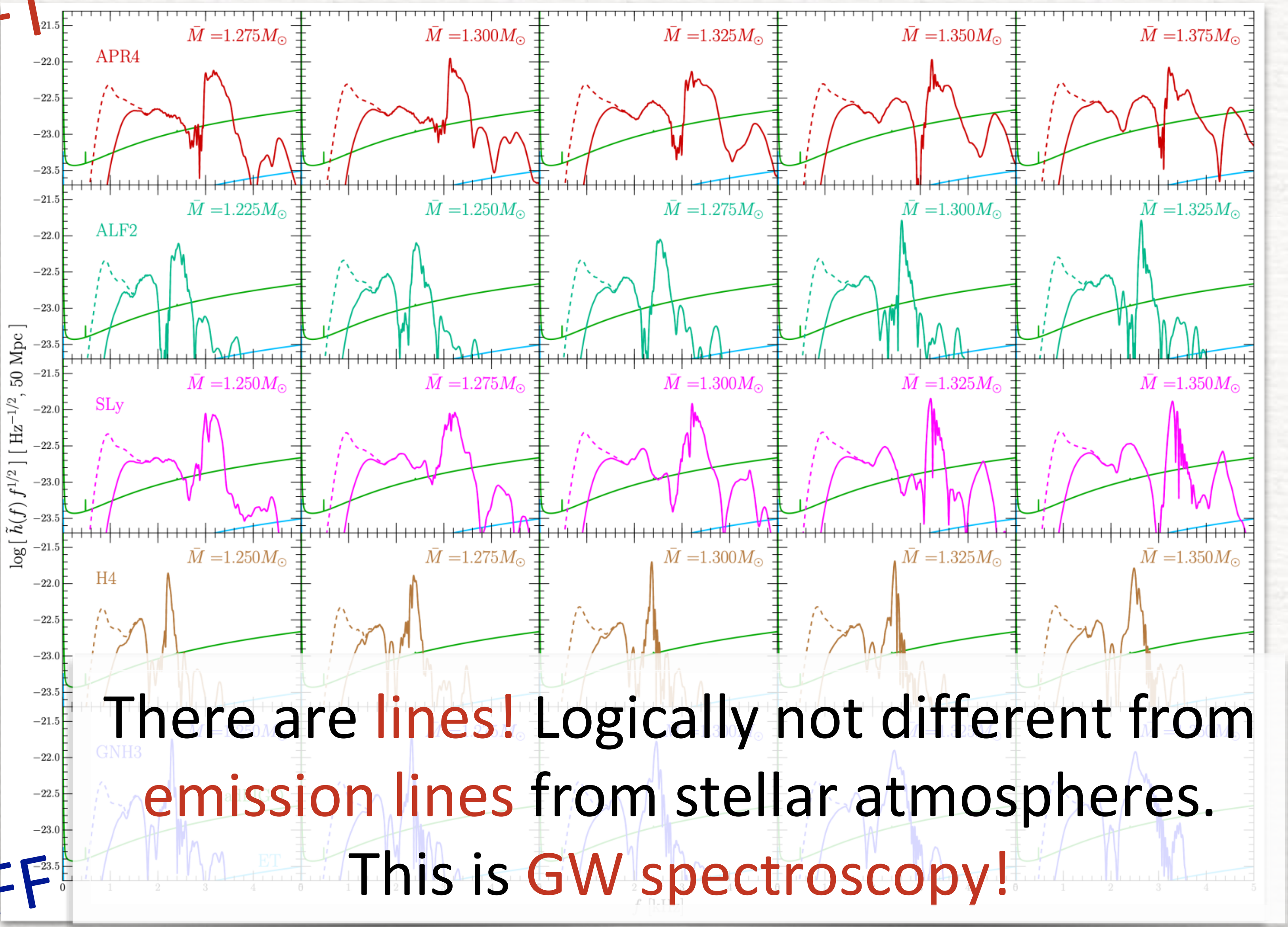

STIFF

There are lines! Logically not different from emission lines from stellar atmospheres.

This is GW spectroscopy!

A new approach to constrain the EOS

Oechslin+2007, Baiotti+2008, Bauswein+ 2011, 2012, Stergioulas+ 2011, Hotokezaka+ 2013, Takami 2014, 2015, Bernuzzi 2014, 2015, Bauswein+ 2015, Clark+ 2016, LR+2016, de Pietri+ 2016, Feo+ 2017, Bose+ 2017 …

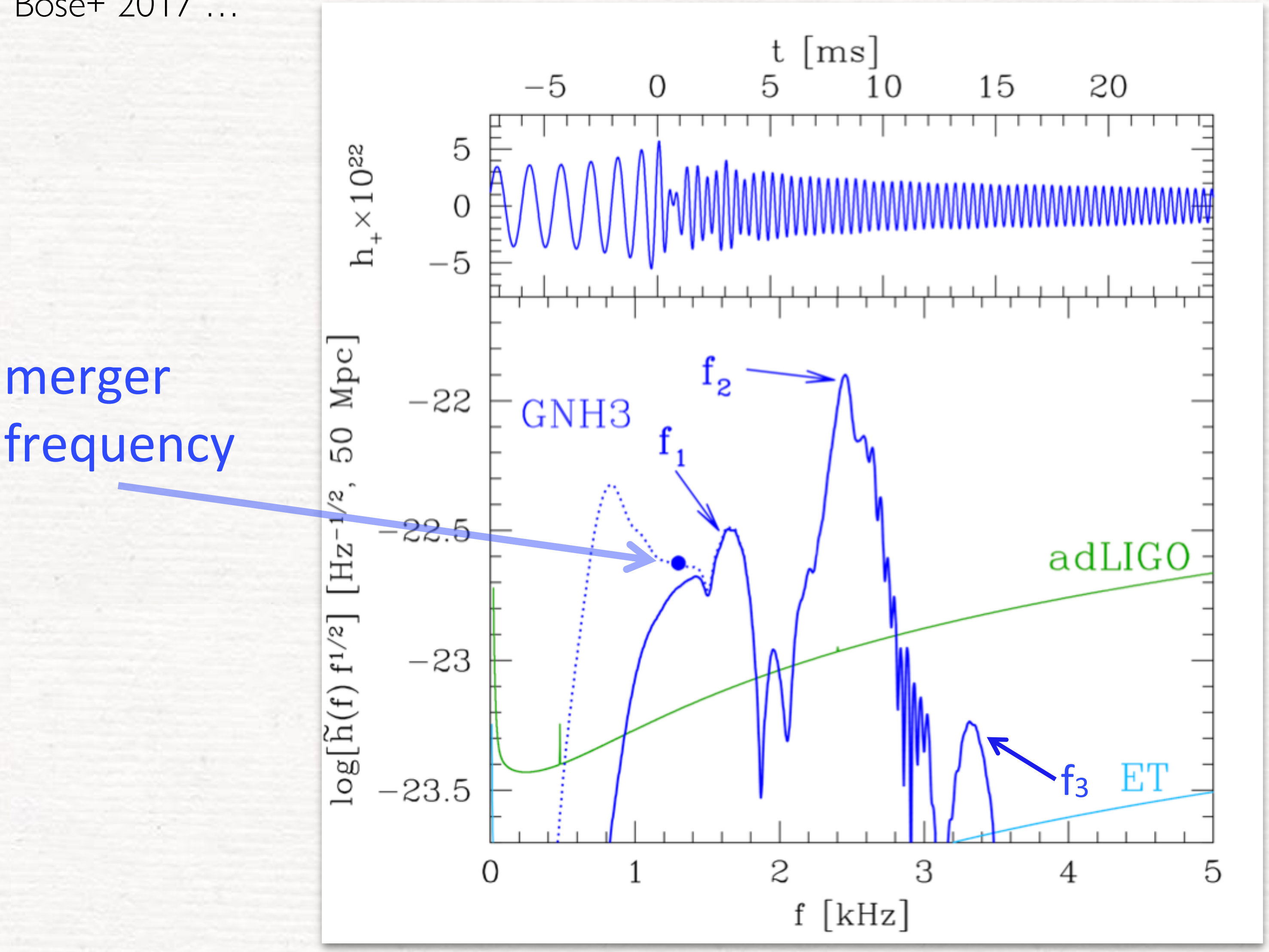

A spectroscopic approach to the EOS

Oechslin+2007, Baiotti+2008, Bauswein+ 2011, 2012, Stergioulas+ 2011, Hotokezaka+ 2013, Takami 2014, 2015, Bernuzzi 2014, 2015, Bauswein+ 2015, Clark+ 2016, LR+2016, de Pietri+ 2016, Feo+ 2017, Bose+ 2017 …

merger frequency

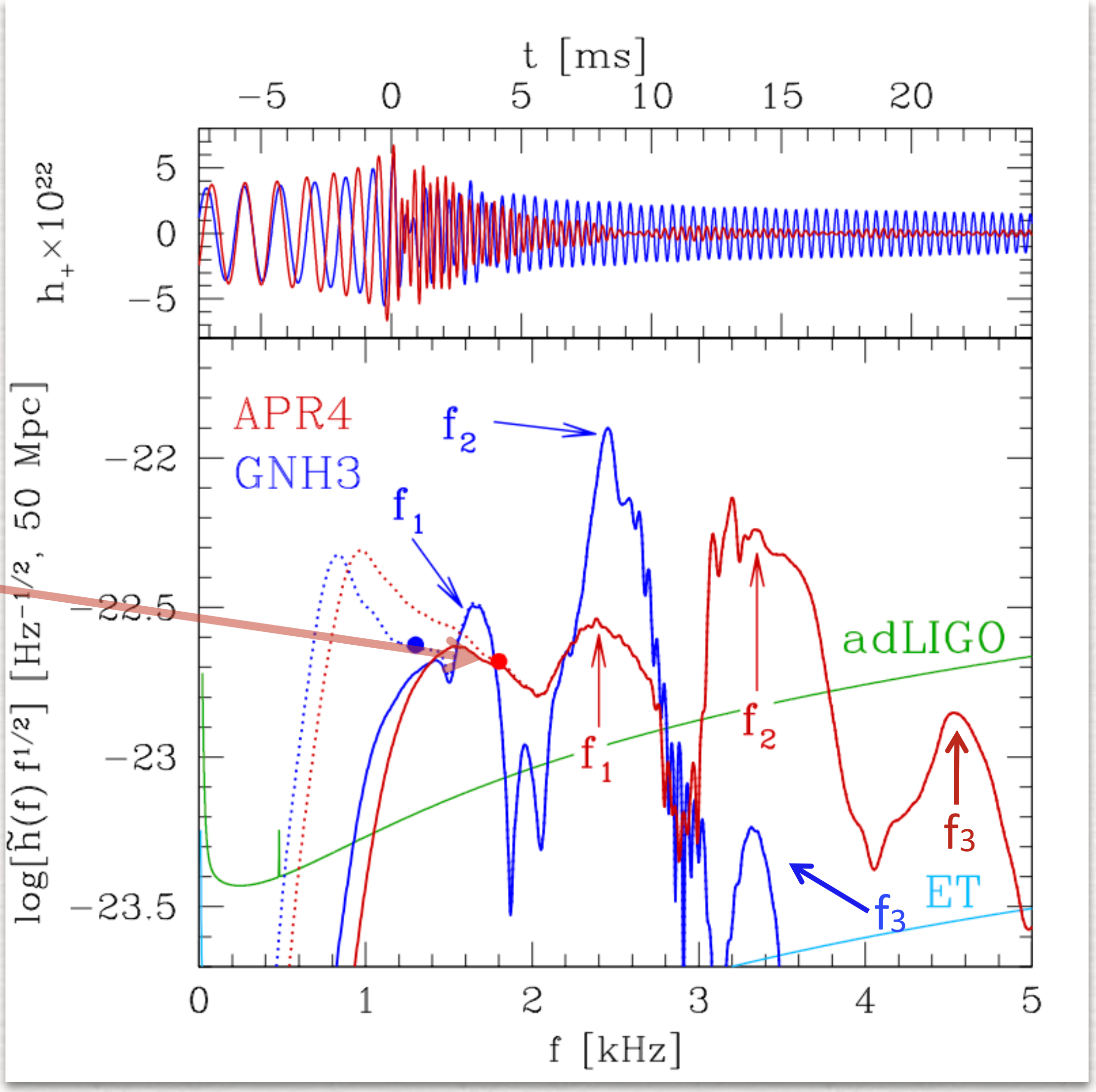

Quasi-universal behaviour: **inspiral**

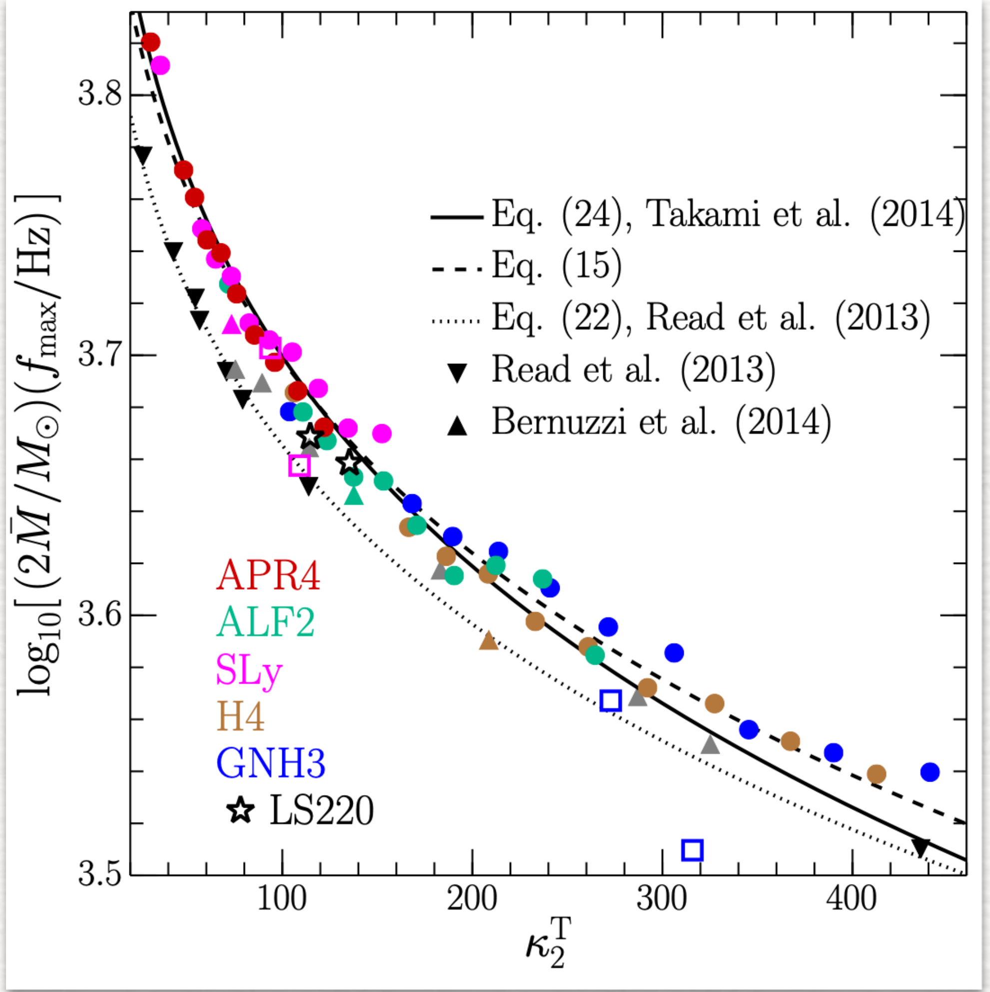

"surprising" result: quasi-universal behaviour of GW frequency at amplitude peak (Read+2013)

Many other simulations have confirmed this (Bernuzzi+ 2014, Takami+ 2015, LR+2016) .

Quasi-universal behaviour in the **inspiral** implies that once f_{max} is measured, so is tidal deformability, hence $I, \ Q, \ M/R$

$$\Lambda = \frac{\lambda}{\bar{M}^5} = \frac{16}{3}\kappa_2^T$$ tidal deformability or Love number

Quasi-universal behaviour: **post-merger**

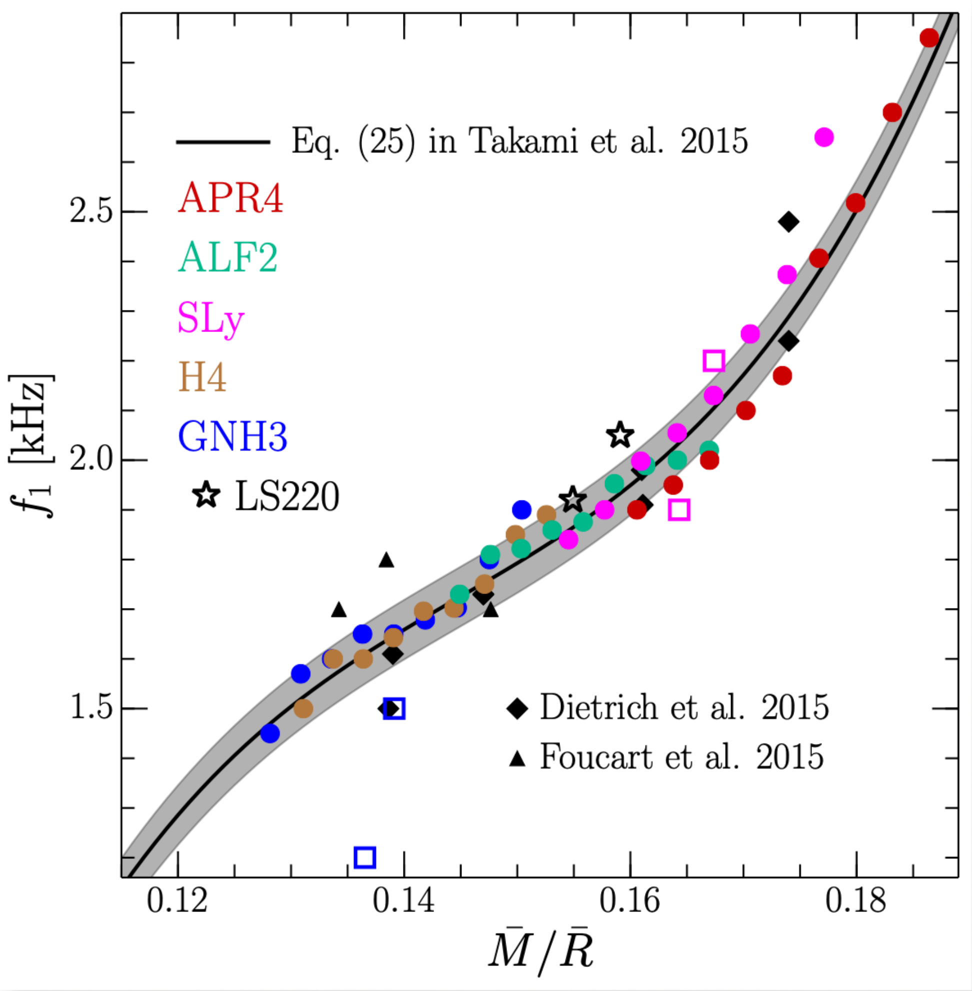

We have found **quasi-universal behaviour:** i.e., the properties of the spectra are only weakly dependent on the EOS.

This has profound implications for the analytical modelling of the GW emission: "what we do for one EOS can be extended to all EOSs."

Quasi-universal behaviour: **post-merger**

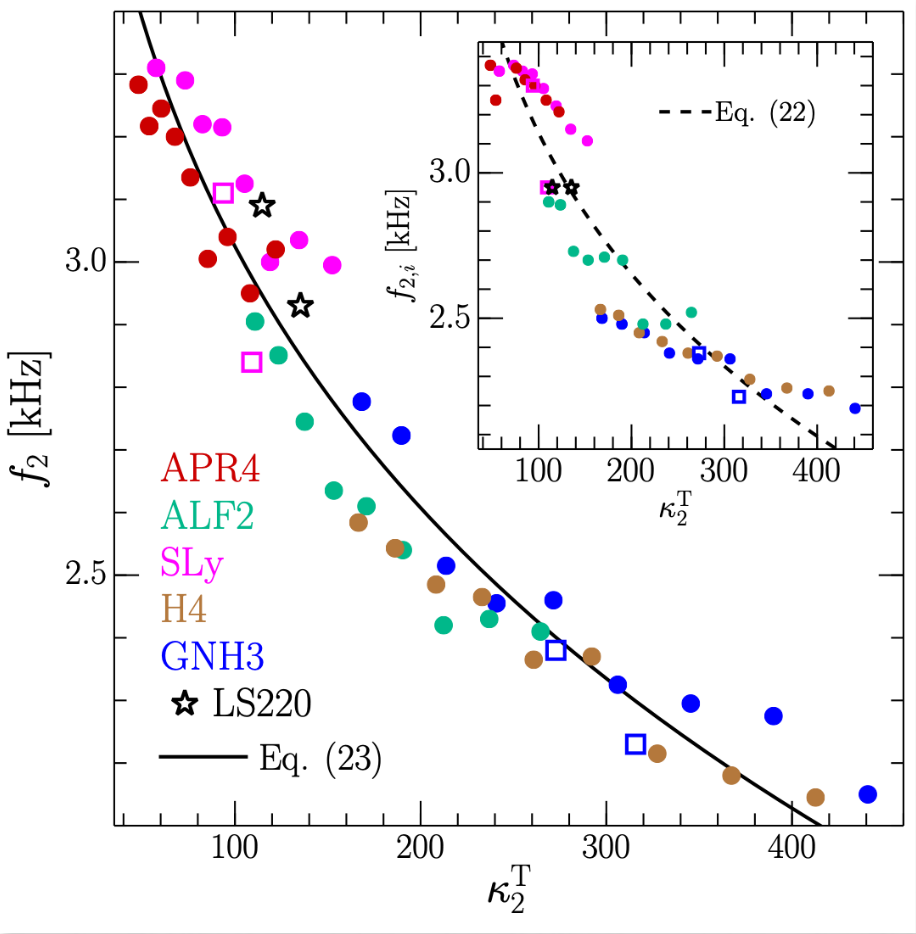

- Correlations with Love number found also for high frequency peak f_2.
- This and other correlations are **weaker** but equally useful.

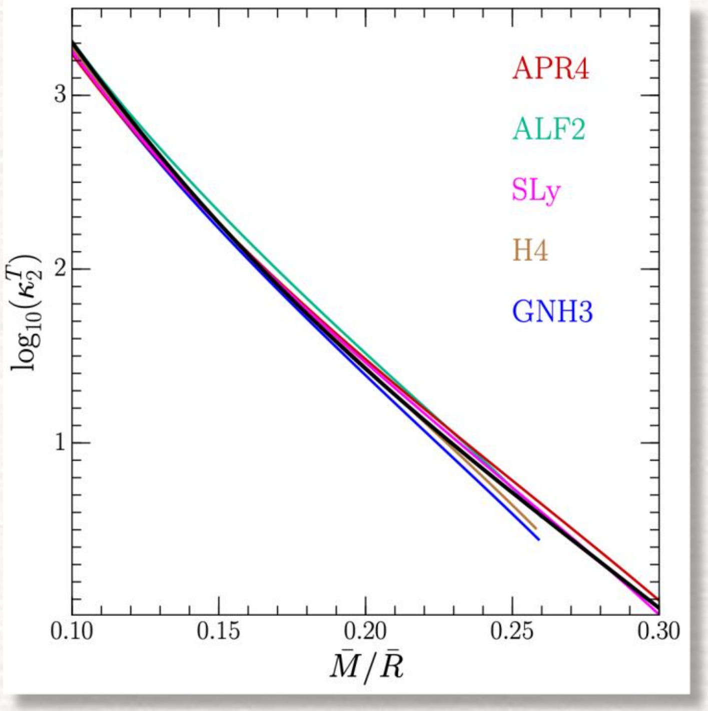

- Important correlation also between **compactness** and **deformability**

GW170817, maximum mass, radii and tidal deformabilities

LR, Most, Weih (2018)

Most, Weih, LR, Schaffner-Bielich (2018)

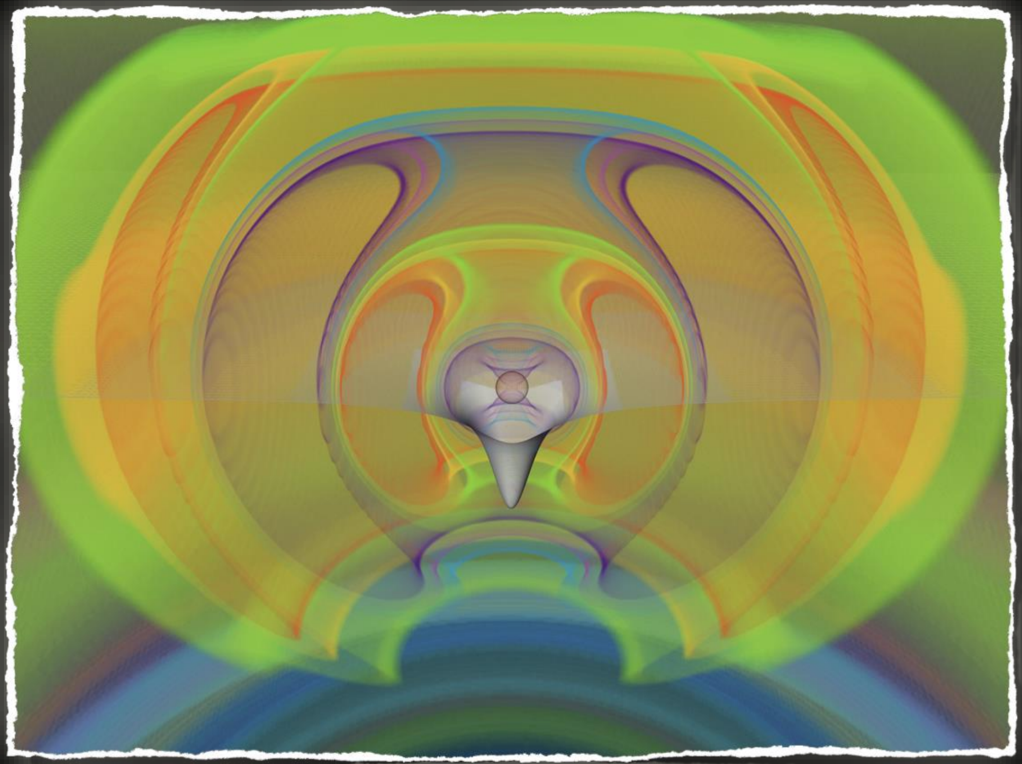

The outcome of GW170817

- The remnant of GW170817 was a hypermassive star, i.e. a differentially rotating object with initial **gravitational** mass $M_1 + M_2 = 2.74^{+0.04}_{-0.01} M_\odot$

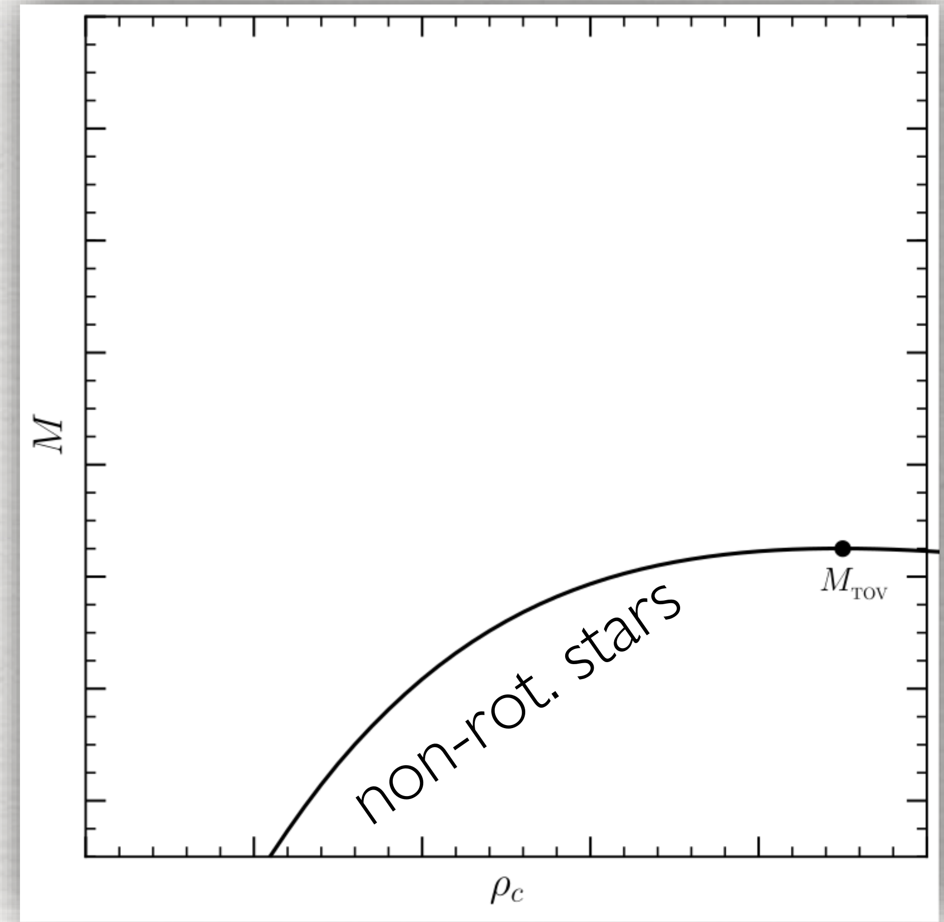

- Sequences of equilibrium models of **nonrotating** stars will have a maximum mass: $M_{\rm TOV}$

The outcome of GW170817

- The remnant of GW170817 was a hypermassive star, i.e. a differentially rotating object with initial **gravitational** mass $M_1 + M_2 = 2.74^{+0.04}_{-0.01} M_\odot$

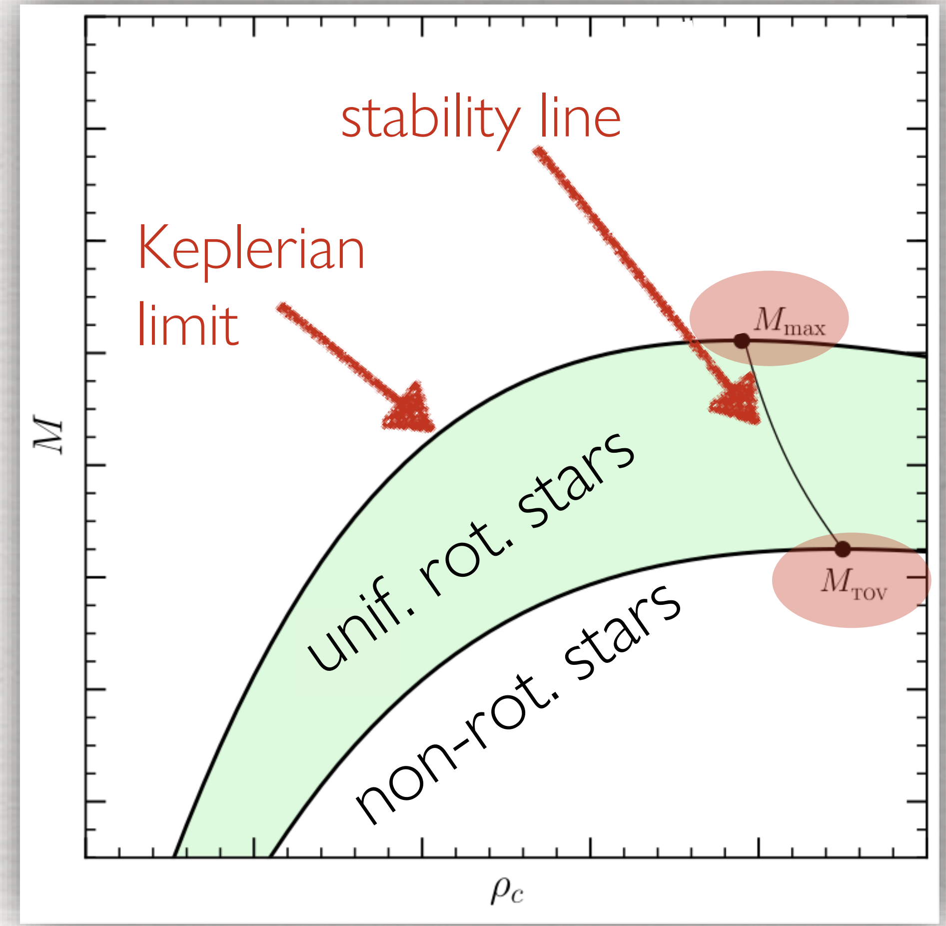

- Sequences of equilibrium models of **nonrotating** stars will have a maximum mass: $M_{\rm TOV}$
- This is true also for **uniformly** rotating stars at mass shedding limit: $M_{\max}$
- $M_{\max}$ simple and **quasi-universal** function of $M_{\rm TOV}$ (Breu & LR 2016)

$$M_{\max} = \left(1.20^{+0.02}_{-0.05}\right) M_{\rm TOV}$$

The outcome of GW170817

- The remnant of GW170817 was a hypermassive star, i.e. a differentially rotating object with initial **gravitational** mass
$$M_1 + M_2 = 2.74^{+0.04}_{-0.01} M_\odot$$

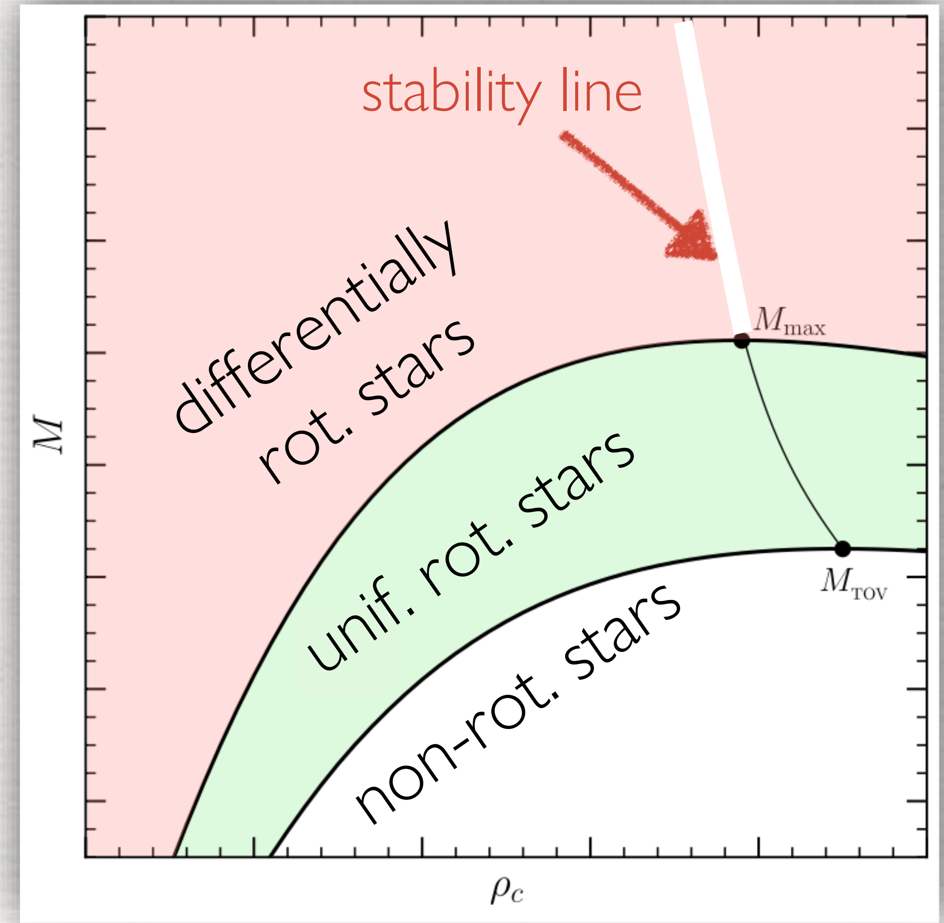

- Green region is for **uniformly** rotating equilibrium models.
- Salmon region is for **differentially** rotating equilibrium models.
- Stability line is simply extended (Weih+18)

The outcome of GW170817

- GW170817 produced object as **"x"**; GRB implies a BH has been formed: **"x"** followed two possible tracks: **fast (2)** and **slow (1)**

- It rapidly produced a BH when still **differentially** rotating (2)
- It lost differential rotation leading to a **uniformly** rotating core (1).
- (1) is much more likely because of large ejected mass (long lived).
- Final mass is near $M_{\mathbf{max}}$ and we know this is universal!

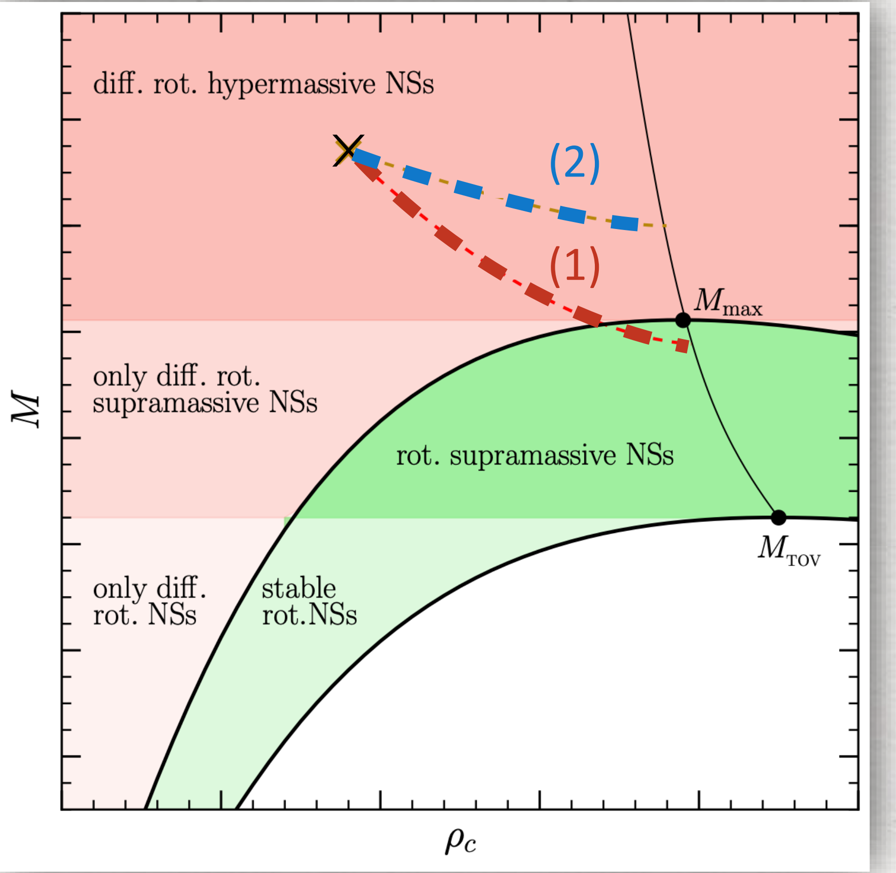

let's recap…

- The merger product of GW170817 was initially **differentially** rotating but collapsed as **uniformly** rotating object.

- Use measured **gravitational** mass of GW170817
- Remove **rest mass** deduced from kilonova emission

- Use **universal relations** and account errors to obtain

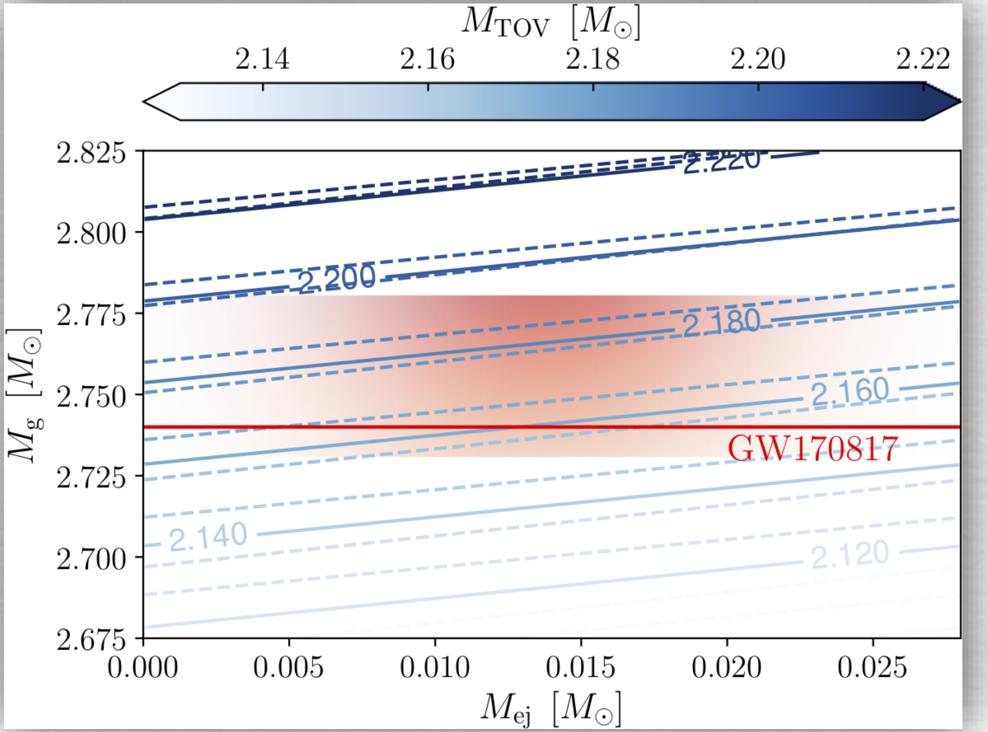

pulsar timing

$$2.01^{+0.04}_{-0.04} \leq M_{\rm TOV}/M_\odot \lesssim 2.16^{+0.17}_{-0.15}$$

universal relations and GW170817; similar estimates

Merging Neutron Stars

- Lecture I: The math of neutron-star mergers
  - Introduction
  - A brief review of General Relativity
  - Numerical relativity of neutron-star mergers
    - The 3+1 decomposition of spacetime
    - ADM equations
    - BSSNOK/ccZ4 formulation
    - Initial data, gauge conditions, excising parts of spacetime and gravitational wave extraction
- Lecture II: The physics/astrophysics of neutron-star mergers
  - Introduction
  - GW170817 - the long-awaited event
  - Determining neutron-star properties and the equation of state using gravitational wave data
  - **Hypermassive neutron stars and the post-merger gravitational wave emission**
  - Detecting the hadron-quark phase transition with gravitational waves

The QCD Phae Diagram

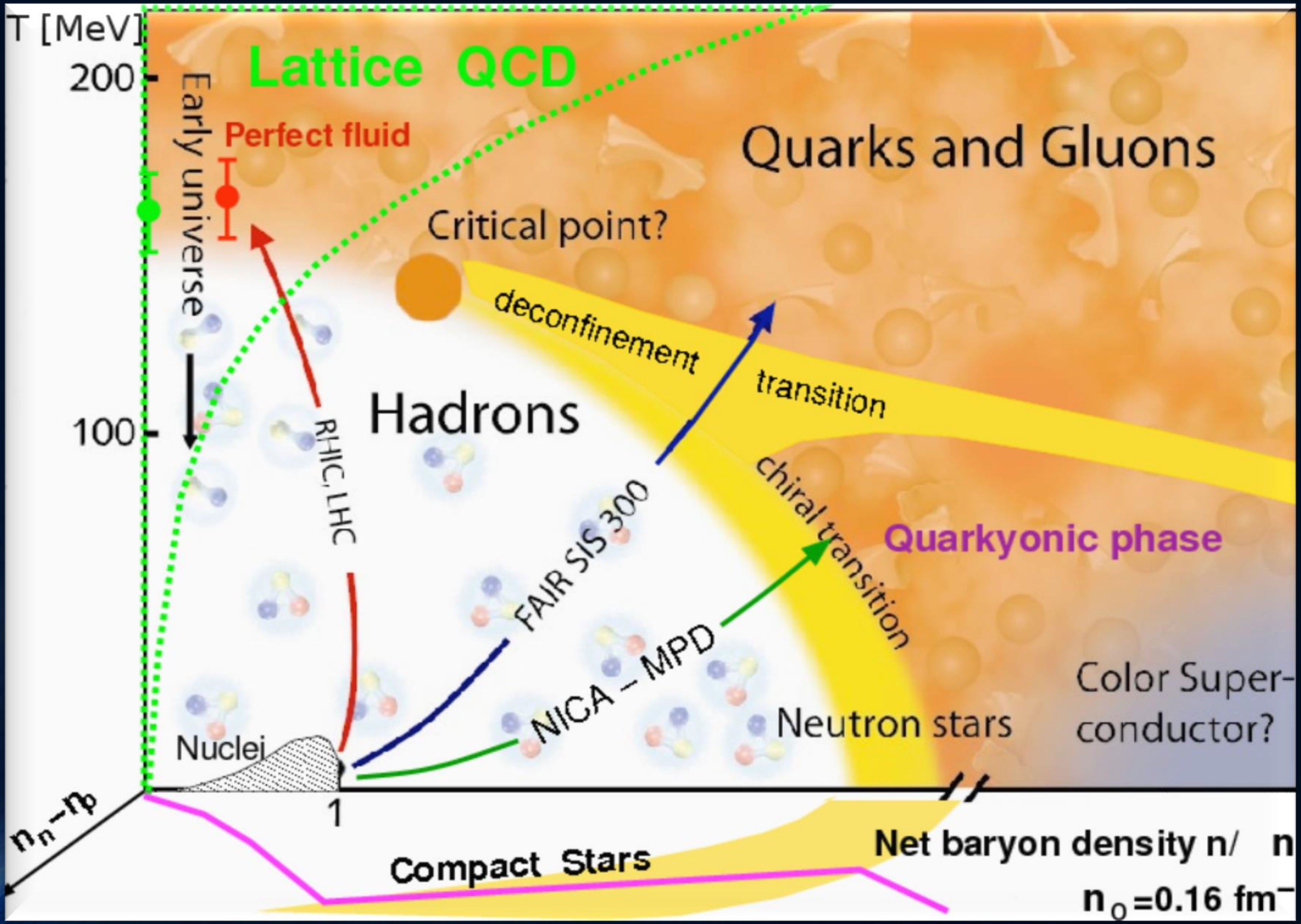

Credits to http://inspirehep.net/record/823172/files/phd_qgp3D_quarkyonic2.png

Hypermassive Neutron Stars in the QCD Phase Diagram

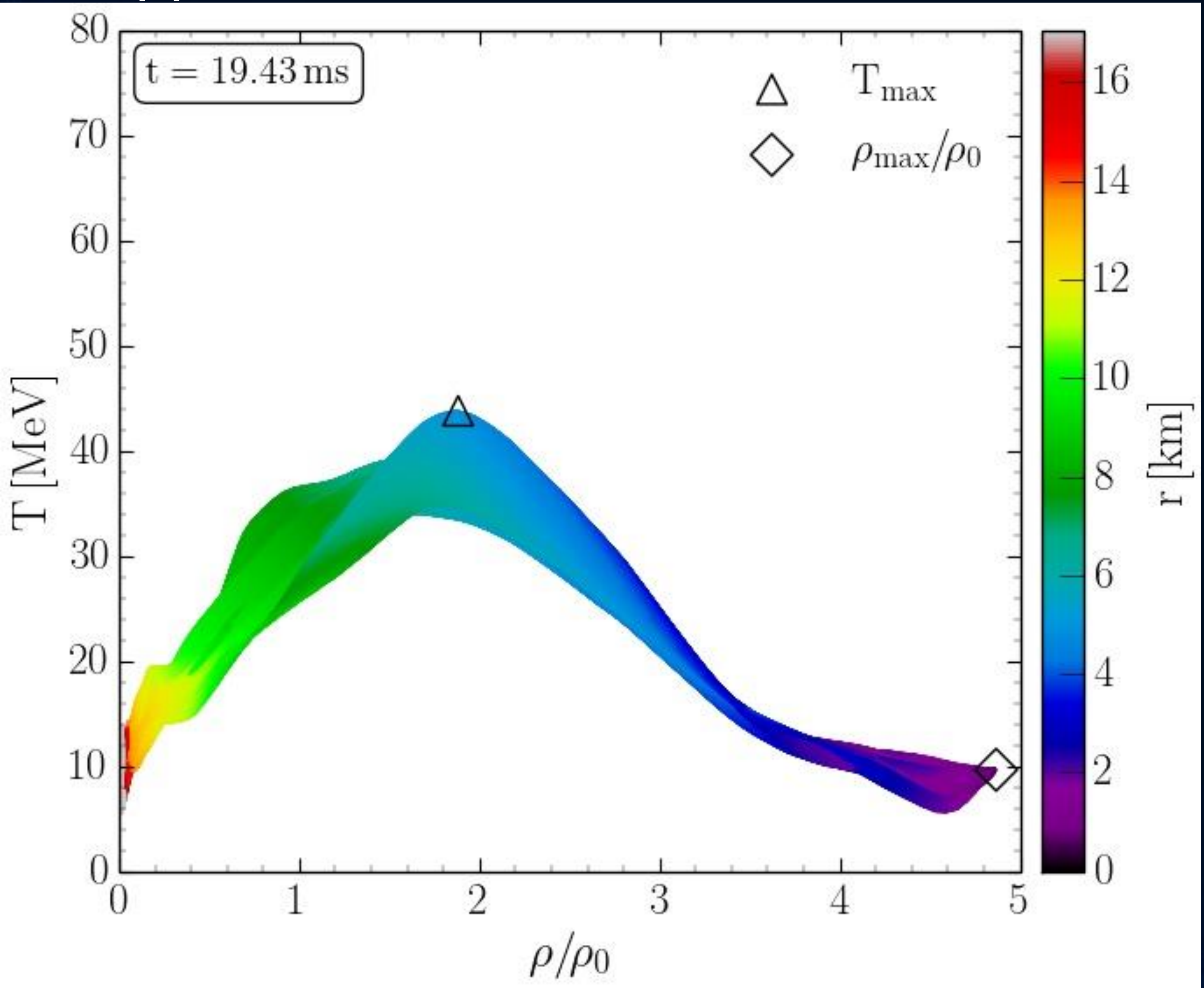

Density-temperature profiles inside the inner area of a hypermassive neutron star simulated within the LS220 EOS (☹ see talk by J.Lattimer) with a total mass of M_{total}=2.7 M_{solar} in the style of a (T- ρ) QCD phase diagram plot at t=19.43 ms after the merger.

The color-coding indicate the radial position r of the corresponding (T- ρ) fluid element measured from the origin of the simulation (x , y) = (0 , 0) on the equatorial plane at z = 0.

The open triangle marks the maximum value of the temperature while the open diamond indicates the maximum of the density.

QCD Phase Diagram: The Late Inspiral Phase

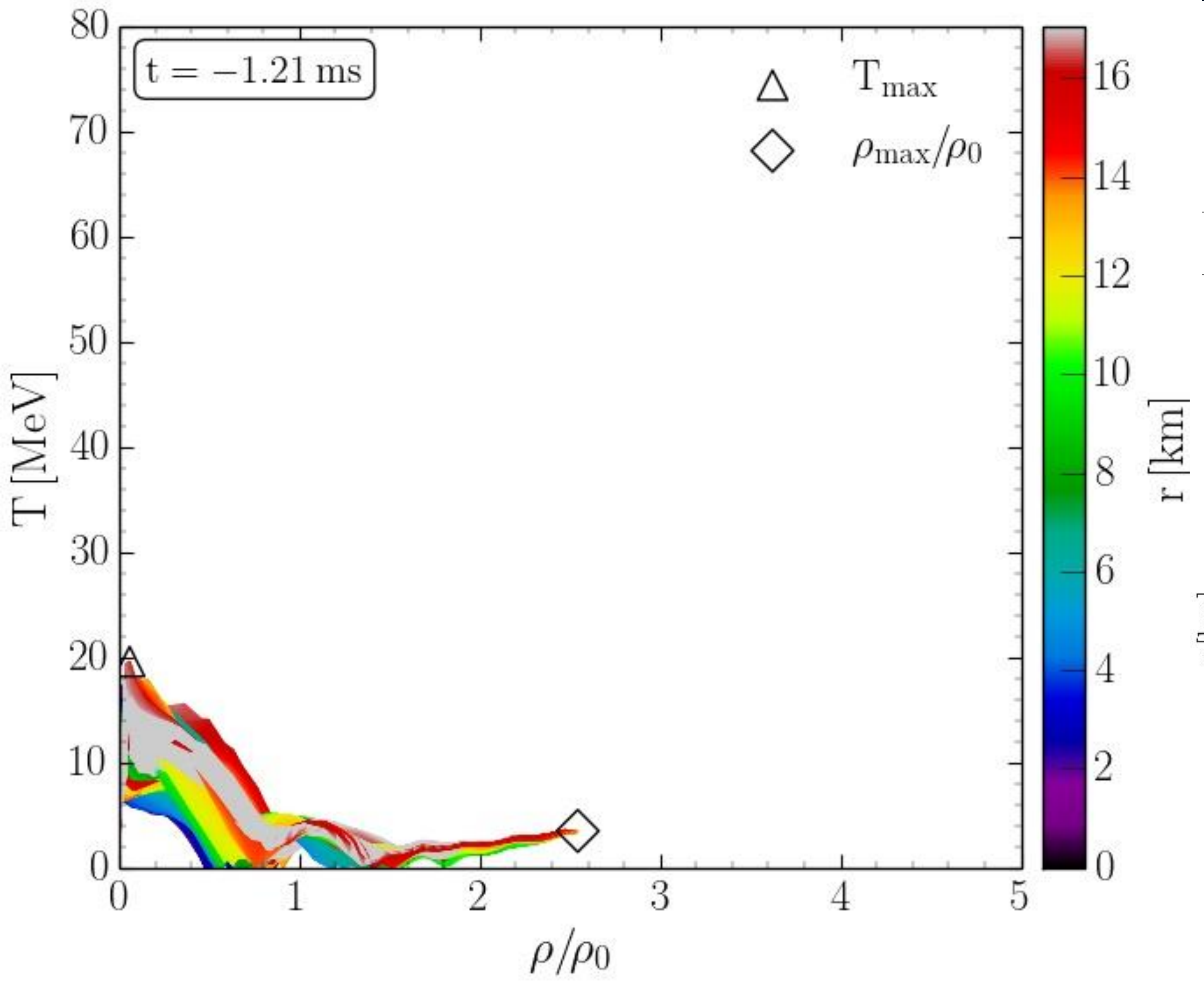

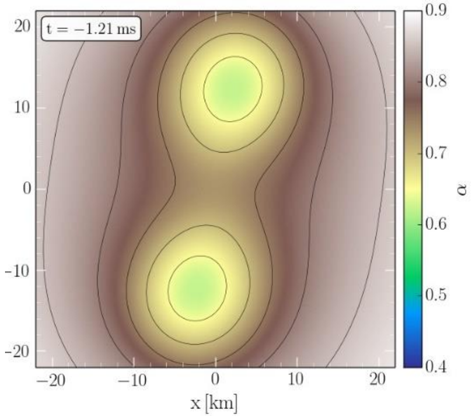

Lapse function α (left)

rest mass density ρ

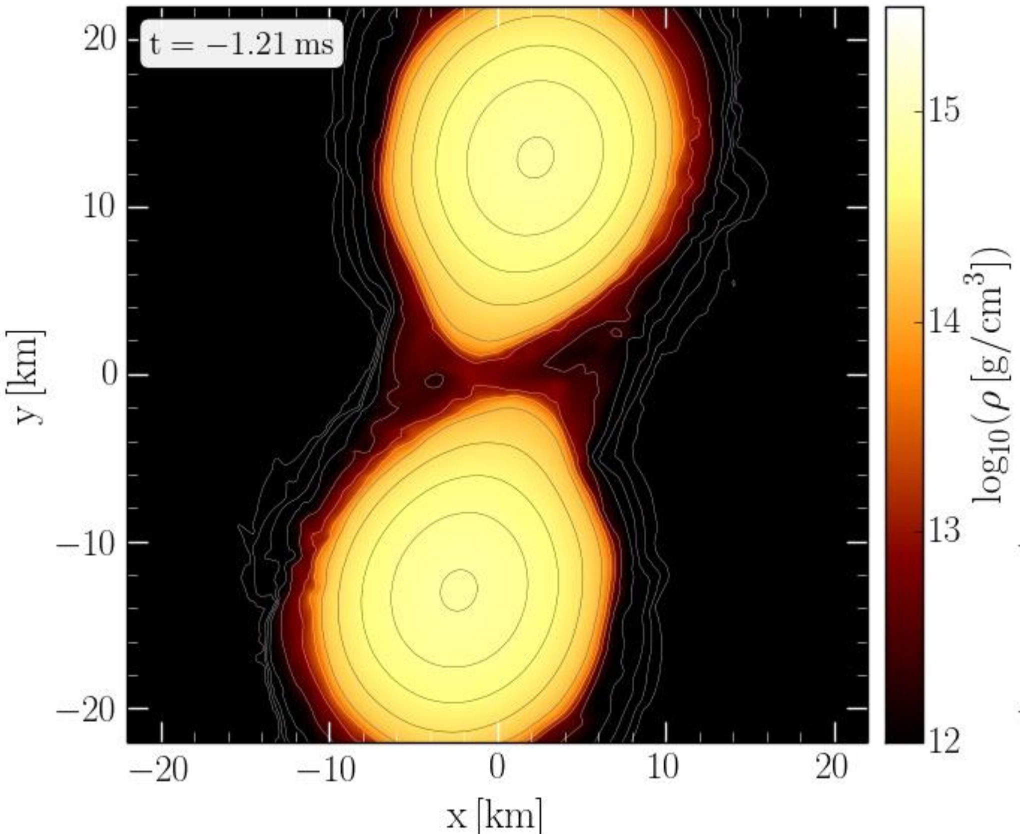

QCD Phase Diagram: The Late Inspiral Phase

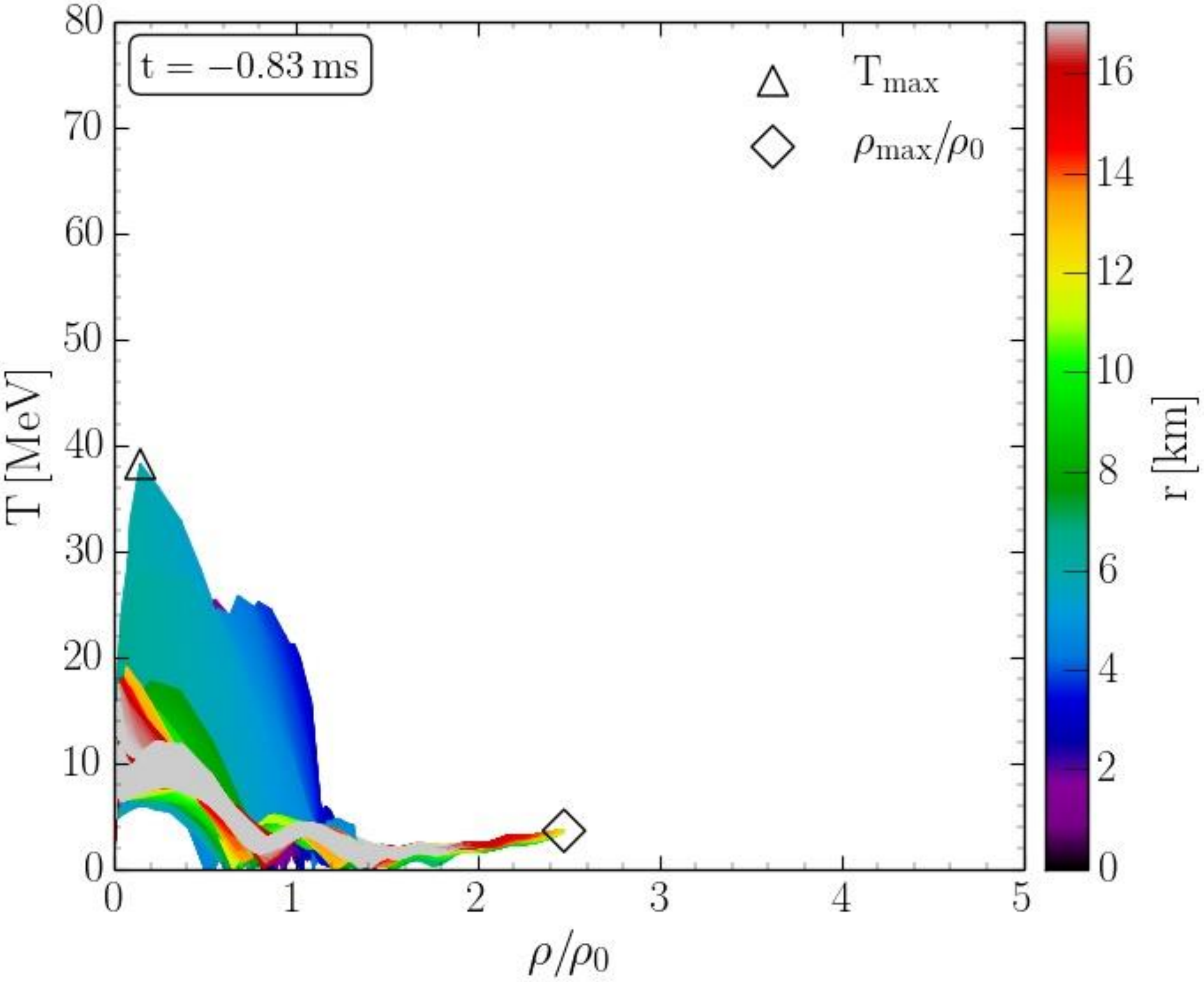

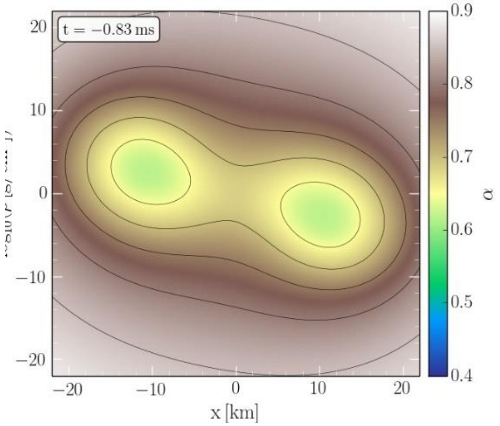

Lapse function α (left)

rest mass density ρ

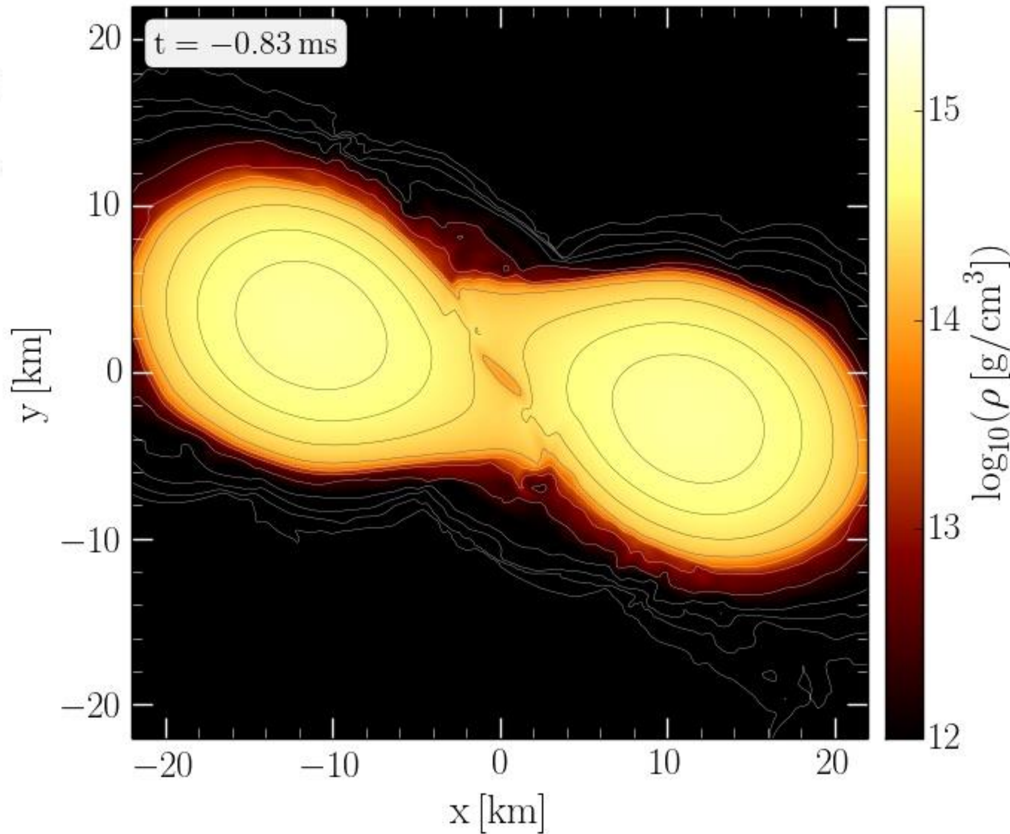

QCD Phase Diagram: The Late Inspiral Phase

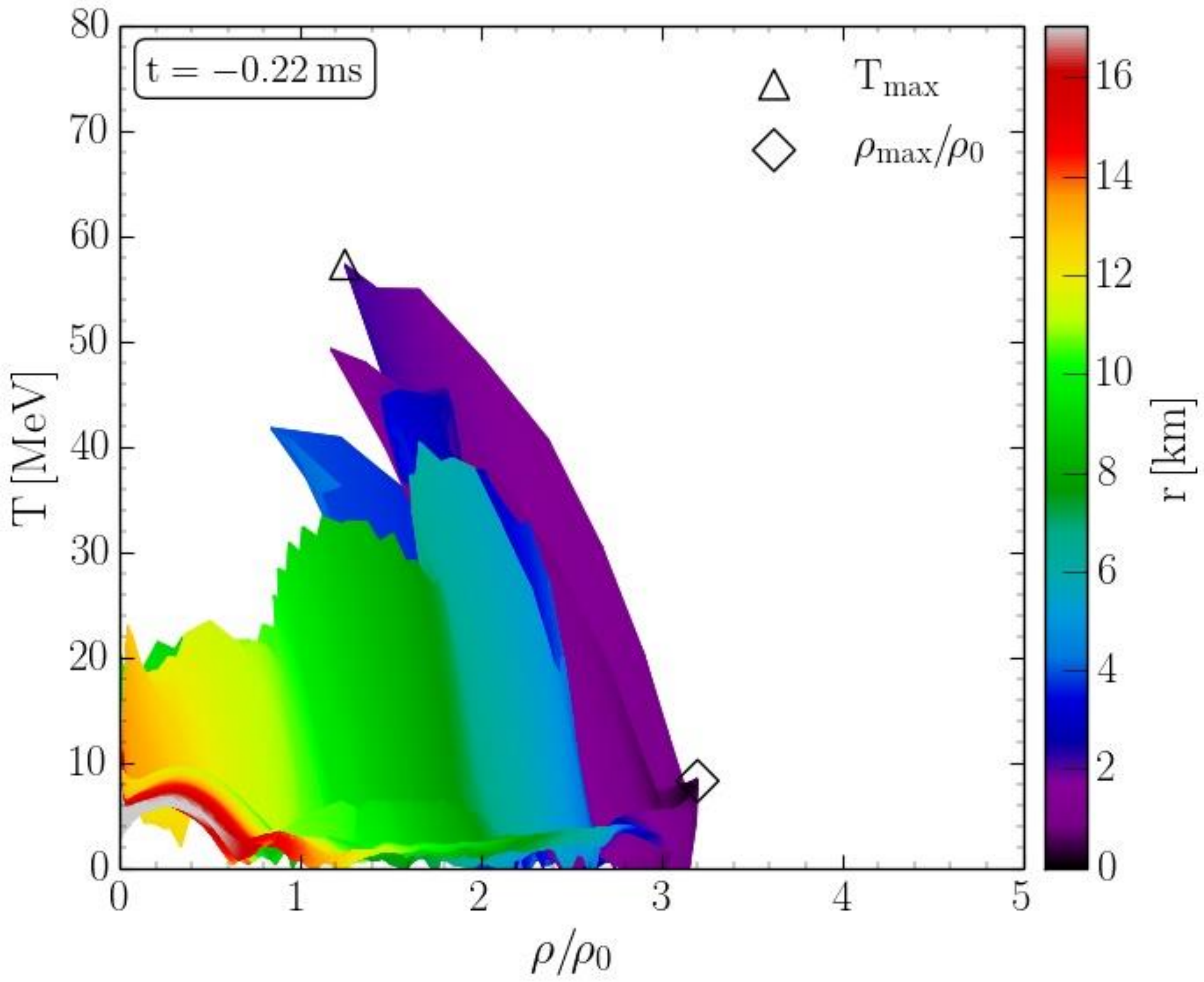

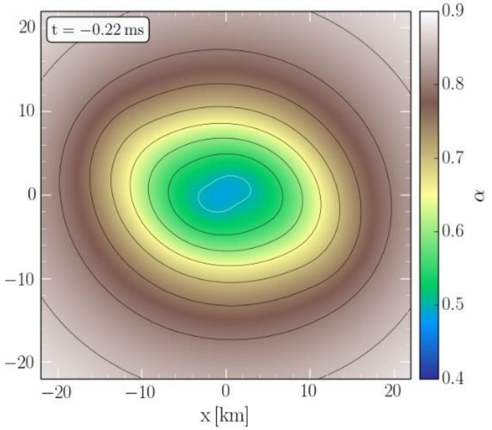

Lapse function α (left)

rest mass density ρ

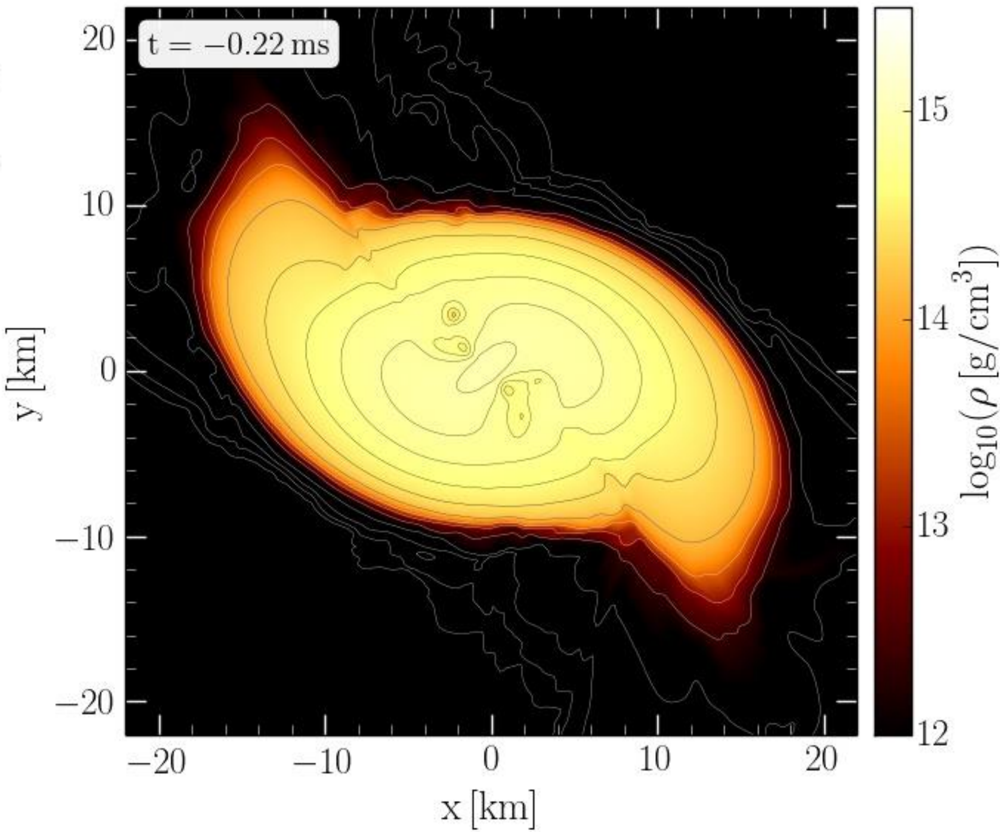

Binary Neutron Star Mergers in the QCD Phase Diagram

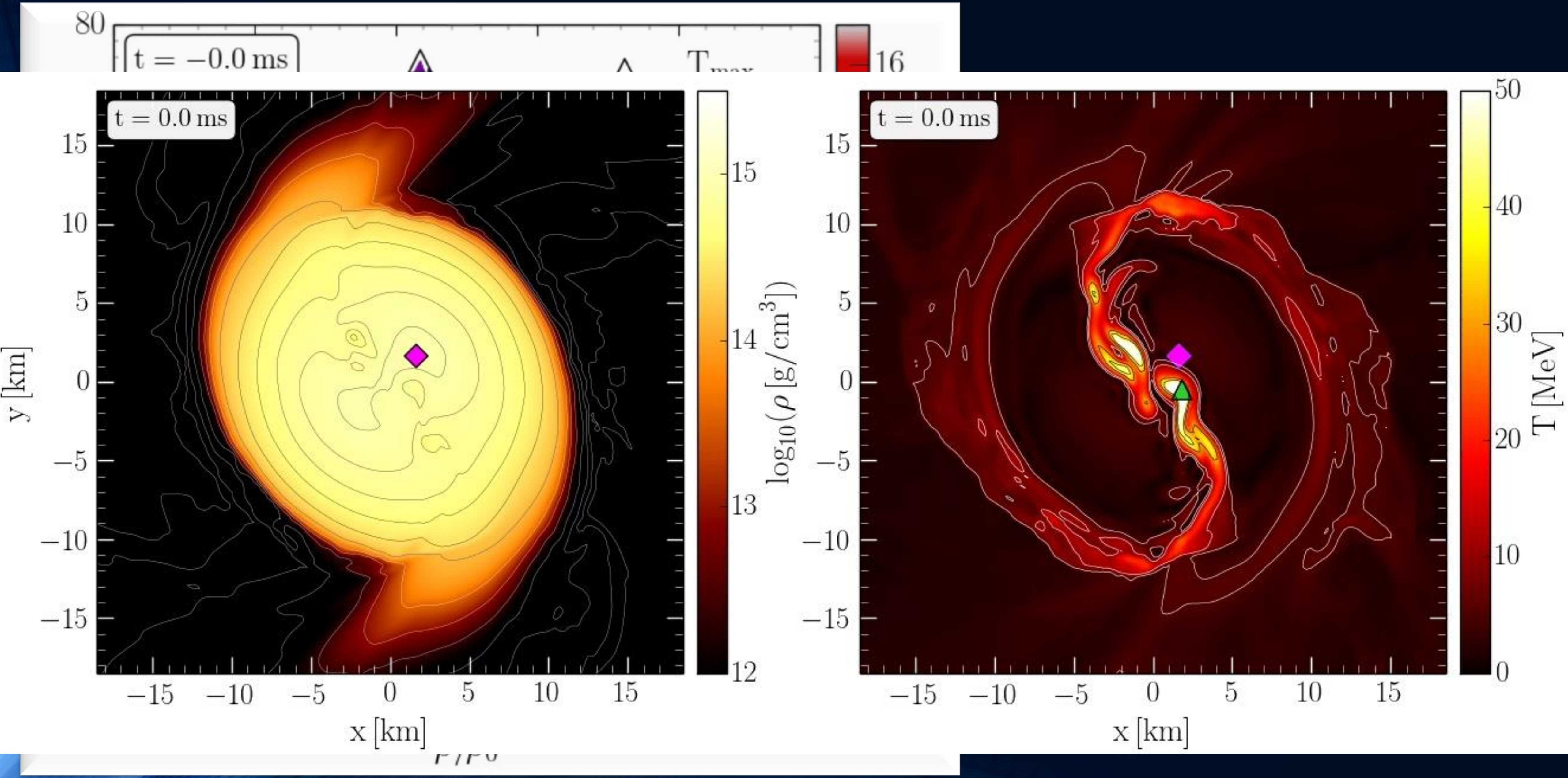

Binary Neutron Star Mergers in the QCD Phase Diagram

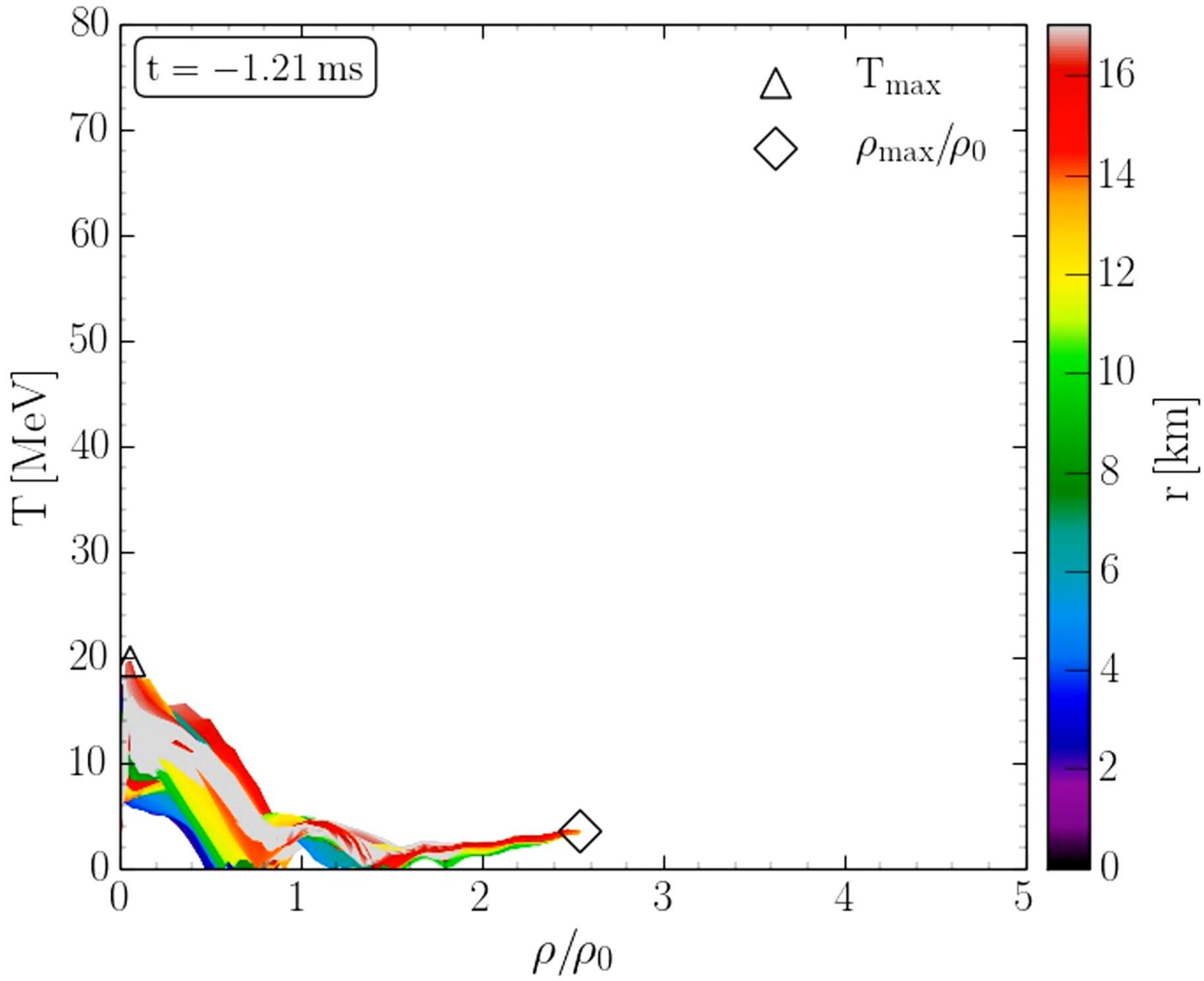

Evolution of hot and dense matter inside the inner area of a hypermassive neutron star simulated within the LS220 EOS with a total mass of M_{total}=2.7 M_{solar} in the style of a (T- ρ) QCD phase diagram plot

The color-coding indicate the radial position r of the corresponding (T- ρ) fluid element measured from the origin of the simulation (x , y) = (0 , 0) on the equatorial plane at z = 0.

The open triangle marks the maximum value of the temperature while the open diamond indicates the maximum of the density.

The Co-Rotating Frame

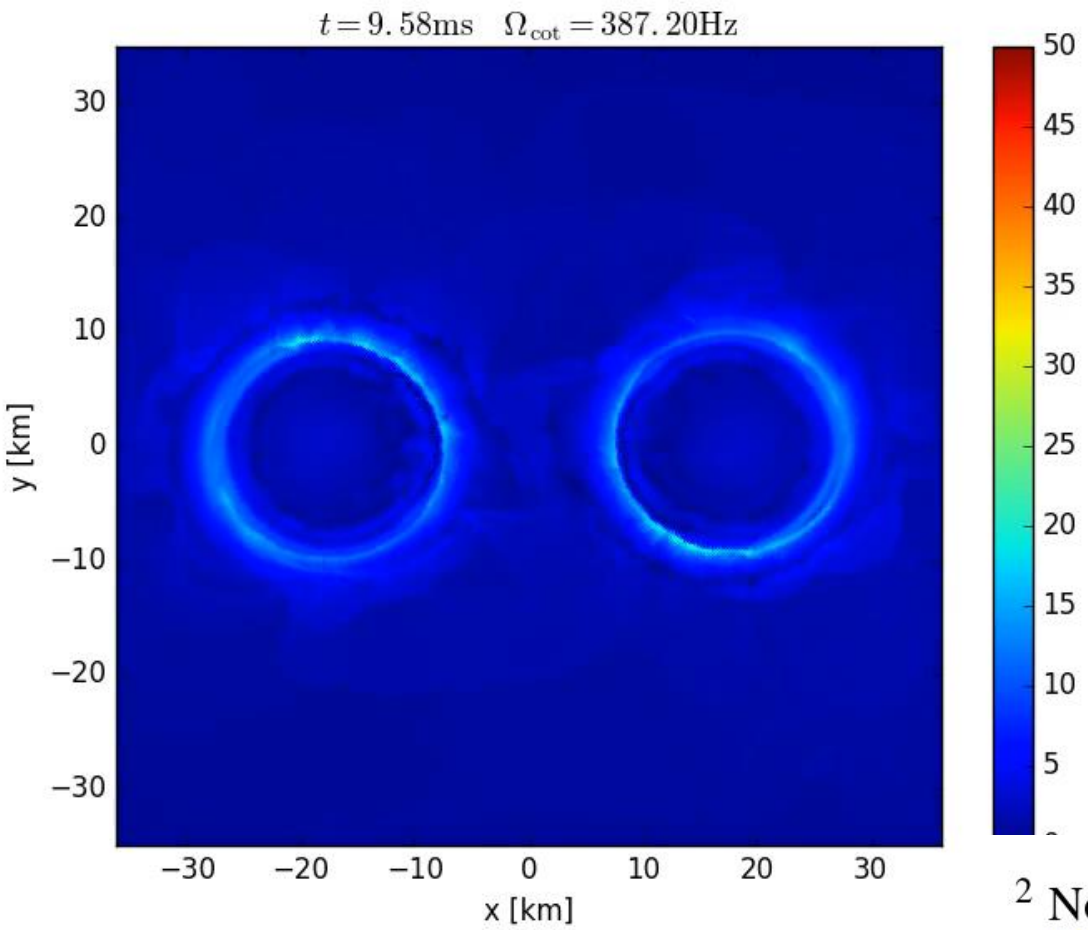

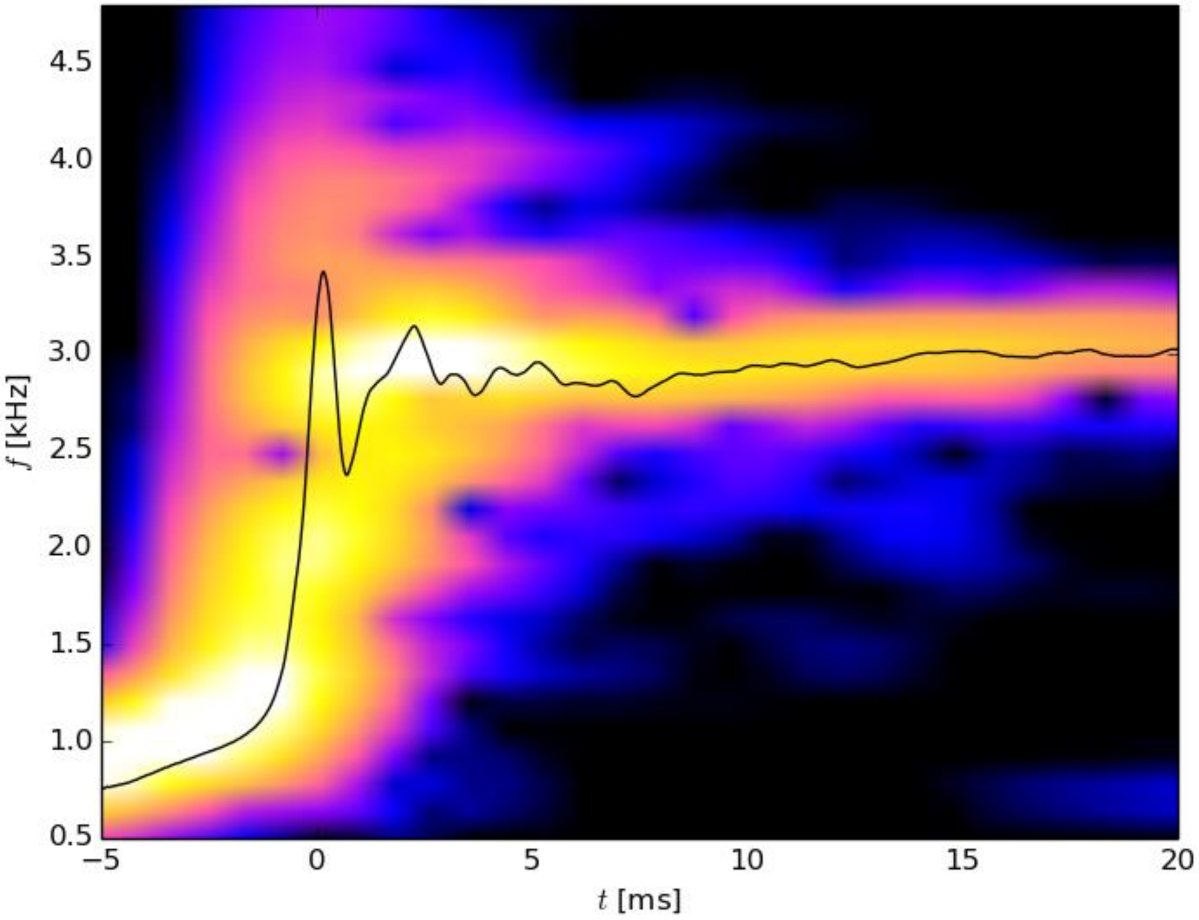

[2] Note that the angular-velocity distribution in the lower central panel of Fig. 10 refers to the corotating frame and that this frame is rotating at half the angular frequency of the emitted gravitational waves, Ω_{GW}. Because the maximum of the angular velocity Ω_{max} is of the order of $\Omega_{GW}/2$ (cf. left panel of Fig. 12), the ring structure in this panel is approximately at zero angular velocity.

Simulation and movie has been produced by Luke Bovard

Density and Temperature Evolution inside the HMNS

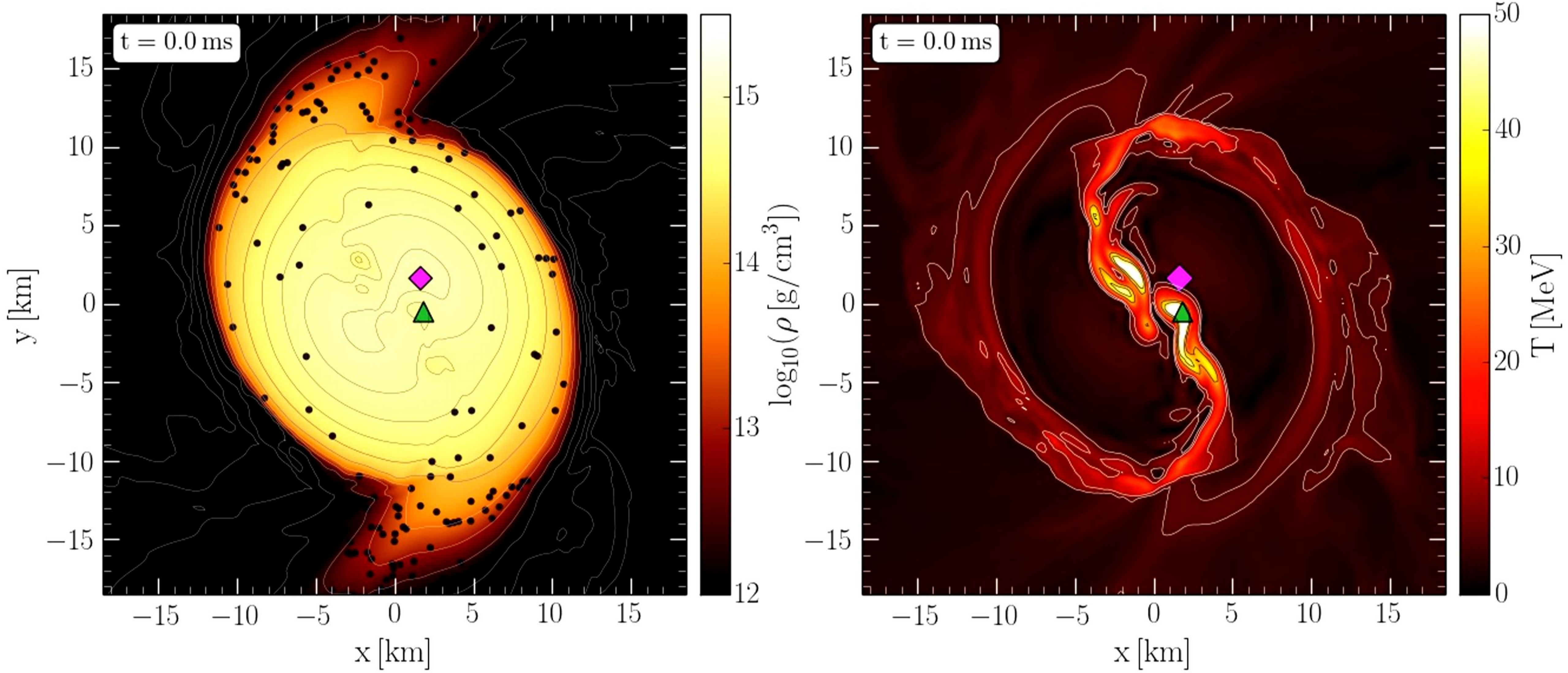

Rest mass density on the equatorial plane

Temperature on the equatorial plane

Binary Neutron Star Mergers in the QCD Phase Diagram

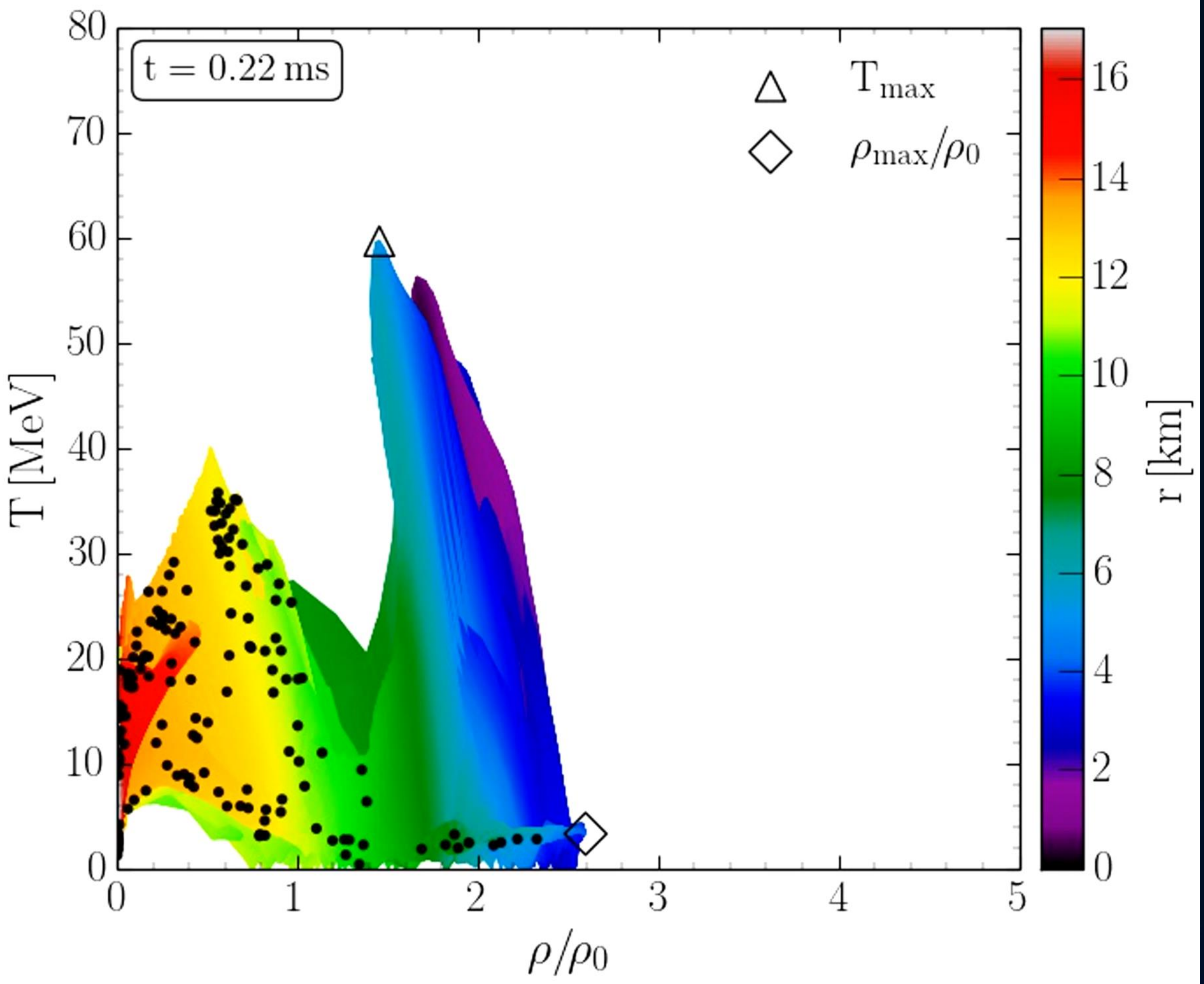

Evolution of hot and dense matter inside the inner area of a hypermassive neutron star simulated within the LS220 EOS with a total mass of M_{total}=2.7 M_{solar} in the style of a (T- ρ) QCD phase diagram plot

The color-coding indicate the radial position r of the corresponding (T- ρ) fluid element measured from the origin of the simulation (x , y) = (0 , 0) on the equatorial plane at z = 0.

The open triangle marks the maximum value of the temperature while the open diamond indicates the maximum of the density.

The Angular Velocity in the (3+1)-Split

The angular velocity Ω in the (3+1)-Split is a combination of the lapse function α , the ϕ-component of the shift vector β^{ϕ} and the 3-velocity v^{ϕ} of the fluid (spatial projection of the 4-velocity **u**):

$$\Omega(x, y, z, t) = \frac{u^{\phi}}{u^{t}} = \alpha\, v^{\phi} - \beta^{\phi}$$

Angular velocity Ω

Lapse function α

Φ-component of 3-velocity v^{φ}

Frame-dragging β^{φ}

(3+1)-decomposition of spacetime:

$$g_{\mu\nu} = \begin{pmatrix} -\alpha^2 + \beta_i \beta^i & \beta_i \\ \beta_i & \gamma_{ij} \end{pmatrix}$$

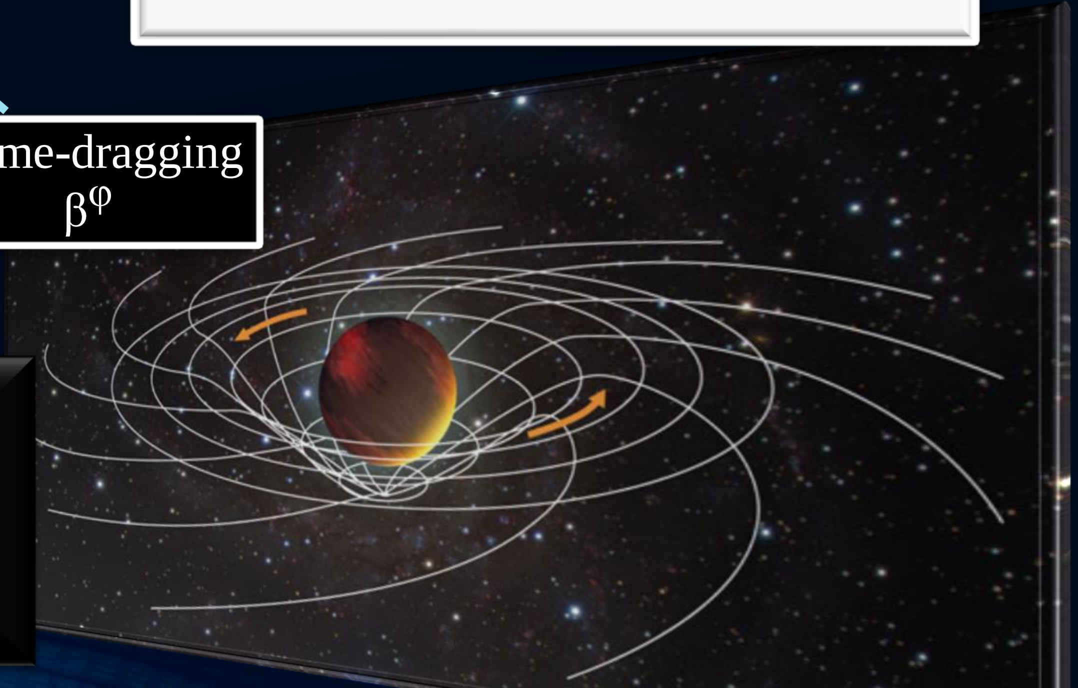

Focus: Inner core of the differentially rotating HMNS

M. Shibata, K. Taniguchi, and K. Uryu, Phys. Rev. D 71, 084021 (2005)
M. Shibata and K. Taniguchi, Phys. Rev. D 73, 064027 (2006)
F. Galeazzi, S. Yoshida and Y. Eriguchi, A&A 541, p. A156 (2012)
W. Kastaun and F. Galeazzi, Phys. Rev. D 91, p. 064027 (2015)

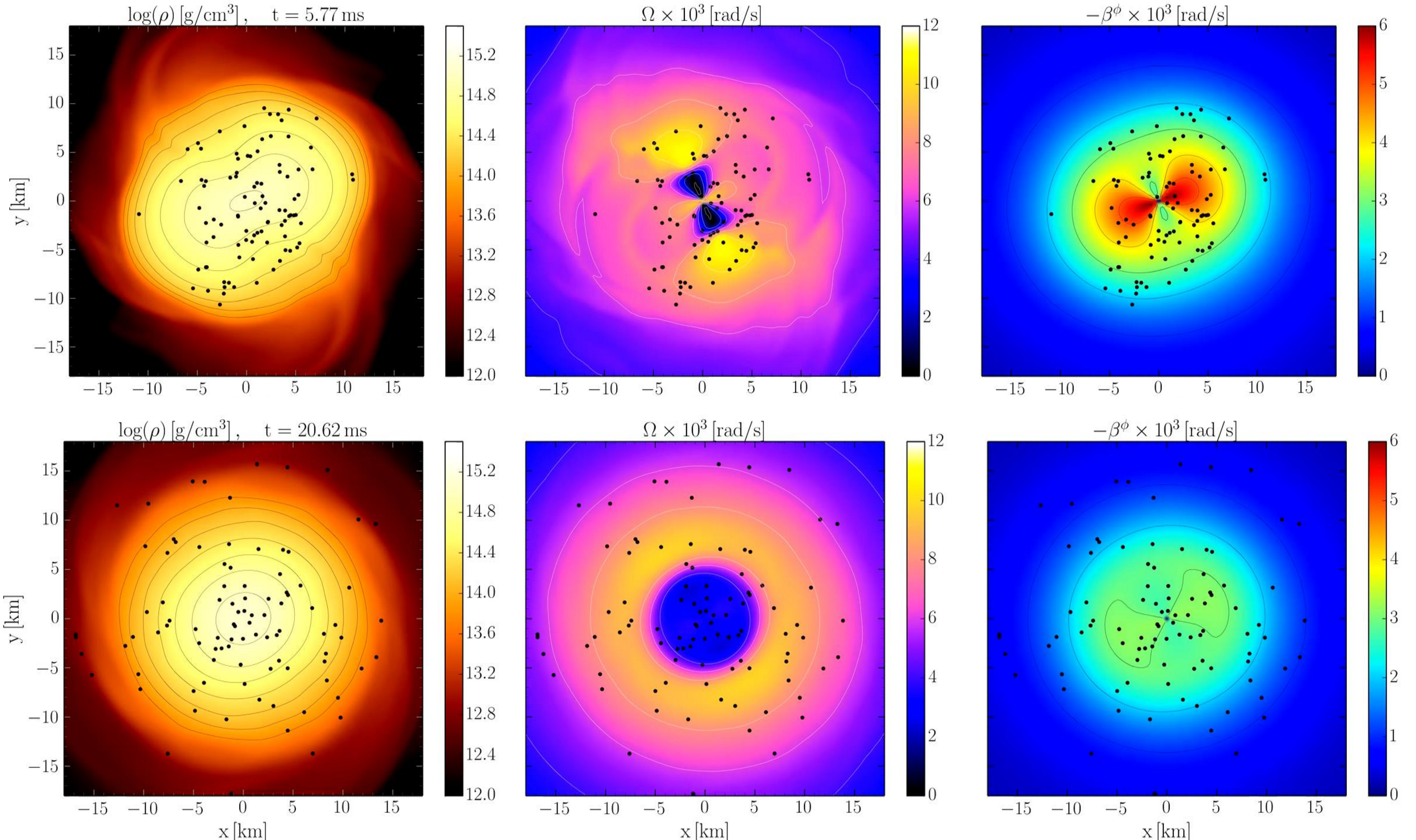

log(ρ) [g/cm³], t = 5.77 ms
Ω × 10³ [rad/s]
−β^φ × 10³ [rad/s]
log(ρ) [g/cm³], t = 20.62 ms
Ω × 10³ [rad/s]
−β^φ × 10³ [rad/s]
y [km]
x [km]

Time-averaged Rotation Profiles of the HMNSs

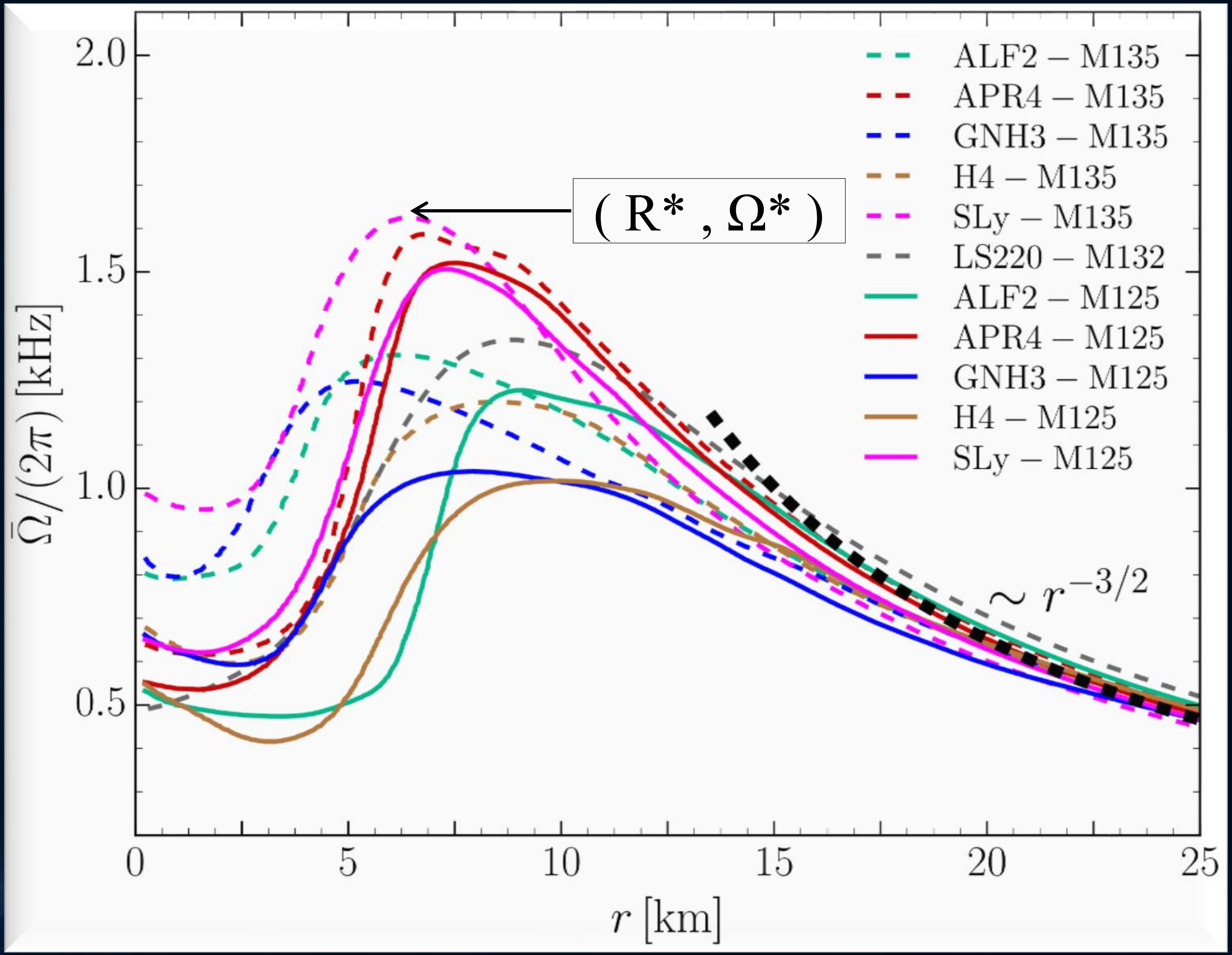

Time-averaged rotation profiles for different EoS
Low mass runs (solid curves), high mass runs (dashed curves).

<u>Soft EoSs</u>:
Sly
APR4

<u>Stiff EoSs</u>:
GNH3
H4

Temperature

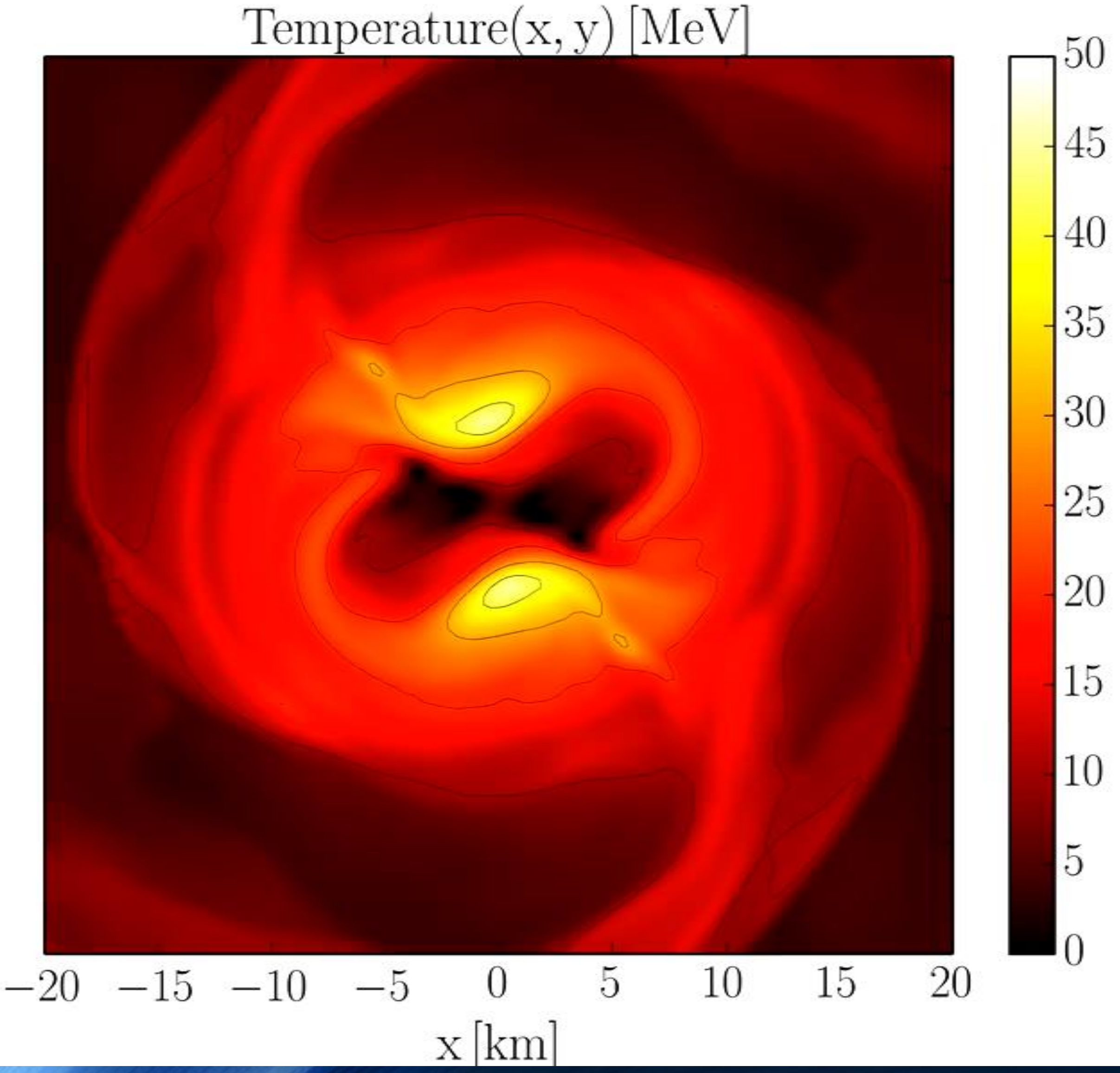

Angular Velocity

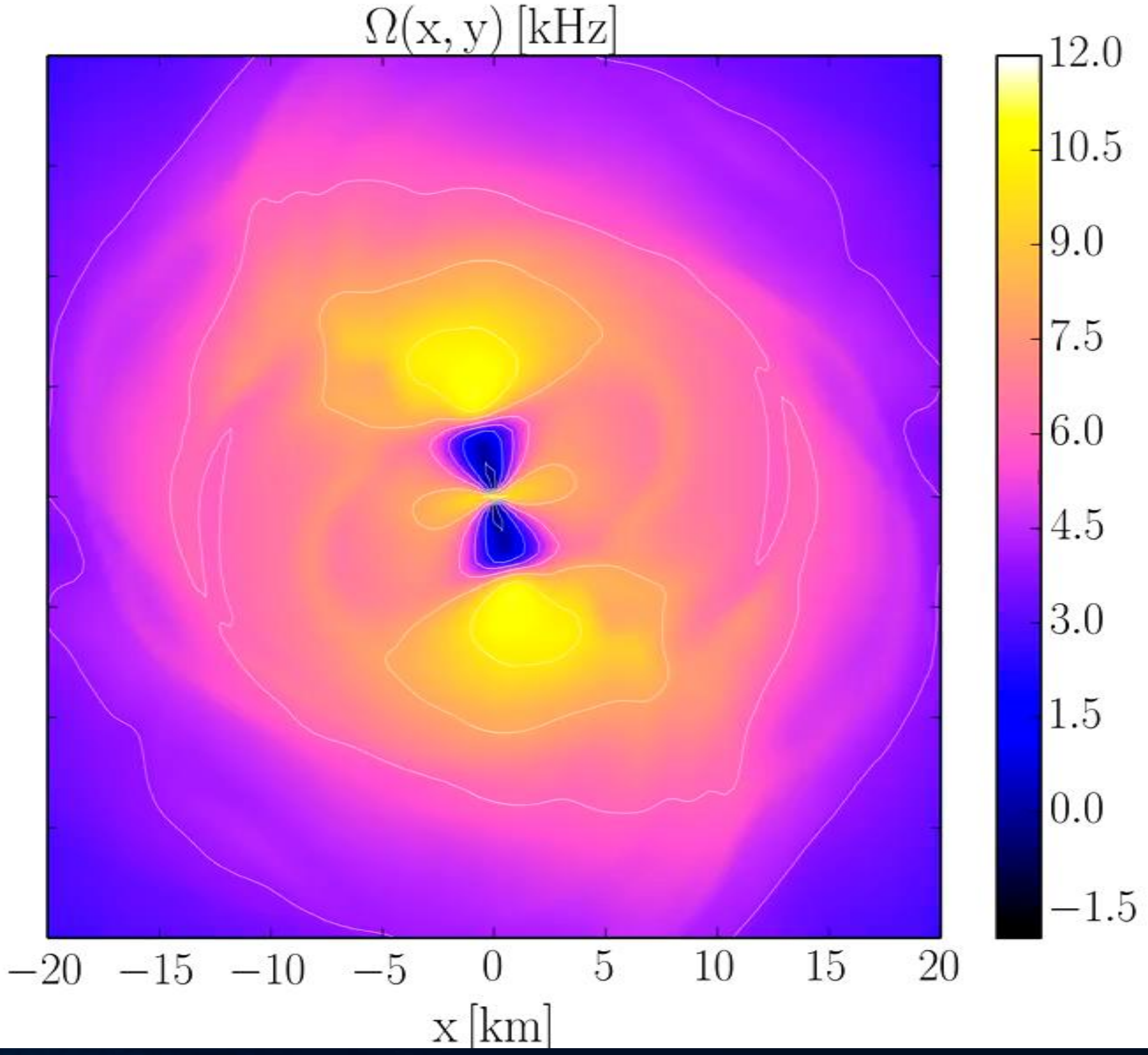

EOS: LS200 , Mass: 1.32 M_{solar} , simulation with Pi-symmetry

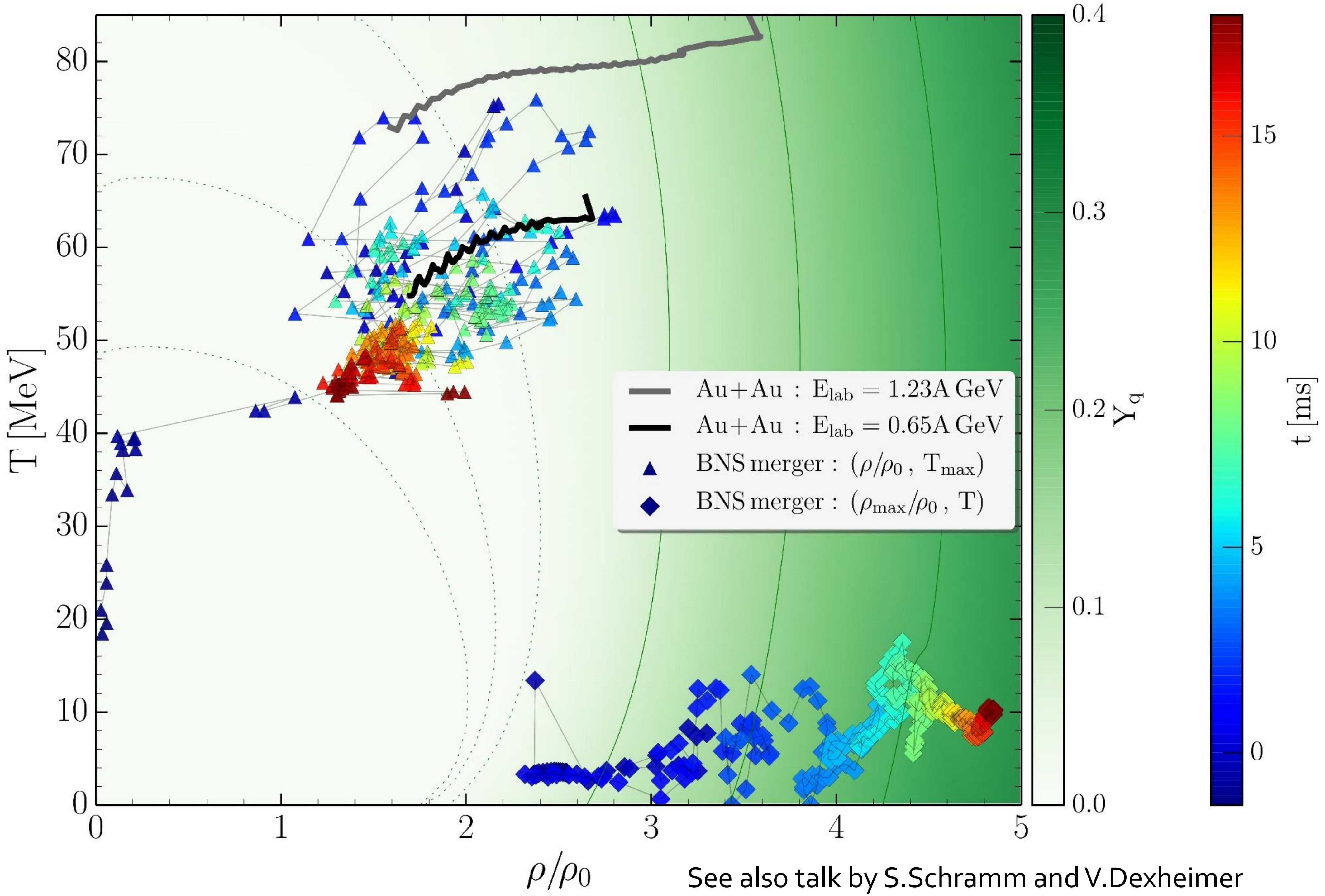

See also talk by S.Schramm and V.Dexheimer

Evolution of the maximum value of the temperature (triangles) and rest mass density (diamonds) at the equatorial plane in the interior of a HMNS using the simulation results of the LS220-M135 run
Color coding of triangles/diamonds: time of the simulation after merger in milliseconds

Grey and black curve: two heavy ion collision simulations within the quark-hadron chiral parity-doublet model

Y_q = Quark fraction

Merging Neutron Stars

- Lecture I: The math of neutron-star mergers
  - Introduction
  - A brief review of General Relativity
  - Numerical relativity of neutron-star mergers
    - The 3+1 decomposition of spacetime
    - ADM equations
    - BSSNOK/ccZ4 formulation
    - Initial data, gauge conditions, excising parts of spacetime and gravitational wave extraction
- Lecture II: The physics/astrophysics of neutron-star mergers
  - Introduction
  - GW170817 - the long-awaited event
  - Determining neutron-star properties and the equation of state using gravitational wave data
  - Hypermassive neutron stars and the post-merger gravitational wave emission
  - Detecting the hadron-quark phase transition with gravitational waves

Phase transitions and their signatures

Most, Papenfort, Dexheimer, Hanauske, Schramm, Stoecker, LR
(2019)

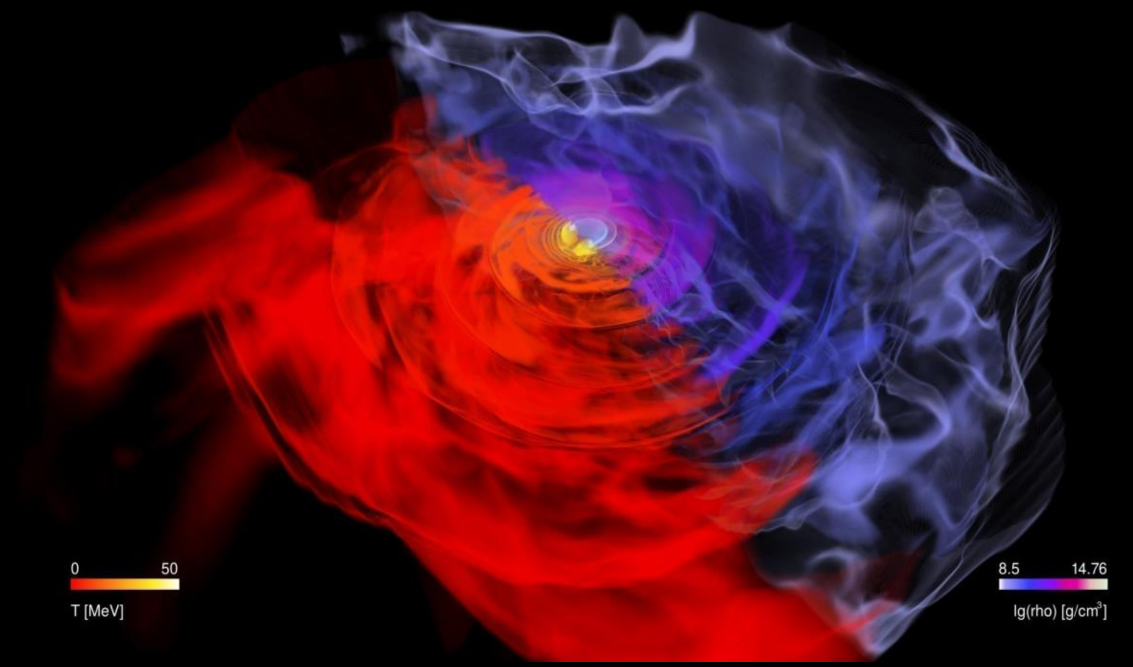

Modelling the EOS

- EOS based on Chiral Mean Field (CMF) and nonlinear SU(3) sigma model
- Includes hyperons and quarks that can be turned on/off
- Uses Polyakov loop to implement a strong first order phase transition
- Includes a cross-over transition at high temperatures

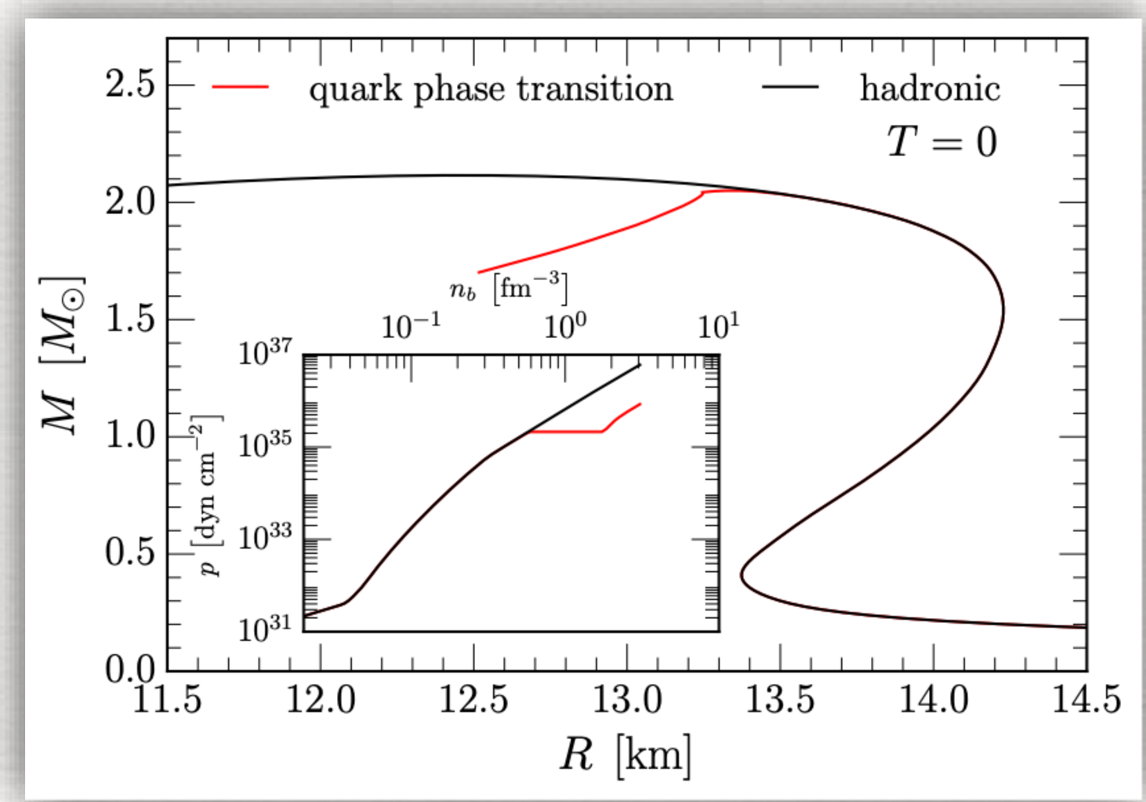

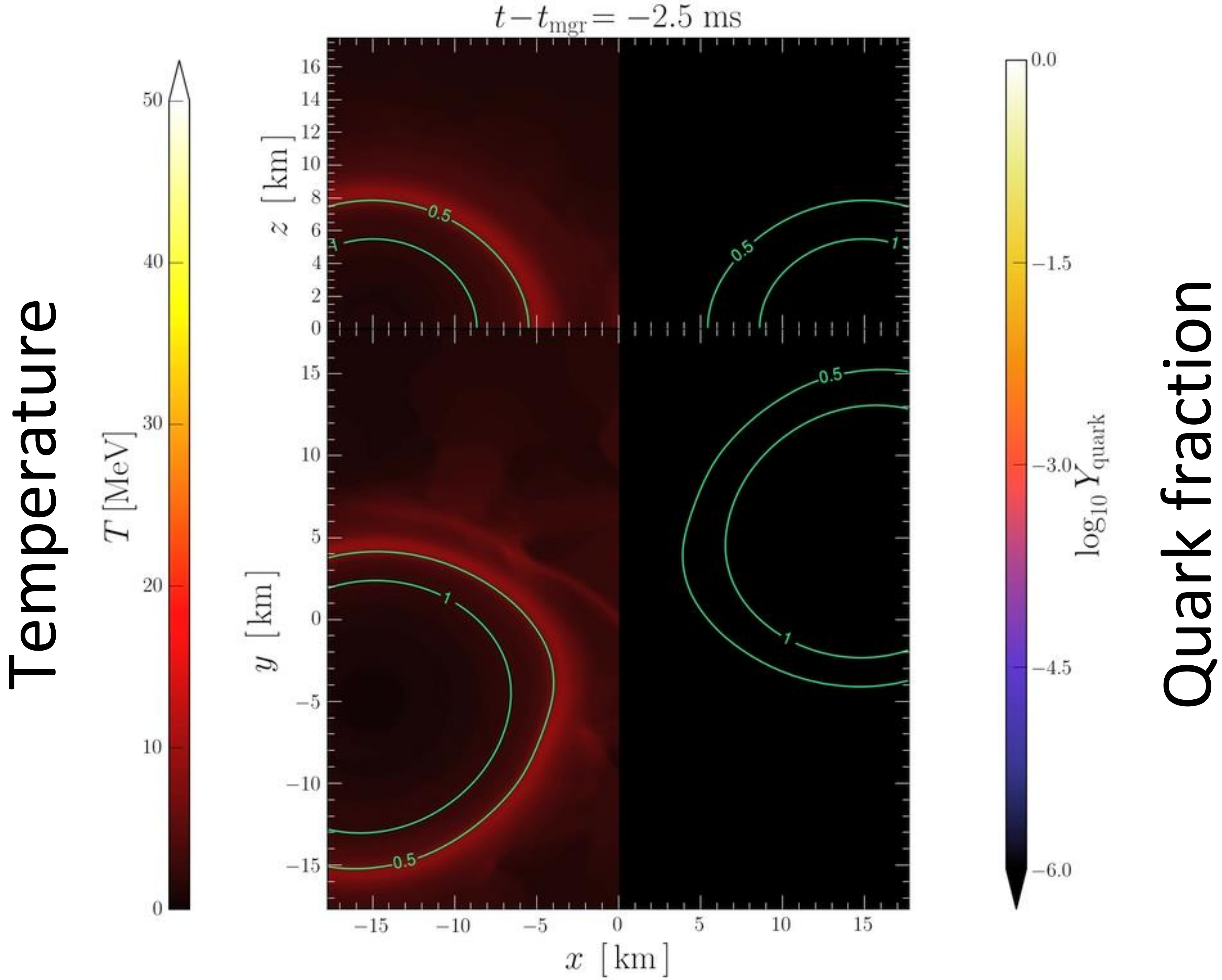
Temperature
$t - t_{mgr} = -2.5$ ms
T [MeV]
z [km]
y [km]
x [km]
$\log_{10} Y_{quark}$
Quark fraction

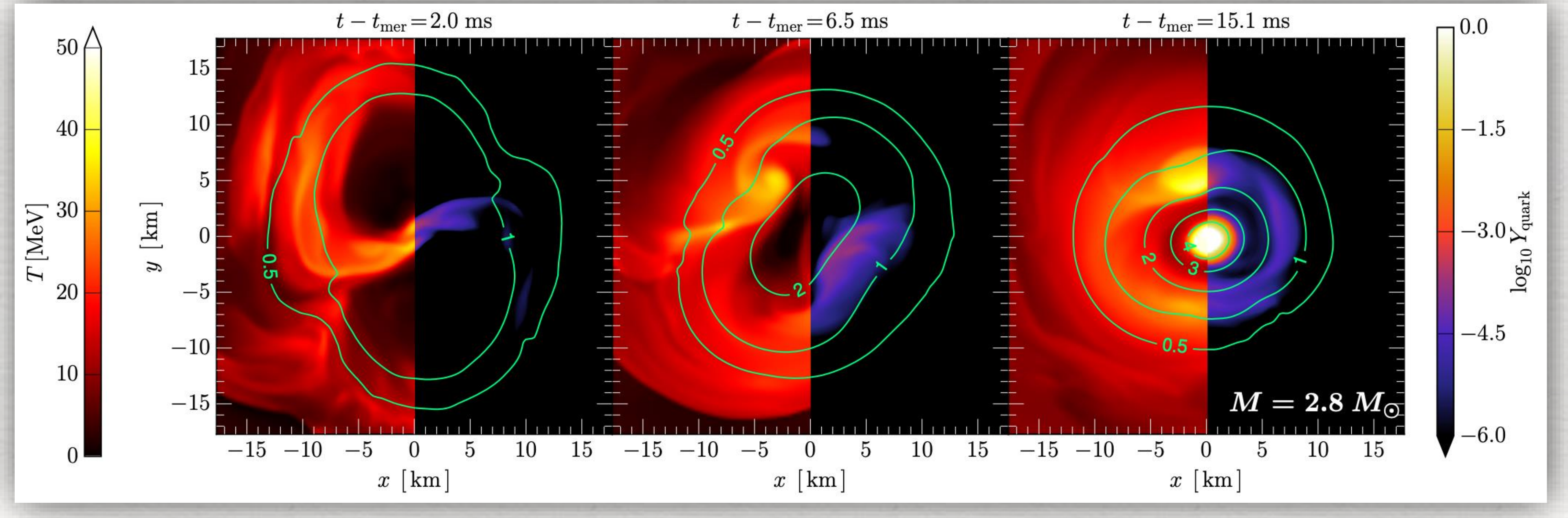

- EOS based on Chiral Mean Field (CMF) model, based on a nonlinear SU(3) sigma model.
- Quarks appear at sufficiently large temperatures and densities.

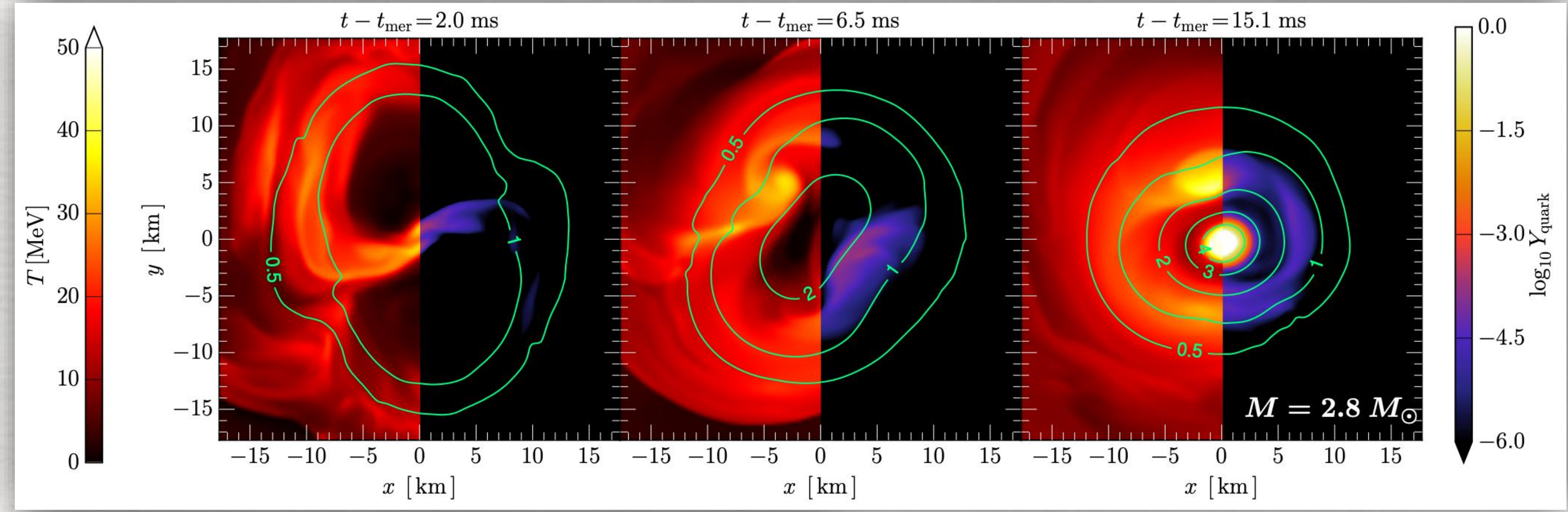

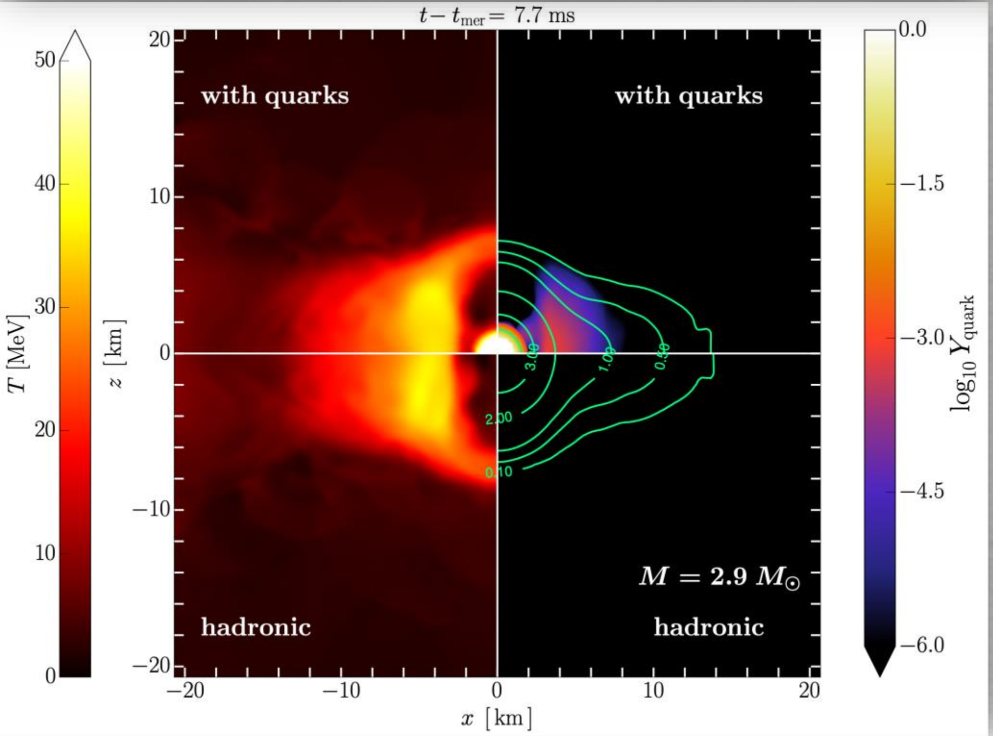

- EOS based on Chiral Mean Field (CMF) model, based on a nonlinear SU(3) sigma model.
- Quarks appear at sufficiently large temperatures and densities.
- For EOS without quarks, the dynamics is very similar, but no PT.

Comparing with the phase diagram

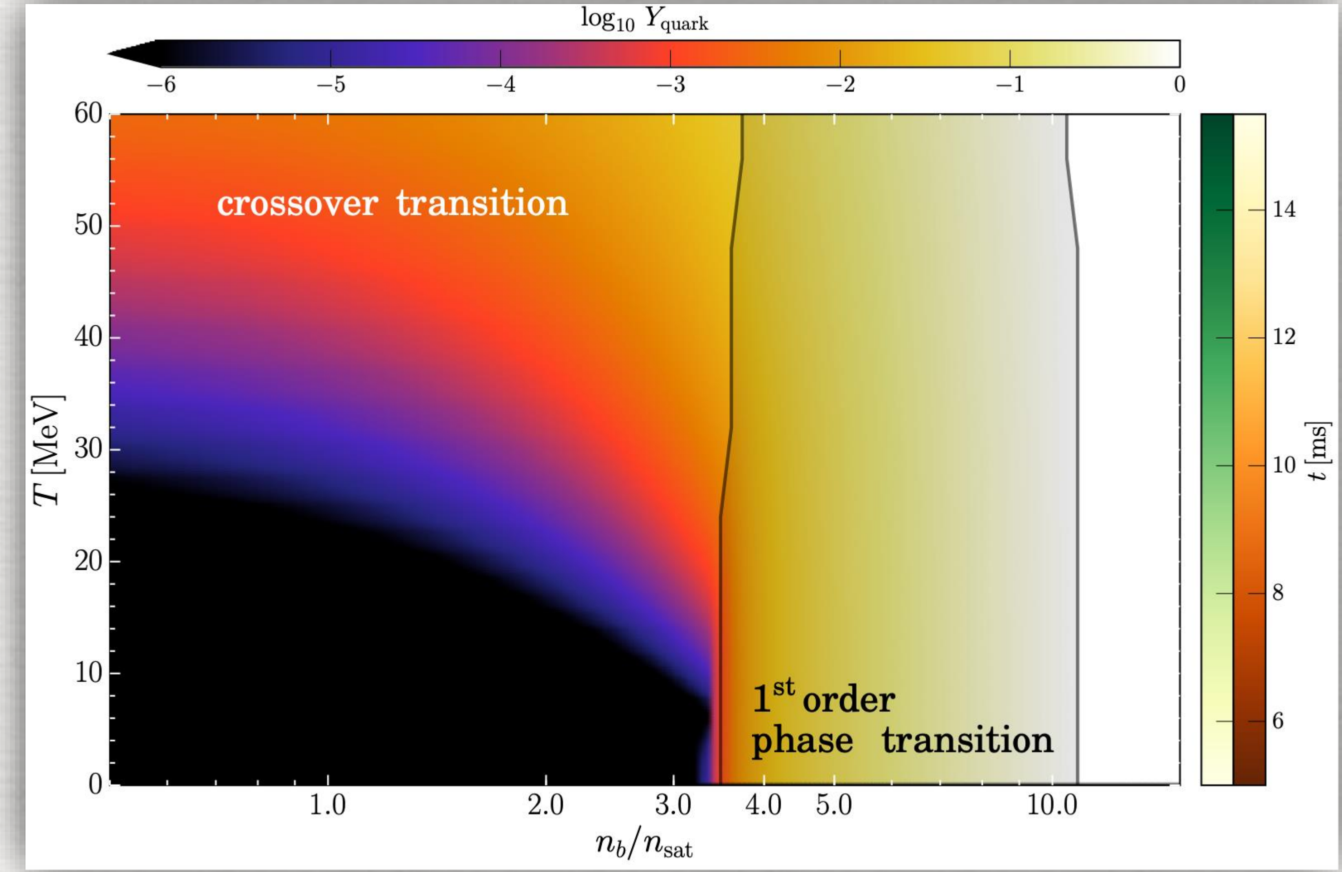

- Phase diagram with quark fraction

Comparing with the phase diagram

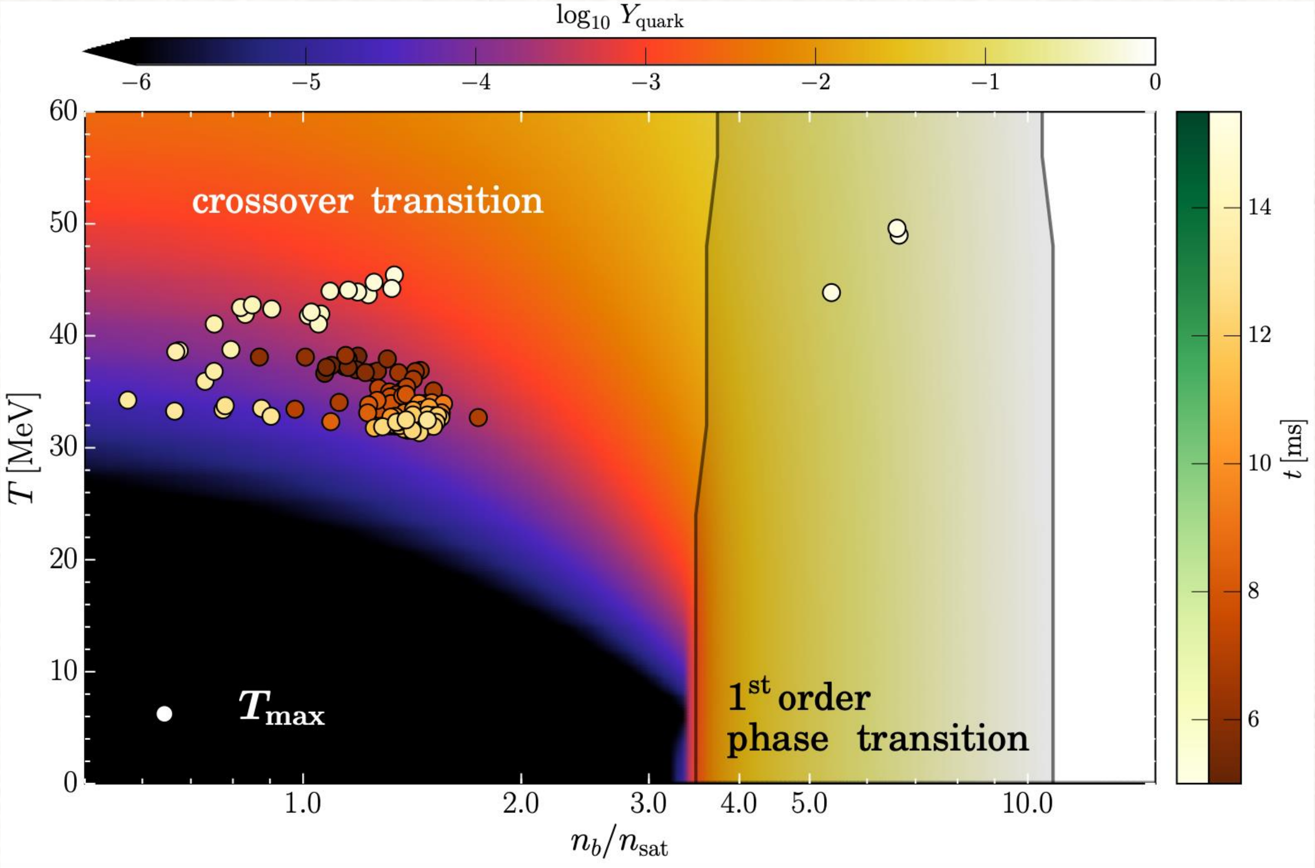

- Phase diagram with quark fraction
- Circles show the position in the diagram of the maximum temperature as a function of time

Comparing with the phase diagram

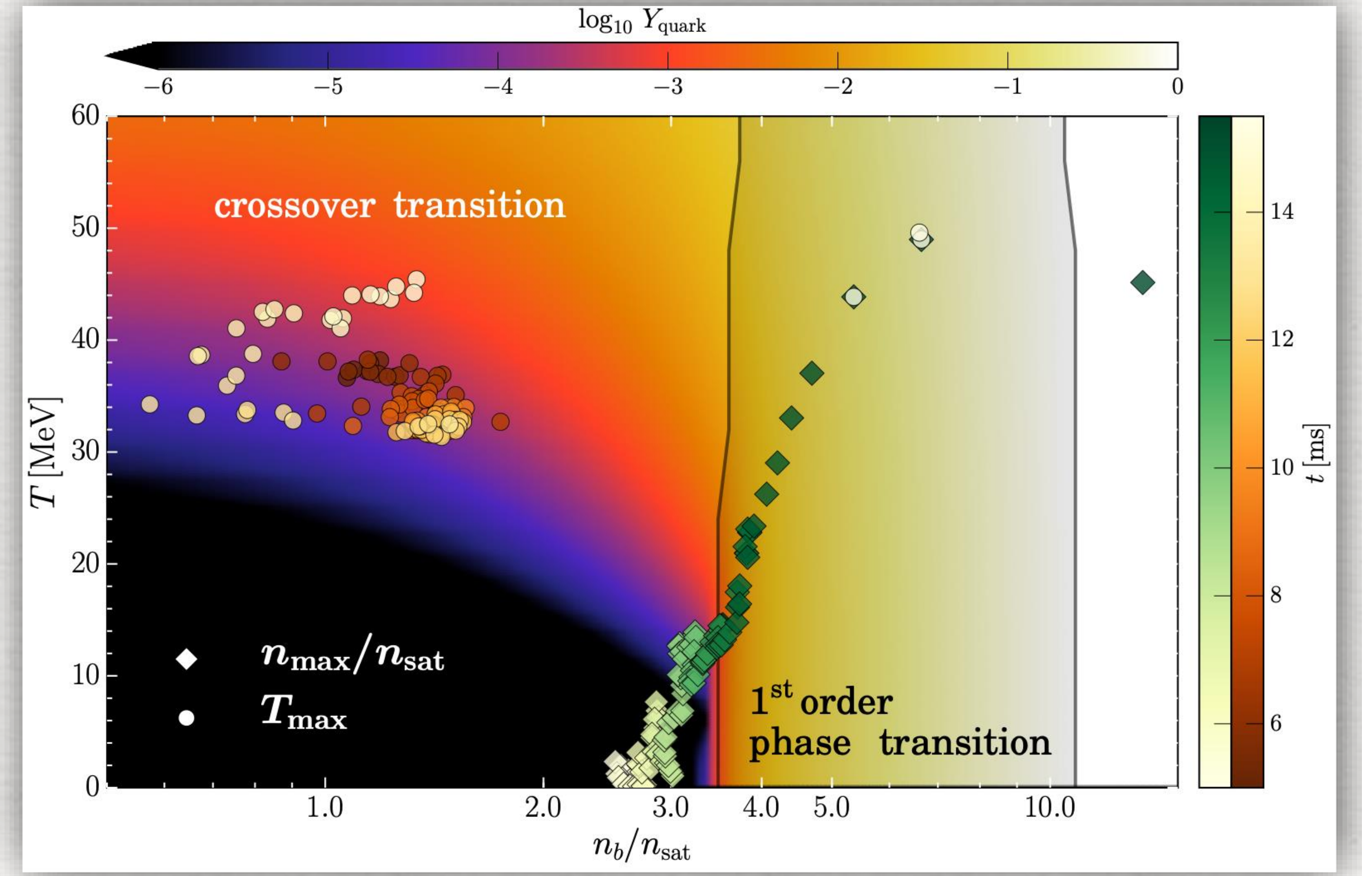

- Reported are the evolution of the max. temperature and density.
- Quarks appear already early on, but only in small fractions.
- Once sufficient density is reached, a full phase transition takes place.

Binary Hybrid Star Mergers and the QCD Phase Diagram

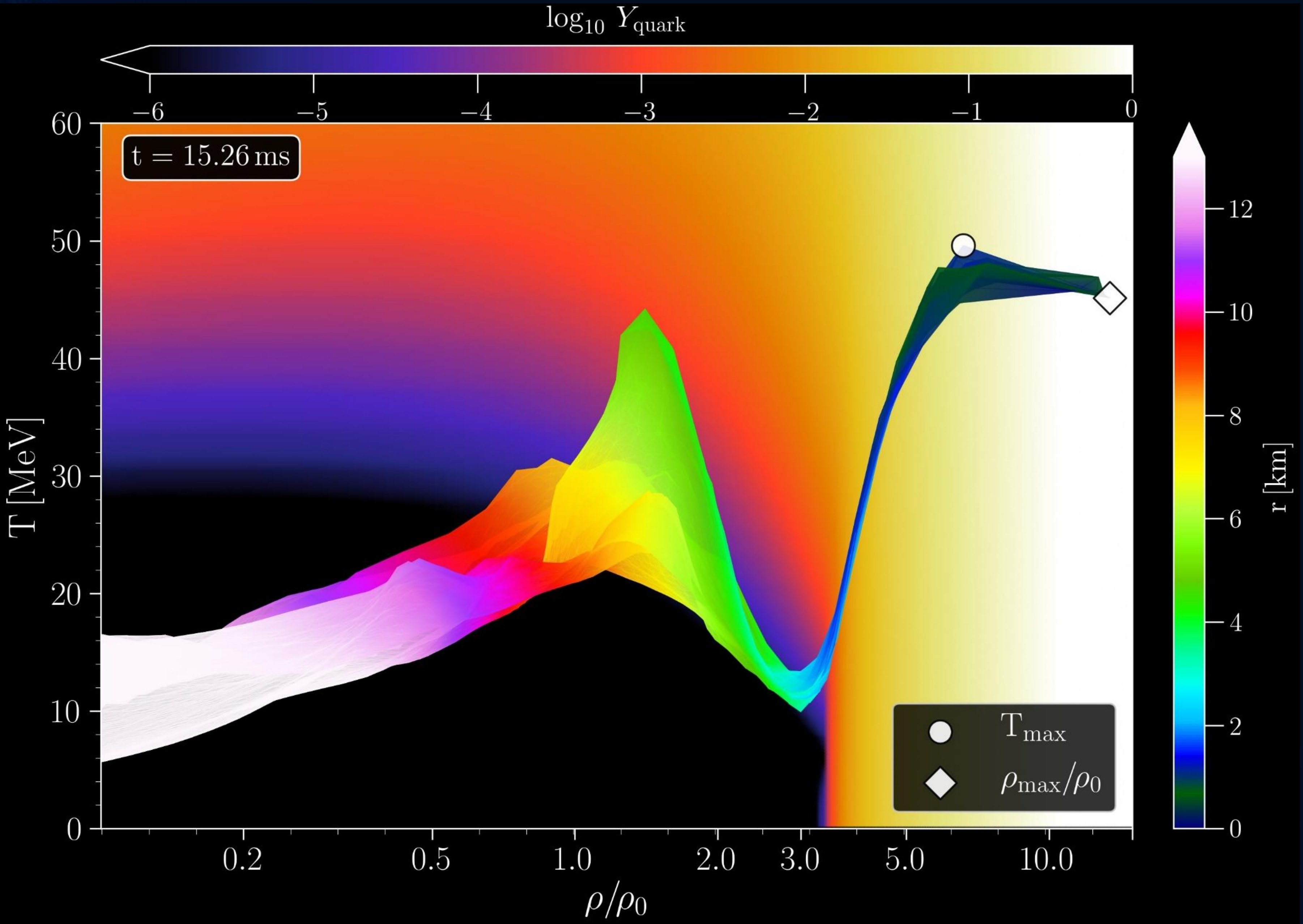

Hot and dense matter inside the inner area of a collapsing hypermassive hybrid star in the style of a (T- ρ) QCD phase diagram plot at a time right before the apparent horizont is formed in its center

The color-coding (right side) indicate the radial position r of the corresponding (T- ρ) fluid element measured from the origin of the simulation (x , y) = (0 , 0) on the equatorial plane at z = 0.
The color-coding (top) indicates the fraction of deconfined quarks.

The open triangle marks the maximum value of the temperature while the open diamond indicates the maximum of the density.

Merger phase

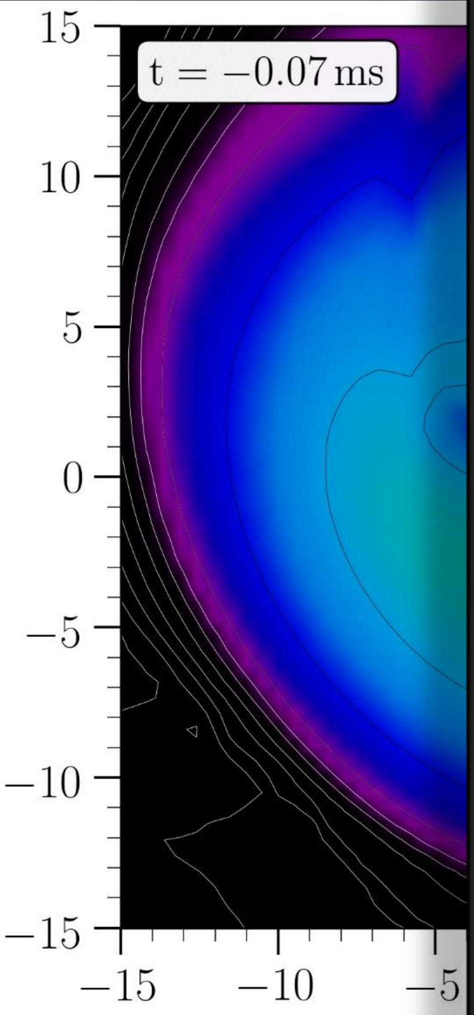

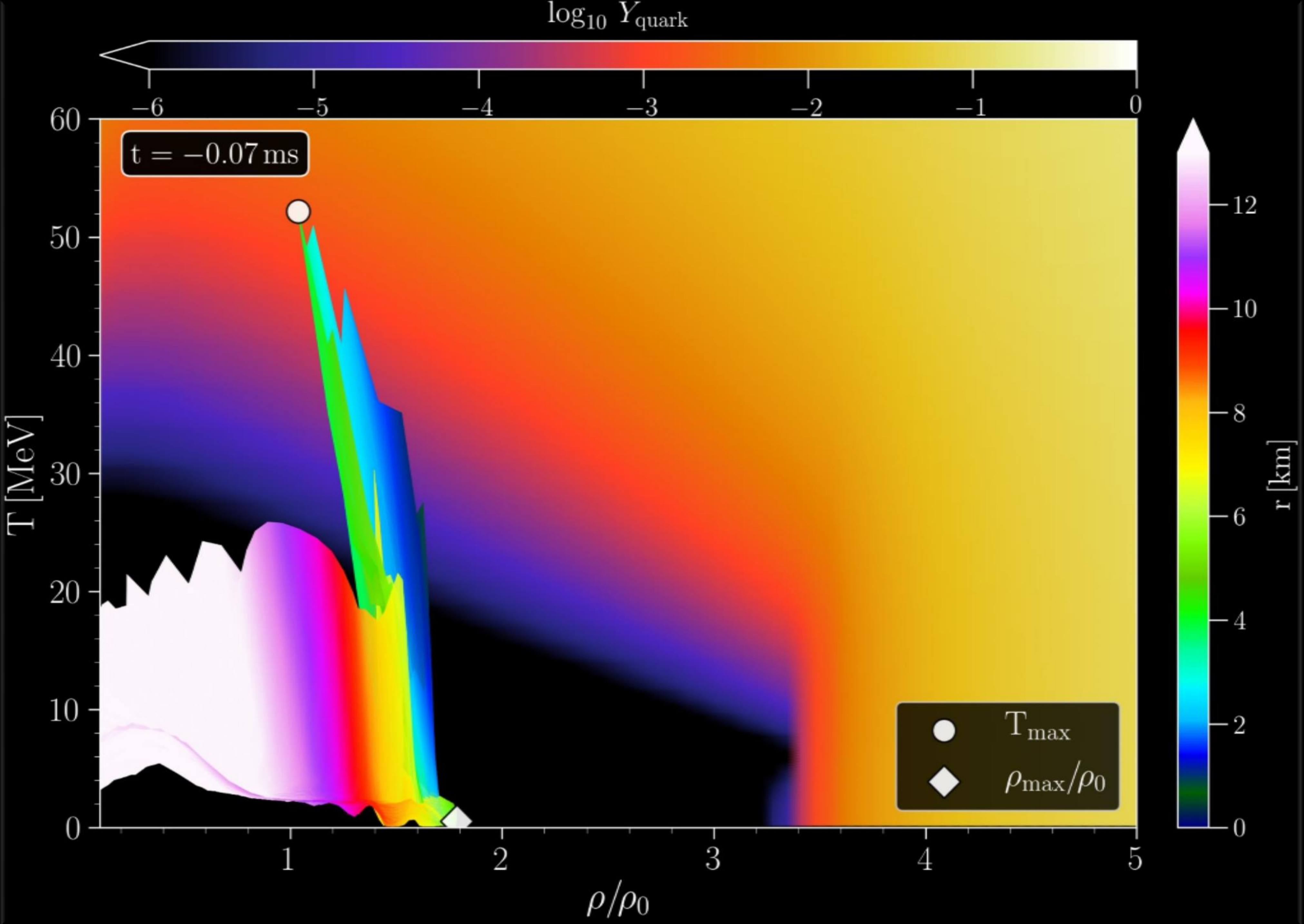

Rest mass density

Post Merger Phase

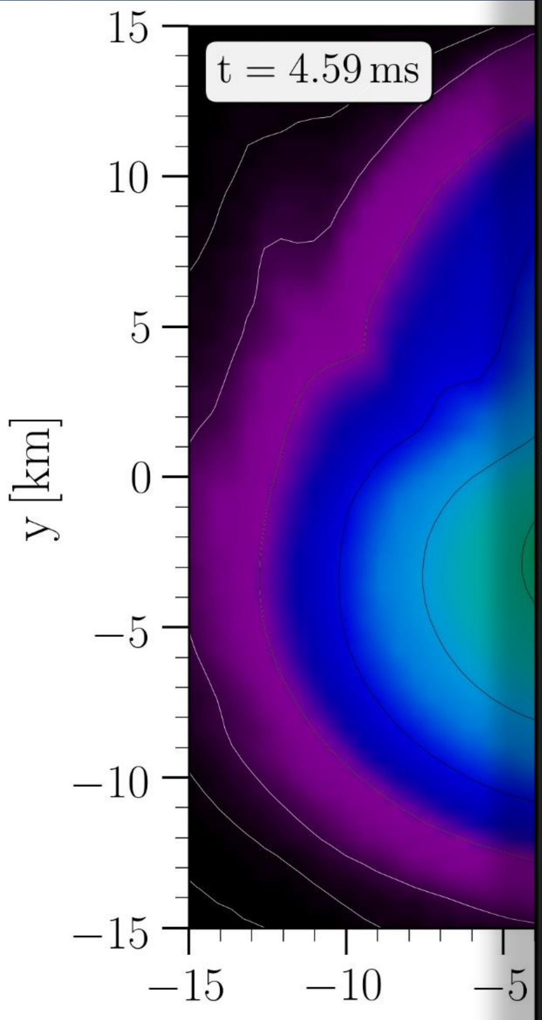

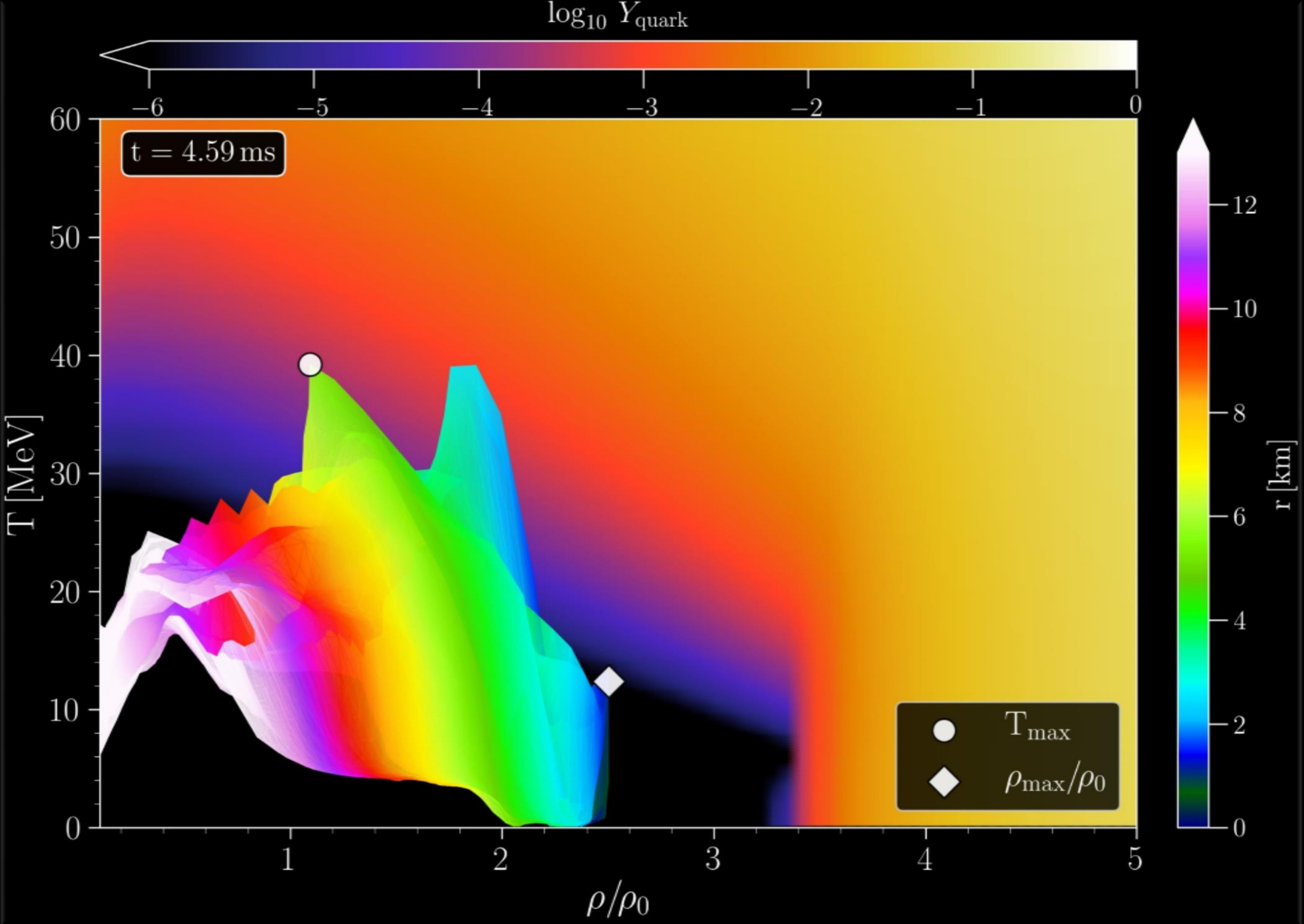

Rest mass density

Post-merger phase

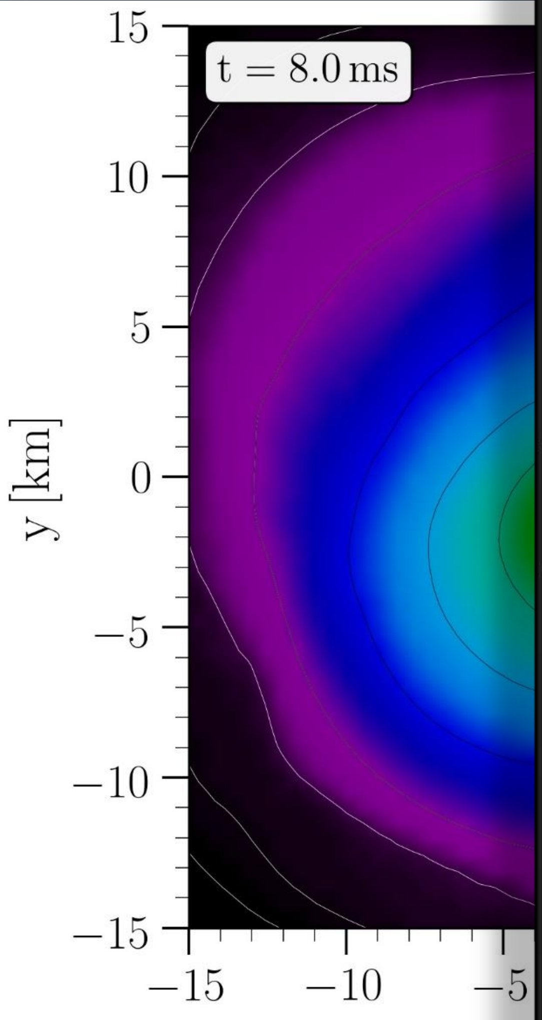

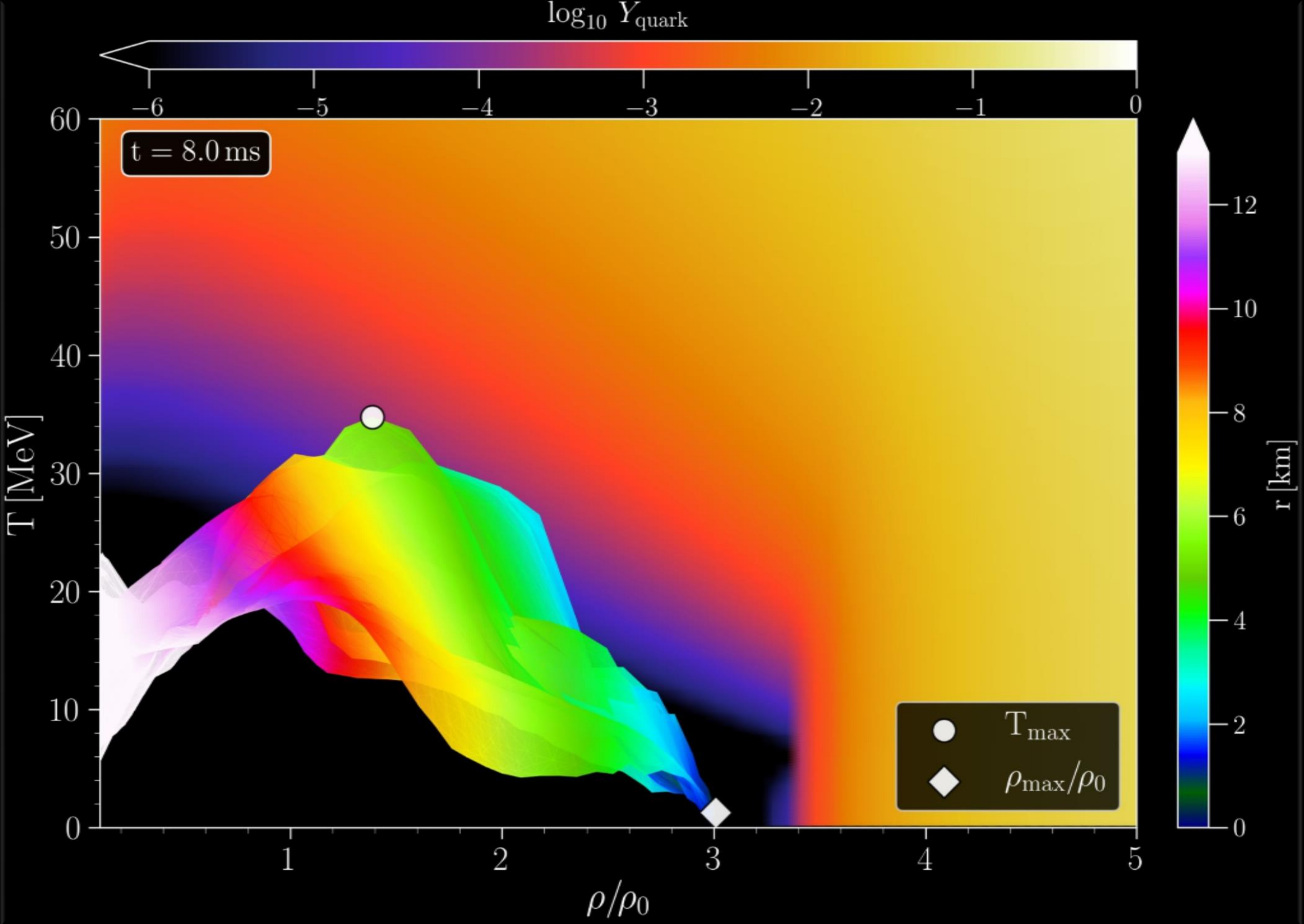

Rest mass density

Post-merger phase

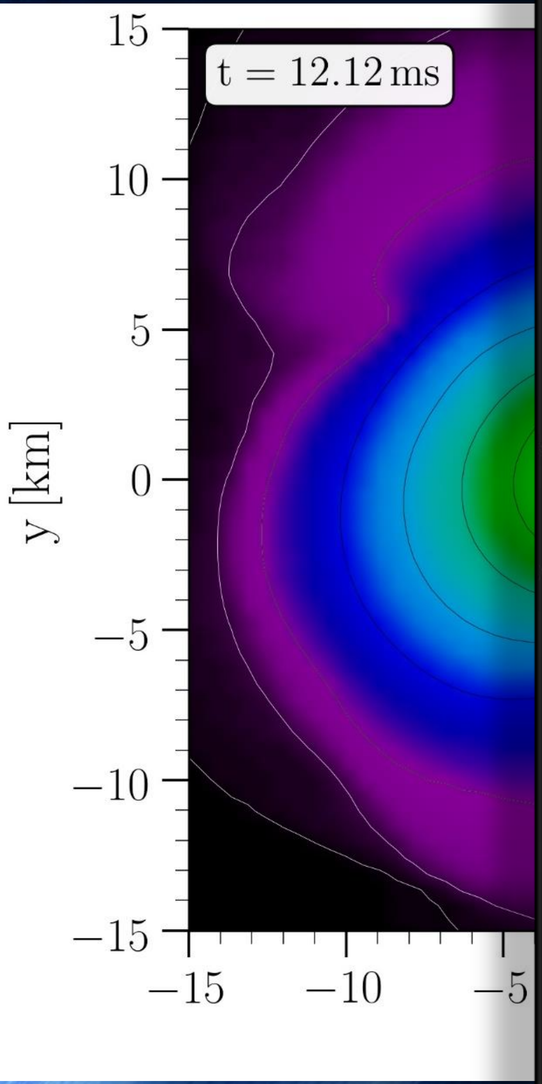

Rest mass density

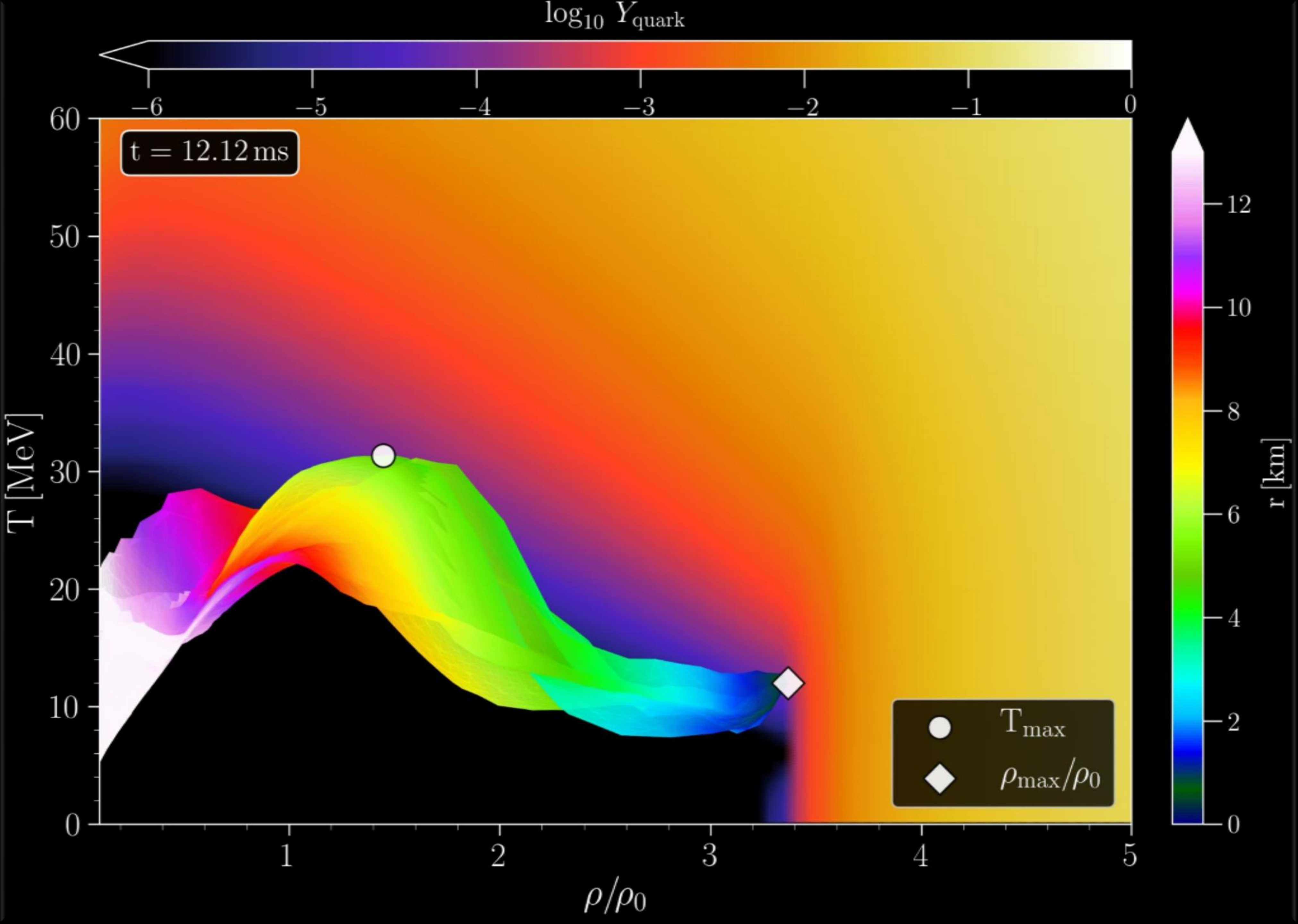

Post-merger phase

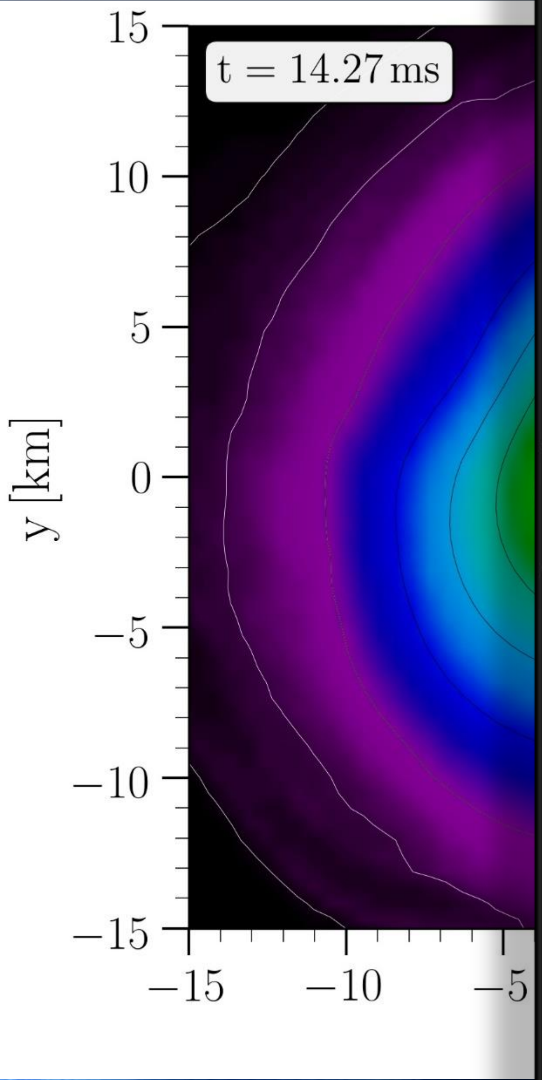

Rest mass density

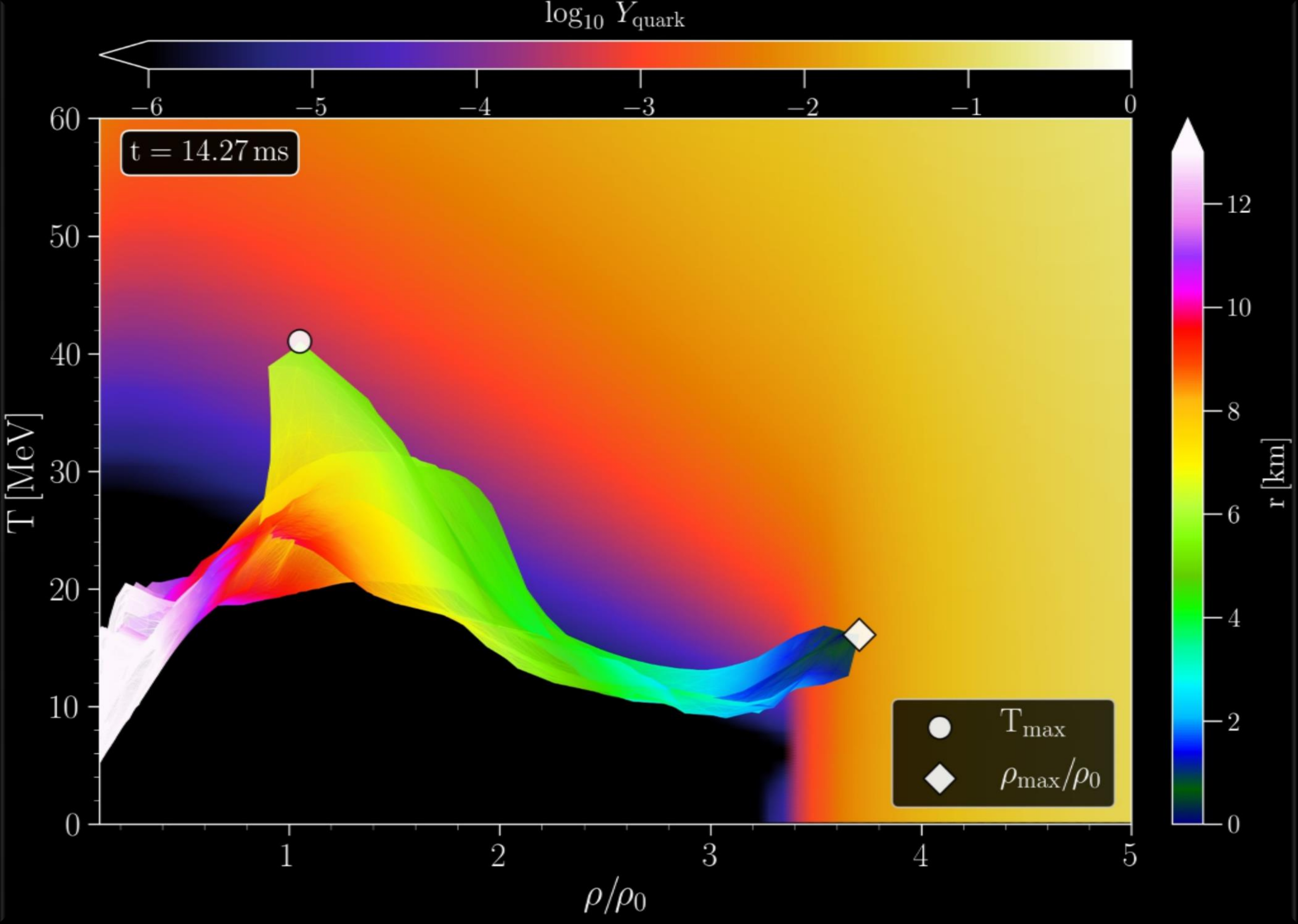

Post-merger phase

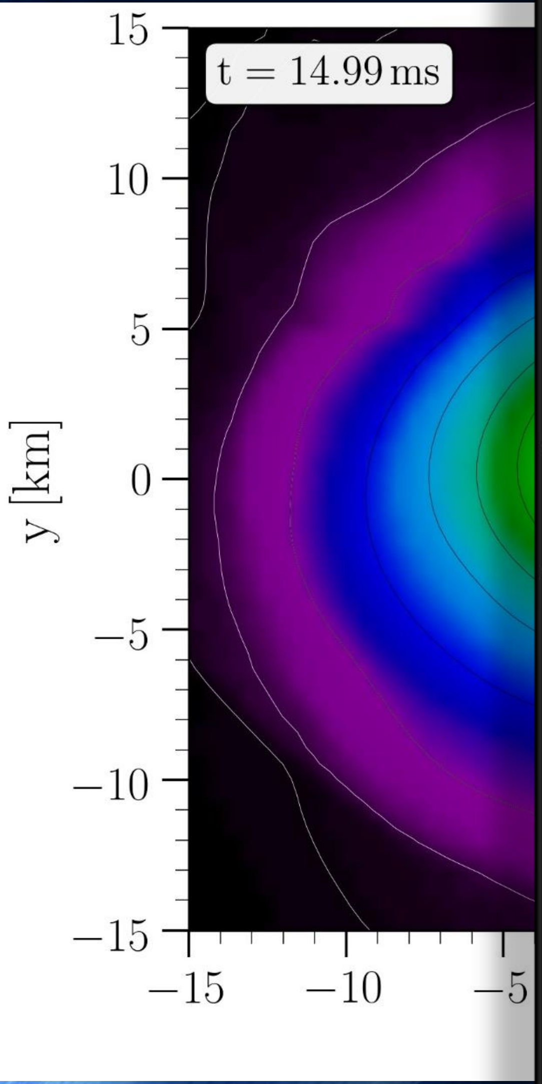

Rest mass density

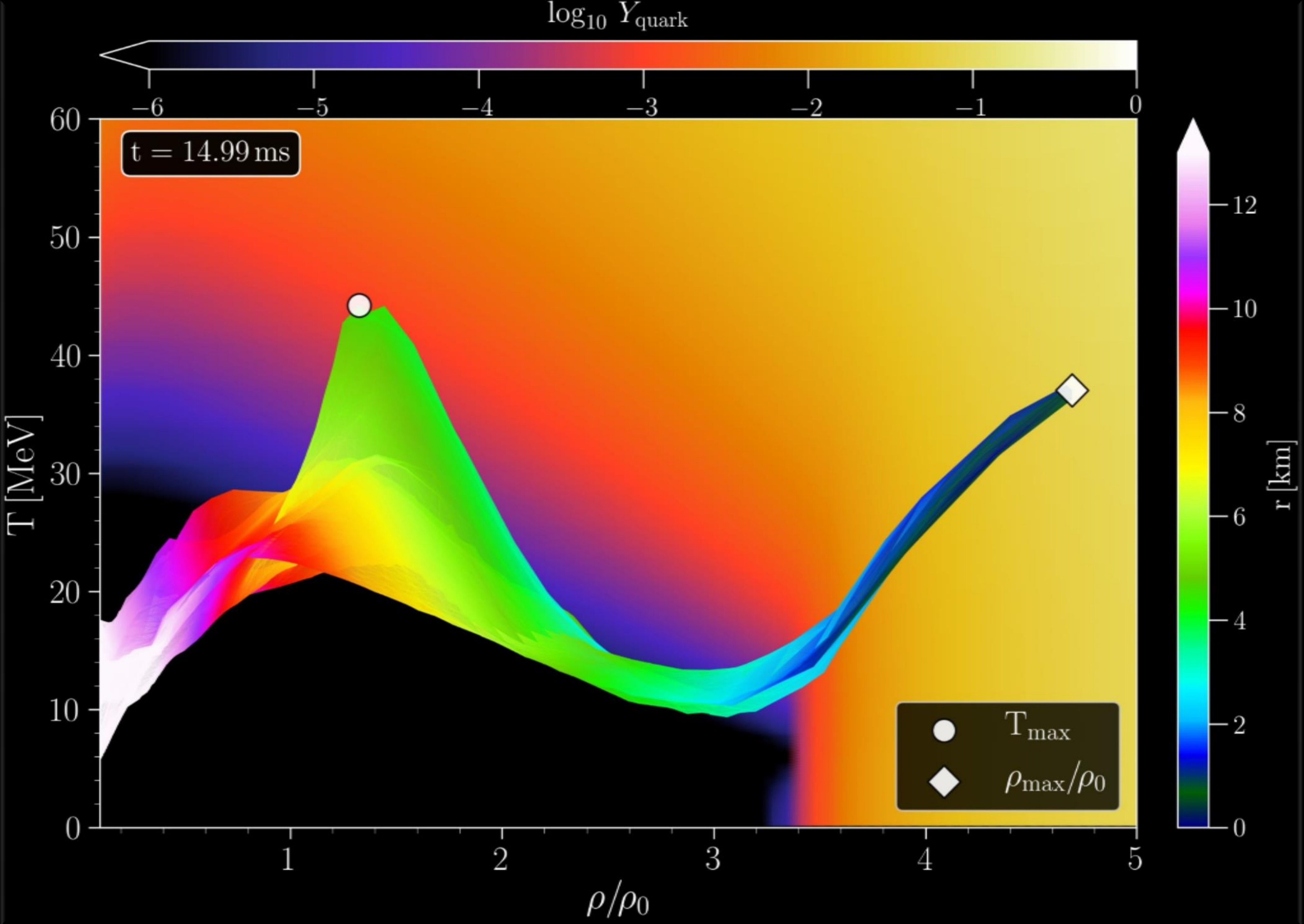

Last picture before tl
apparent horizon form

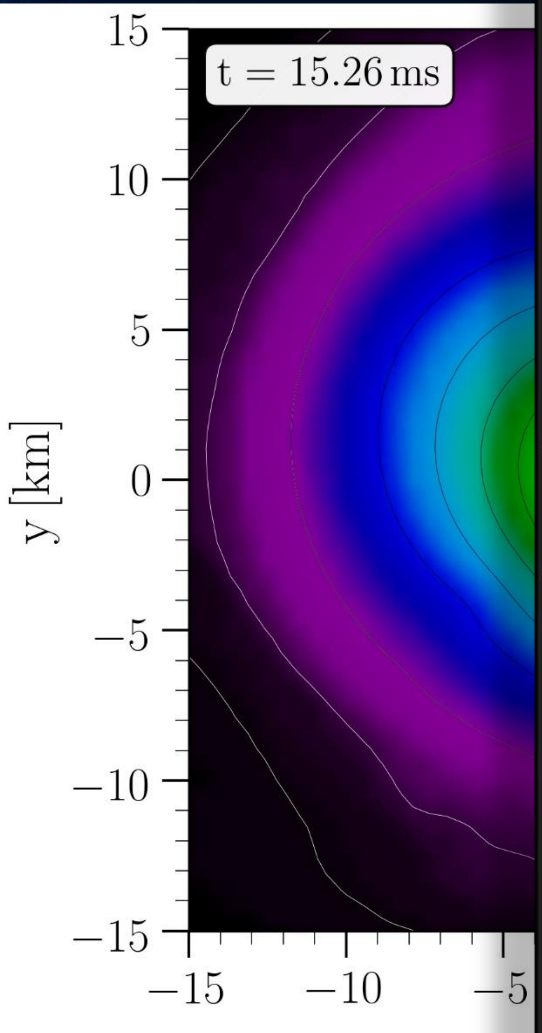

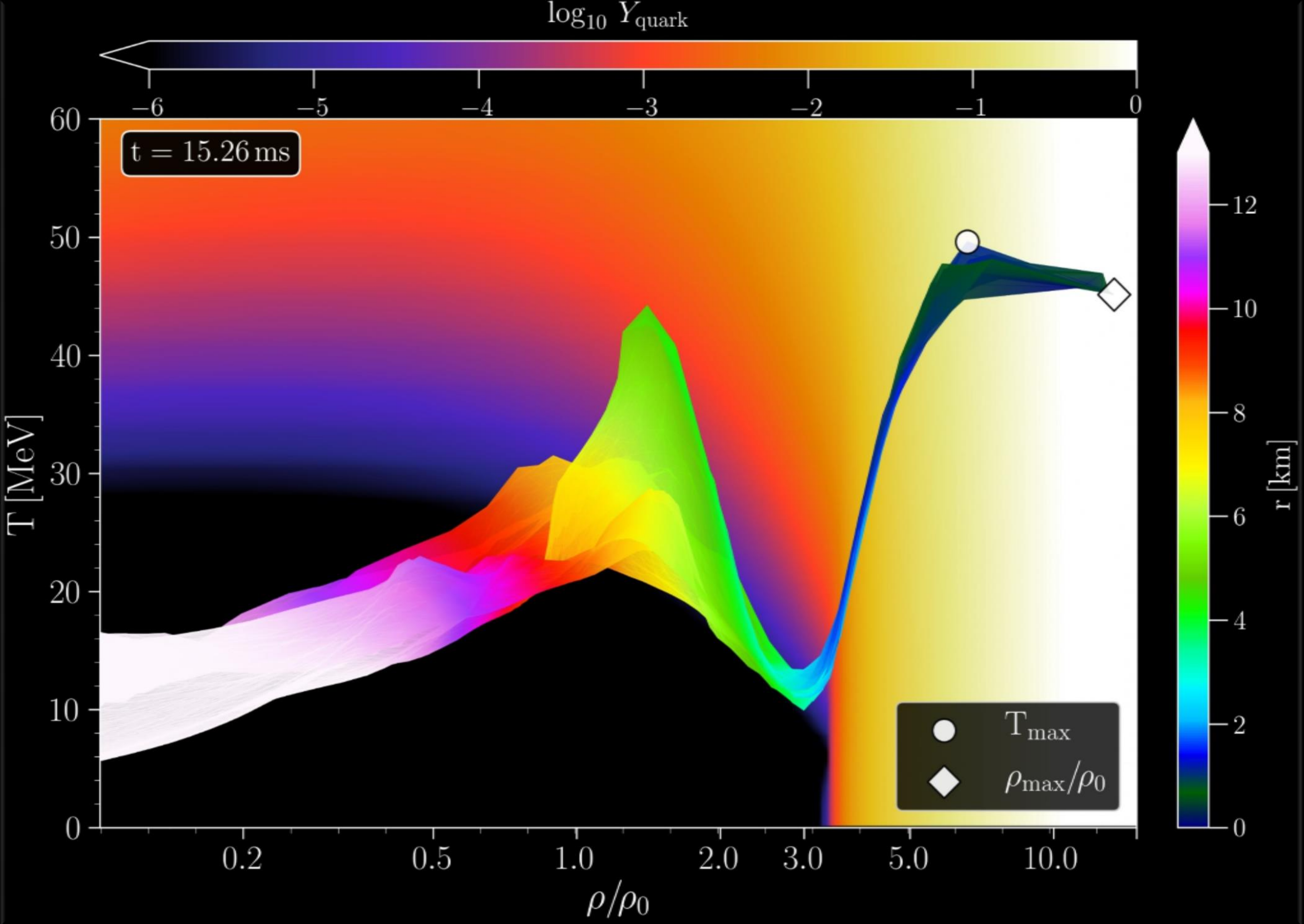

Rest mass density

Gravitational-wave emissiom

"low-mass" binary

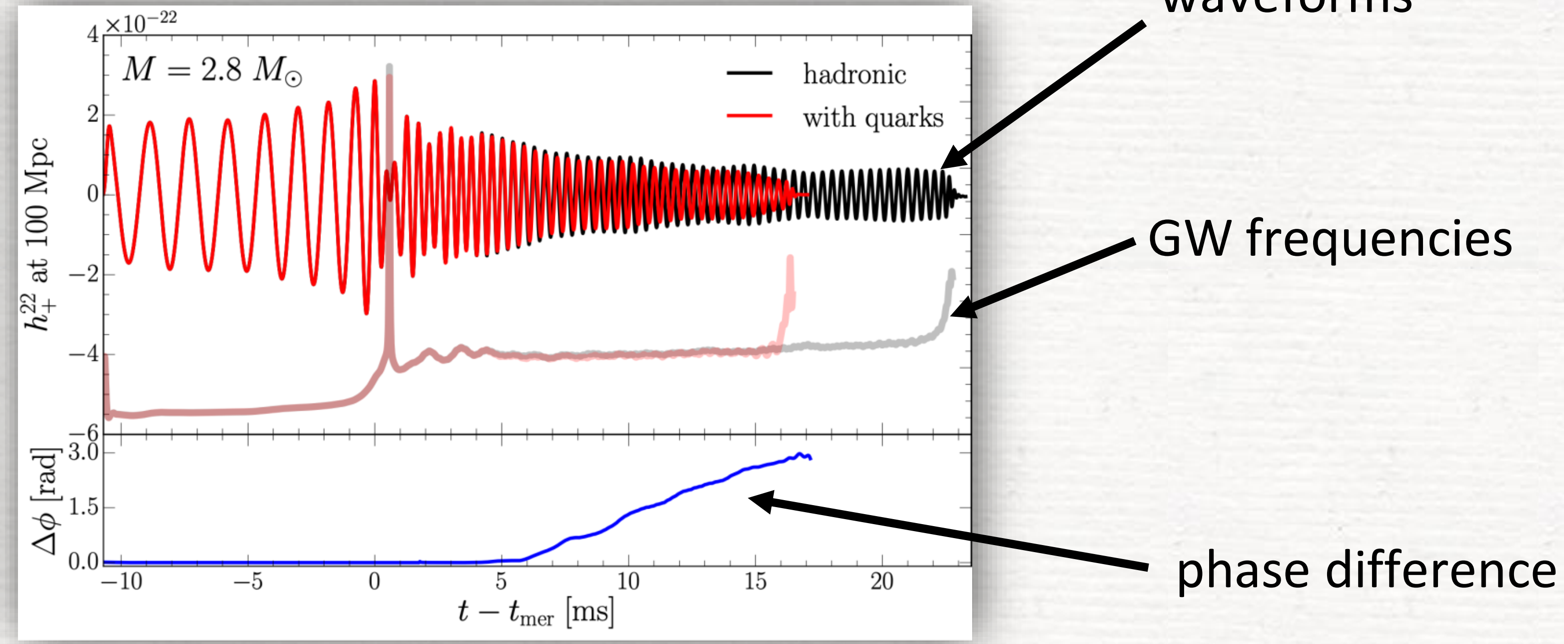

- In **low-mass binary**, after ~ 5 ms, quark fraction is large enough to change quadrupole moment and yield differences in the waveforms.
- Note the phase difference is **zero** in the inspiral.
- Sudden softening of the phase transition leads to collapse and **large difference** in phase evolution.

Gravitational-wave emissiom

“low-mass” binary “high-mass” binary

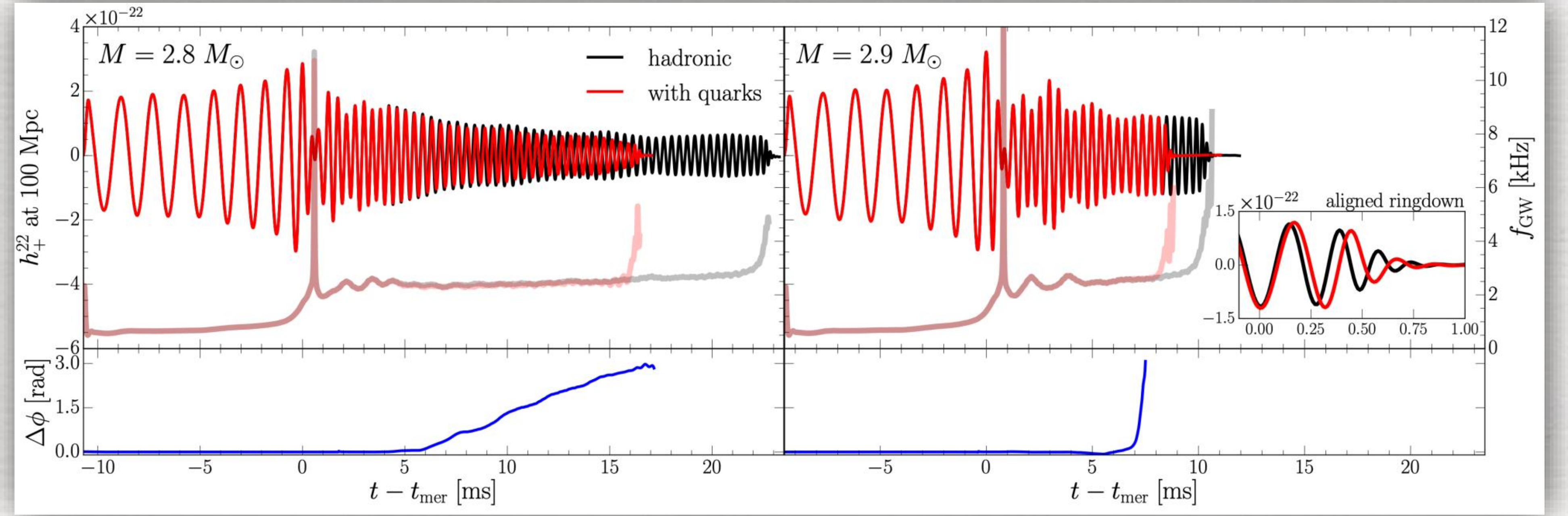

- In **low-mass binary**, after ~ 5 ms, quark fraction is large enough to change quadrupole moment and yield differences in the waveforms.
- In **high-mass binary**, phase transition takes place rapidly after ~ 5 ms. Waveforms a

Observing mismatch between **inspiral** (fully hadronic) and **post-merger**

Binary Hybrid Star Mergers and the QCD Phase Diagram

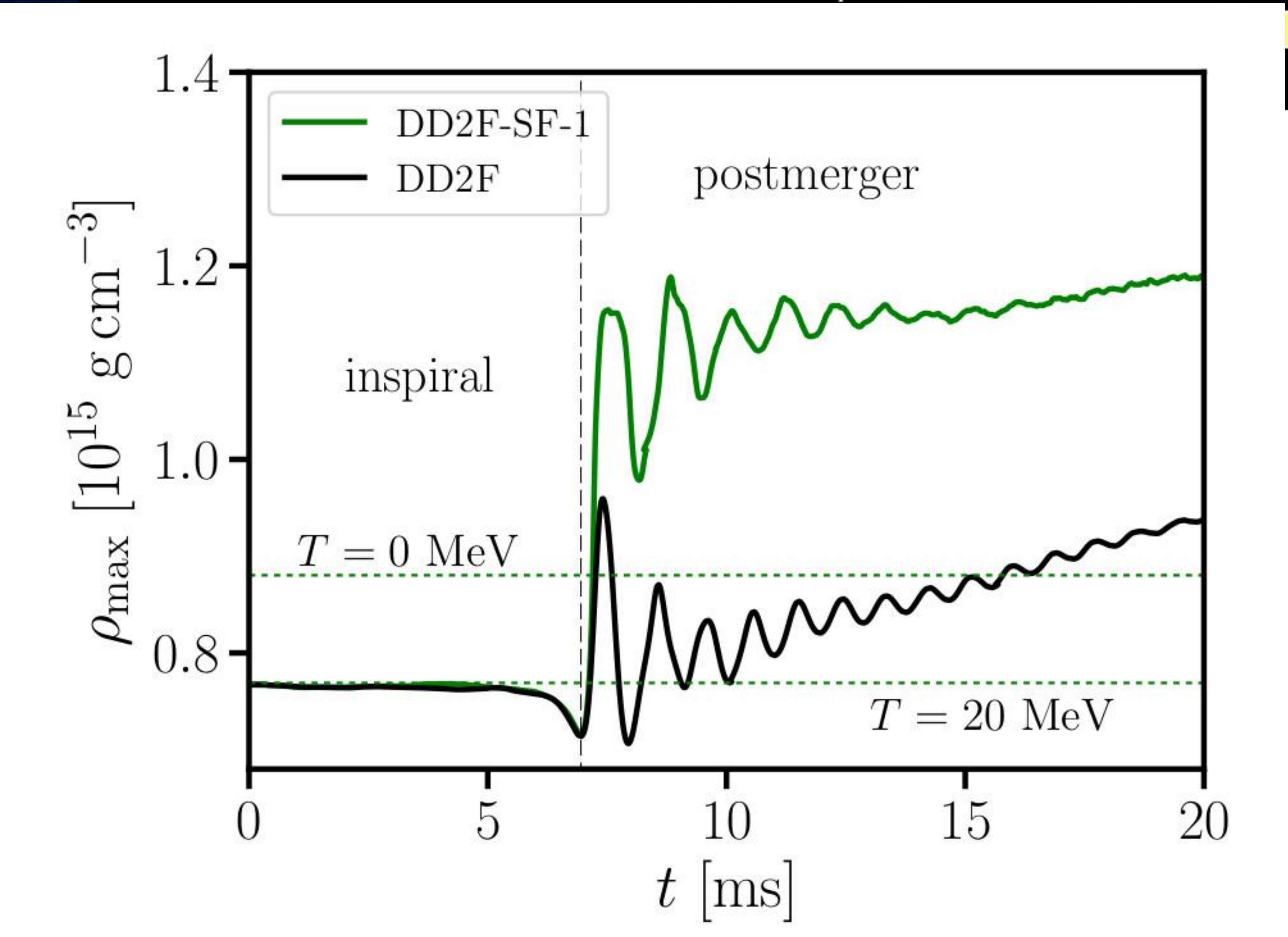

Hot and dense matter inside the inner area of a hypermassive

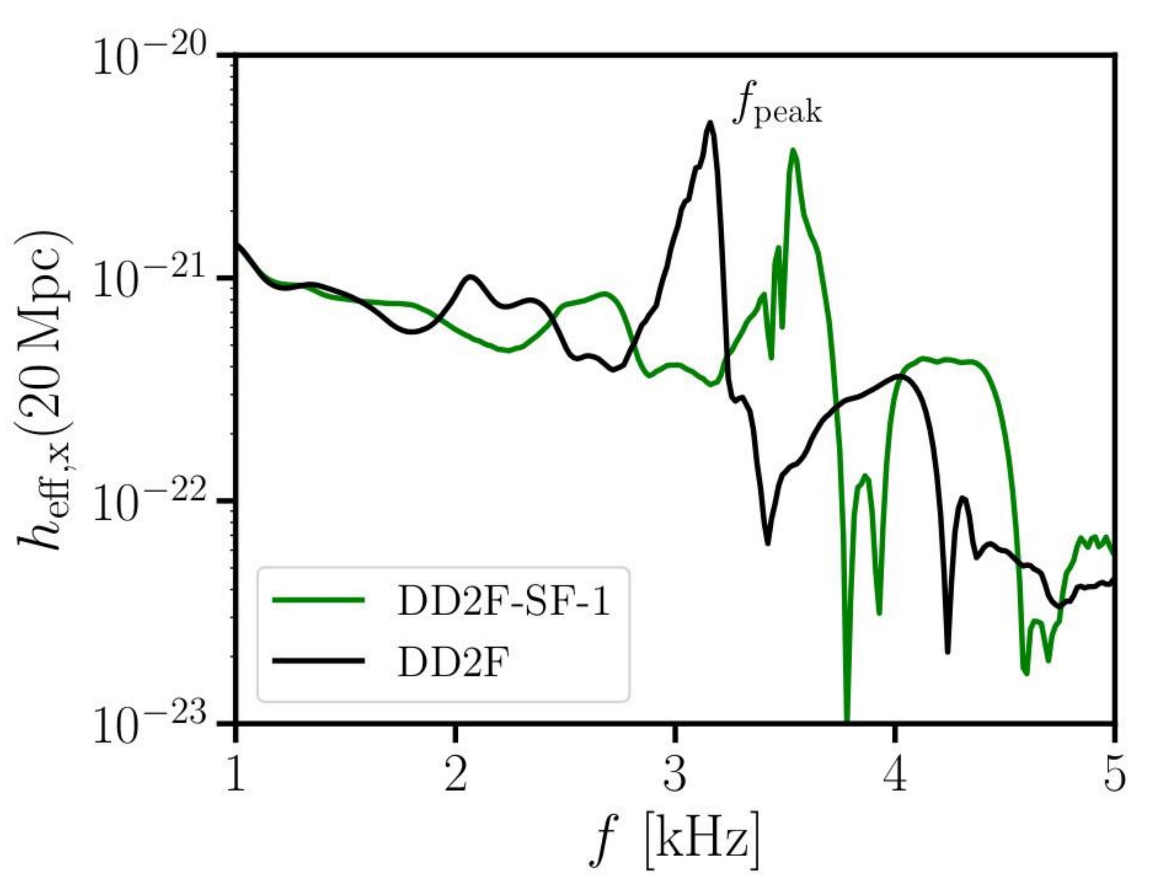

A.Bauswein, N.U.F. Bastian, D.B.Blaschke, K.Chatziioannou, J.A.Clark, T.Fischer and M.Oertel
„Identifying a first-order transition in neutron star mergers through gravitational waves", PRL 2019

E.R.Most, L.J.Papenfort, V.Dexheimer, M.Hanauske, S.Schramm, H.Stöcker and L.Rezzolla
„Signatures of quark-hadron phase transitions in general-relativistic neutron-star mergers„, PRL 2019

Evolution of Tracer-particles tracking individual fluid elements in the equatorial plane of the HMNS at post-merger times

Rotational behavior of deconfined quark matter

Different rotational behaviour of the quark-gluon-plasma produced in non-central ultra-relativistic heavy ion collisions
L. Adamczyk et.al., "Global Lambda-hyperon polarization in nuclear collisions: evidence for the most vortical fluid", Nature 548, 2017

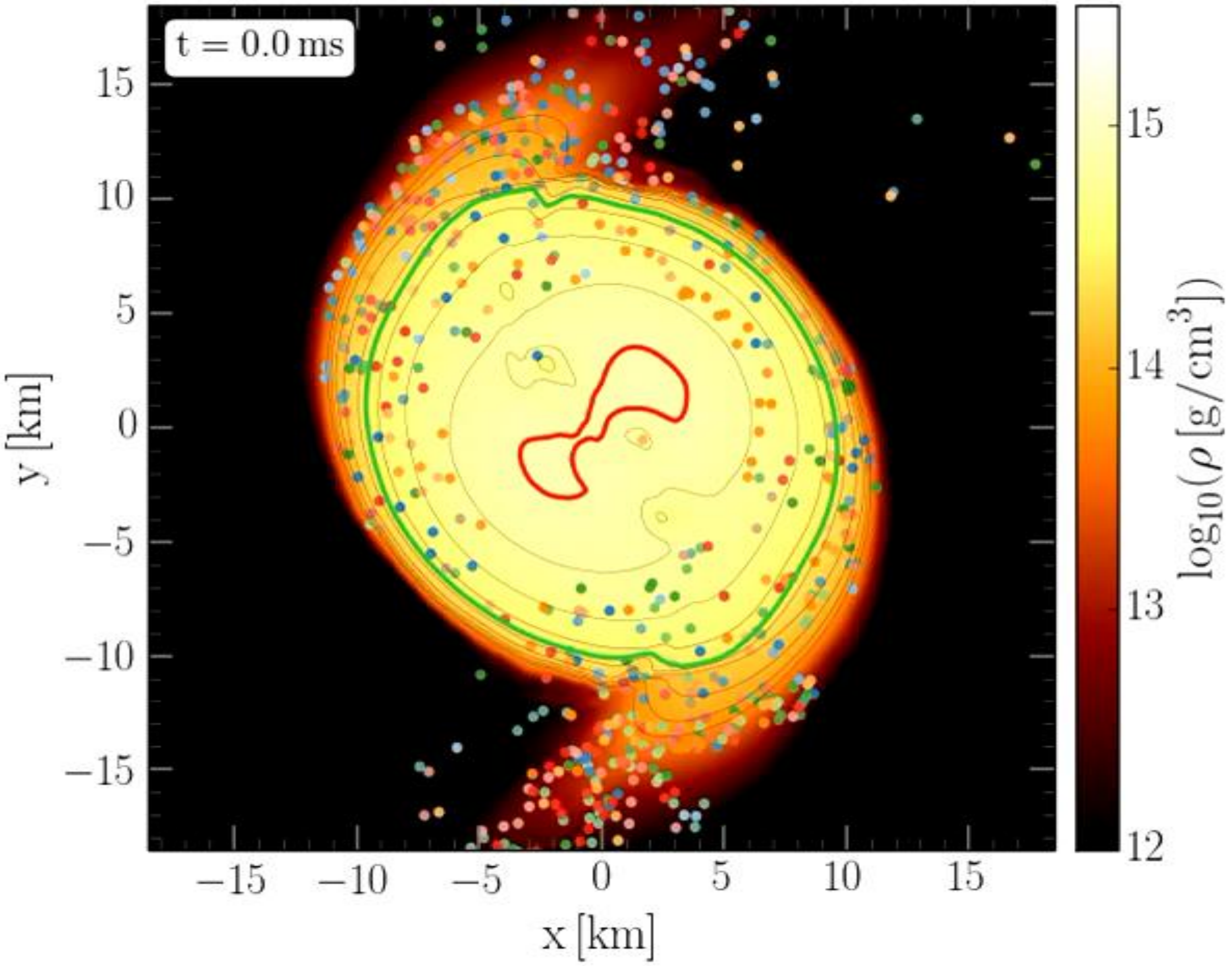

Recap (I)

- Spectra of post-merger shows clear "**quasi-universal**" peaks
- GW spectroscopy possible with post-merger signal
- Unless binary very close, peaks have SNR ~ 1. Multiple signals can be stacked and SNR will increase coherently.
- Only inspiral detected in GW170817 but new limits set on:

Maximum mass

$$2.01^{+0.04}_{-0.04} \leq M_{\rm TOV}/M_\odot \lesssim 2.16^{+0.17}_{-0.15}$$

Typical radii and tidal deformabilities

$$12.00 < R_{1.4}/{\rm km} < 13.45 \quad \tilde\Lambda_{1.4} > 375$$

hadronic EOSs

$$8.53 < R_{1.4}/{\rm km} < 13.74 \quad \tilde\Lambda_{1.4} \gtrsim 35 \quad \tilde\Lambda_{1.7} \lesssim 460$$

phase transitions

- Phase transition can take place after merger leading to clear signatures: misma

Recap (II)

- **Mergers** lead naturally to EM counterparts (GRB, kilonova).
- Magnetic fields unlikely to be detected during the inspiral but **important** after the merger: instabilities and EM counterparts.
- **Electromagnetic counterparts** and a **jet** are **likely** to be produced but the details of this picture are still **far from clear**.
- **Mergers** lead to tiny but important ejected matter and macronova emission.
- "high-*A*" nucleosynthesis very robust (little dependence on EOS and mass ratio) and good agreement with solar abundances.

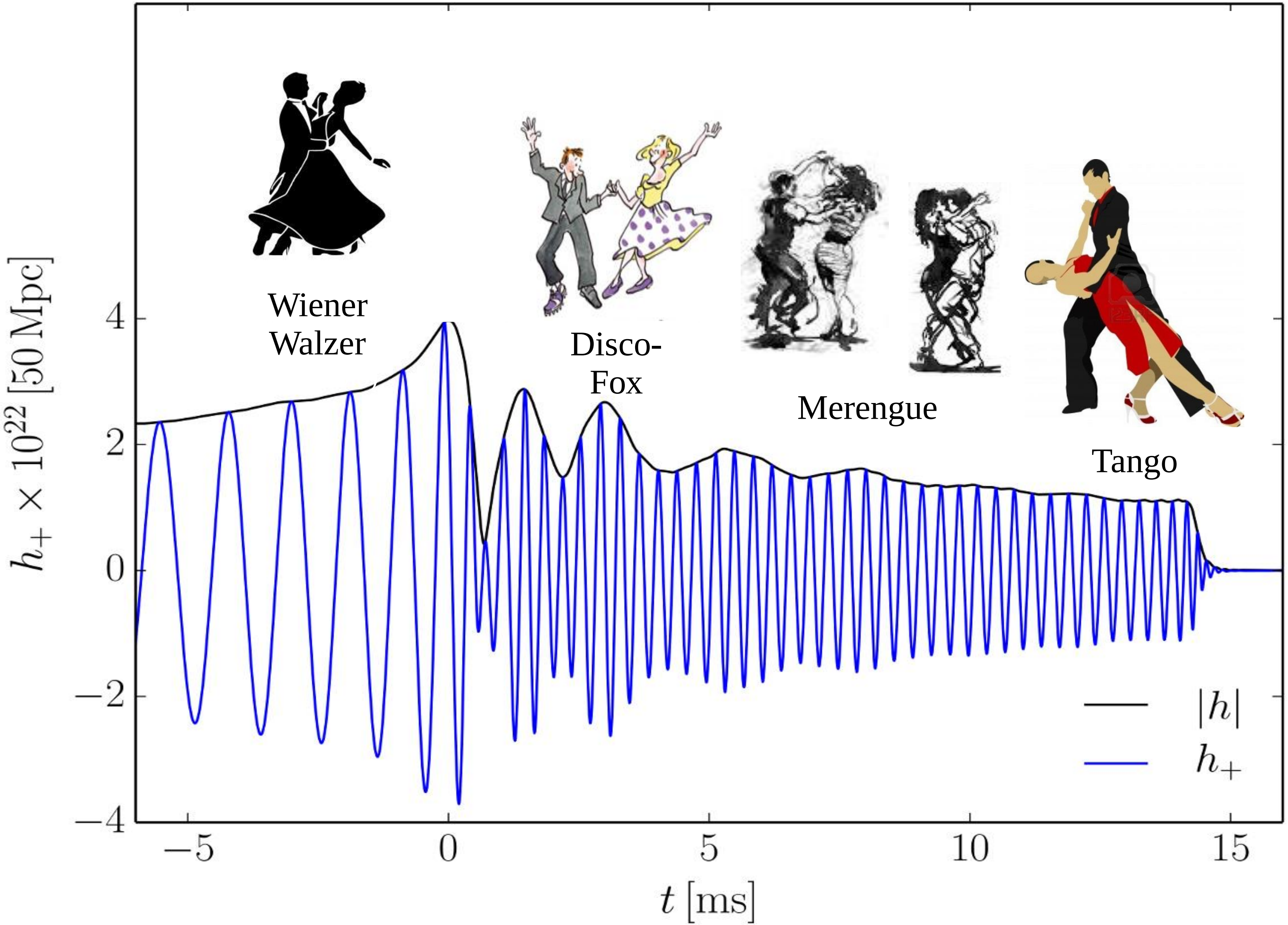
Wiener
Walzer
Disco-
Fox
Merengue
Tango
$h_+ \times 10^{22}$ [50 Mpc]
t [ms]
$|h|$
h_+
4
2
0
−2
−4
−5
0
5
10
15

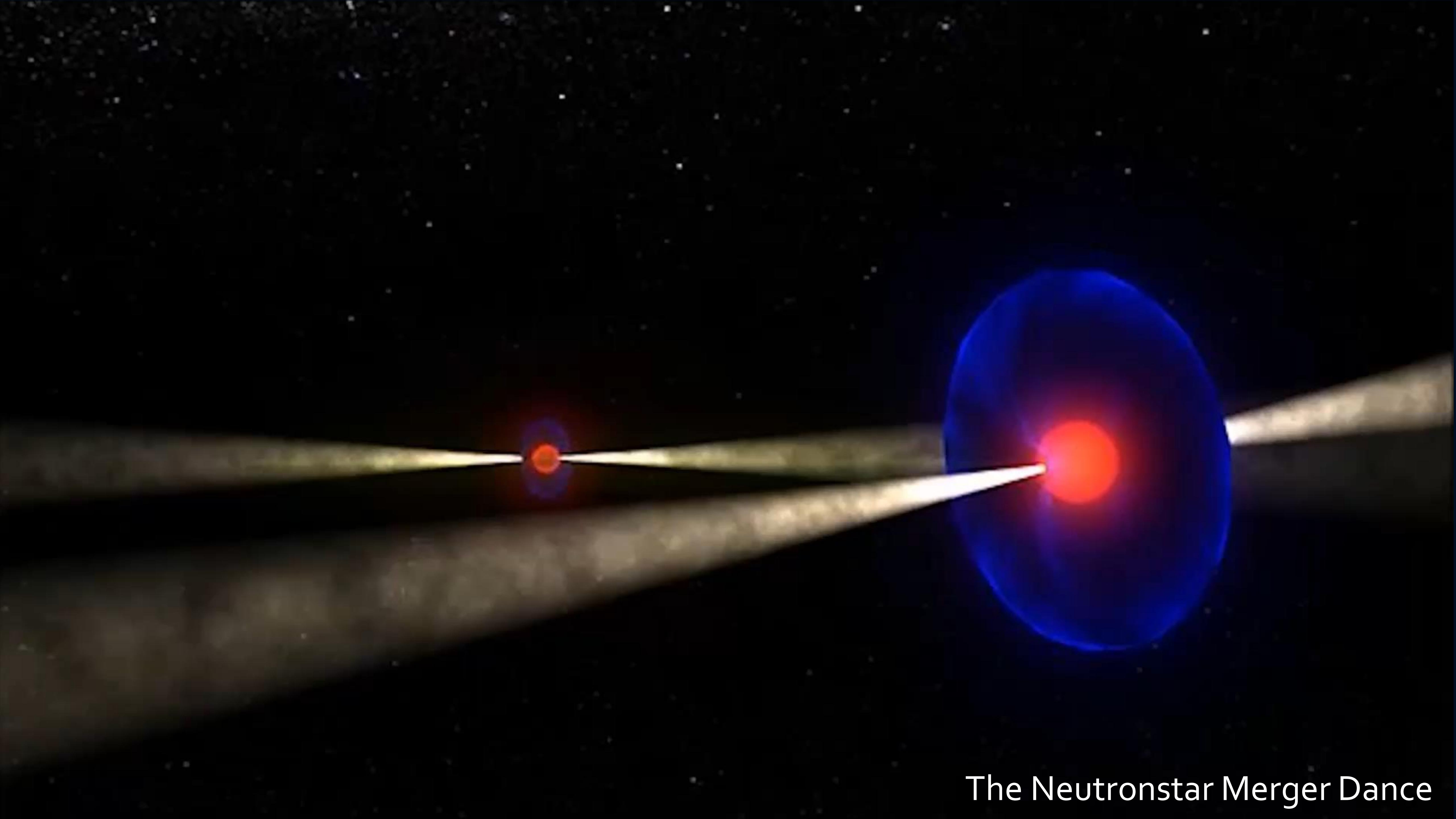

The Neutronstar Merger Dance

Physik der sozio-ökonomischer Systeme mit dem Computer *von* Dr.phil.nat.Dr.rer.pol. Matthias Hanauske

Physik sozio-ökonomischer Systeme mit dem Computer (Physics of Socio-Economic Systems with the Computer) Vorlesung WS 2017/2018, Fr. 15-17.00 Uhr, PC-Pool 01.120

Zusätzlich zur Vorlesung werden ab dem 27.10.2017 freiwillige Übungstermine eingerichtet, die jeweils freitags, eine Stunde vor der Vorlesung im PC-Pool 01.120 stattfinden (Fr. 14-15.00 Uhr).

Diese Vorlesung gibt eine Einführung in das interdisziplinäre Forschungsfeld der *Physik sozio-ökonomischer Systeme*. In sozio-ökonomischen Systemen, wie z.B. bei Finanzmärkten, sozialen Netzwerken, Verkehrssystemen oder wissenschaftliche Kooperationsnetzwerken, sind die dem System zugrunde liegenden Akteure ständigen Entscheidungssituationen ausgesetzt, wobei der Erfolg und die Auswirkung der individuell gewählten Strategie von den Entscheidungen der anderen beteiligten Akteuren abhängt. Die (evolutionäre) Spieltheorie und die Physik komplexer Netzwerke stellen die beiden Grundsäulen der theoretischen Beschreibung und mathematischen Formulierung solcher Systeme dar. Im ersten Teil des Kurses werden die grundlegenden Konzepte der Spieltheorie thematisiert und die Studierenden erlernen, unter Verwendung von Computeralgebra-Systemen (Maple und Mathematica) deren Anwendung auf diverse Spielklassen. Neben den endlichen Zweipersonen-Spielen und N-Personen-Spielen wird auch auf die evolutionäre Entwicklung ganzer Spieler-Populationen eingegangen